

Neuronal alterations in chronic cerebral *Toxoplasma gondii* infection

Dissertation

zur Erlangung des akademischen Grades

**doctor rerum naturalium
(Dr. rer. nat.)**

genehmigt durch die Fakultät für Naturwissenschaften
der Otto-von-Guericke Universität Magdeburg

von: DVM, MSc (Neuroscience) Alexandru Parlog
geb. am 26.März 1982 in Tulcea, Rumänien

Gutachter: Prof. Dr. med. Dirk Schlüter
Prof. Dr. med. Ralf Ignatius

eingereicht am 20.November 2014

verteidigt am 20.April 2015

Acknowledgements

Foremost, I would like to express my sincere gratitude to my advisor, Dr. Ildiko Rita Dunay for accepting me as a member of her team and for the continuous support during my research odyssey. Despite the challenging moments, we both experienced, your enthusiasm, motivation and devotement for work and science have been inspirational for me, through my entire studies. Thank you!

This thesis would not have been possible without the support and conjugated work of: Dr. Laura Adela Harsan, Dr. Karl Heinz Smalla, Dr. Marta Zagrebelsky, Marianna Weller, Dr. Marco van Ham, Dr. Dominik von Elverfeldt, Prof. Dr. Dirk Schlüter, Prof. Dr. Martin Korte, Dr. Eike Budinger, Prof. Dr. Christian Mawrin and Prof. Dr. Lothar Jänsch. I want to express my gratitude to all these collaborators who believed in me and in the project, and who engaged in this work, along with me, with all their energy and enthusiasm. Thank you all!

Dear Luisa and Aindrila, thank you very much for the great adventure I've been through while working together in the same group. It was really fun and rewarding to spend time with you, and I must say I could never hope for better colleagues. The rest you know it... 😊

Dear Dana, thank you very much for your technical assistance and support with the western blots and for making sure that I always had, in due time, all the materials needed for the experiments.

I would like to thank my colleagues from AG Bruder and AG Schlüter, as well as to all the people from the Institute of Medical Microbiology and Hospital Hygiene, for the excellent collegial and working relations we had. It was a pleasure and an honor to be one of you!

To my family, Laura, Mihai, Mum, Dad, it is useless to mention how grateful I am towards you for your love, encouragements and tremendous support. You know that already, but I'd like to say it one more time. Thank you for always being there for me!

I gratefully acknowledge the funding received towards my PhD, for two years (2012-2014), from the Faculty of Medicine at Otto-von-Guericke University of Magdeburg, in the form of a doctoral scholarship.

Publications

Part of this work is published under the following title:

Parlog A, Harsan LA, Zagrebelsky M, Weller M, Elverfeldt von D, Mawrin C, Korte M, Dunay IR. Chronic murine toxoplasmosis is defined by subtle changes in neuronal connectivity. *Dis Model Mech*, April 2014. **7**: 459-69.

Other publications:

Möhle L*, **Parlog A***, Pahnke J, Dunay IR. Spinal cord pathology in chronic experimental *Toxoplasma gondii* infection. *Eur J Microbiol Immunol (Bp)*, March 2014. **4** : 65–75. *First two authors contributed equally to this work.

Parlog A, Schlüter D, Dunay IR. *Toxoplasma gondii* induced neuronal alterations. *Parasite Immunol*. November 2014. doi: 10.1111/pim.12157.

Abstract

Toxoplasma gondii (*T. gondii*) is an obligate intracellular parasite that is widely distributed throughout all warm-blooded animals and humans, with a high tropism for the central nervous system (CNS). Recent studies correlate chronic *T. gondii*-infection with behavioral changes in rodents; additionally, seropositivity in humans is reported to be associated with behavioral and neuropsychiatric diseases. However, little is known about the underlying neurobiological mechanisms by which *T. gondii* might trigger certain neuropsychiatric illnesses.

In this study we investigated whether the described behavioral changes in a murine model of chronic toxoplasmosis are associated with changes in synaptic plasticity and brain neuronal circuitry. In mice chronically infected with *T. gondii*, magnetic resonance imaging (MRI) data analysis displayed the presence of heterogeneous lesions scattered throughout all brain areas. However, a higher density of lesions was observed within specific regions such as the somatosensory cortex (SSC). Further histopathological examination of these brain areas indicated the presence of activated resident glia and recruited immune cells accompanied by limited alterations of neuronal viability. *In vivo* diffusion-tensor MRI analysis of neuronal fiber density within the infected regions revealed connectivity abnormalities in the SSC. Altered fiber density was confirmed by morphological analysis of individual pyramidal and granule neurons, showing a reduction in dendritic arborization and spine density within the SSC, as well as in the hippocampus. Further evaluation of synaptosome fraction from chronically infected mice by proteomic analysis and western blot, revealed significant changes in key synaptic proteins, such as PSD95, Synaptophysin, NR1, NR2A and NR2B. These persistent impacts of the infection on synaptic efficacy might trigger cognitive and neuropsychiatric abnormalities.

Taken together, these findings indicate that upon latent infection with *T. gondii*, marked neuroanatomical and neurofunctional changes occur in CNS regions that are relevant for normal behavior, suggesting a potential explanation for the behavioral alterations, and establish a murine model for translational studies of chronic toxoplasmosis.

Table of contents

Acknowledgements	II
Publications	III
Abstract	IV
Table of contents	V
List of abbreviations	VIII
List of figures and tables	X
Introduction	1
1. Brief description of <i>T. gondii</i> - basic morphology and life cycle	1
1.1. Tachyzoites	2
1.2. Bradyzoites	3
1.3. Sporozoites	4
1.4. Life cycle of <i>T. gondii</i>	4
2. Immune response and pathogenesis of <i>Toxoplasma gondii</i> infection	6
2.1. Immunopathogenesis of cerebral toxoplasmosis	6
3. Toxoplasmosis in Humans	10
3.1. Congenital toxoplasmosis	10
3.2. Acute toxoplasmosis	10
3.3. Chronic toxoplasmosis	11
3.3.1. Cognitive, motor and personality alterations associated with <i>T. gondii</i> infection	11
3.3.2. Association of latent <i>T. gondii</i> infection and psychiatric disorders	12

4.	<i>Toxoplasma gondii</i> infection and animal behavior	14
5.	Hypotheses for specific behavior changes in intermediate hosts	15
5.1.	Cyst location in the CNS	15
5.2.	<i>T. gondii</i> modulates dopamine production	15
5.3.	<i>T. gondii</i> can functionally “silence” neurons	16
5.4.	Proteins injected by <i>T. gondii</i> can manipulate host cell	16
5.5.	Persistent behavioral changes after parasite clearance	17
6.	Neuroplasticity and neuroinflammation	18
6.1.	Overview on neuronal anatomy and plasticity	18
6.2.	The impact of neuroinflammation on neuroconnectivity	19
6.2.1.	Central neuroinflammation	20
6.2.2.	Neuroinflammation via peripheral mediators	21
<u>Aims</u>		23
<u>Materials and Methods</u>		25
1.	Animals and <i>T. gondii</i> infection	25
2.	<i>In vivo</i> Magnetic Resonance Imaging	26
2.1.	Data acquisition	26
2.2.	Data post-processing	27
3.	Histopathological analysis	28
4.	Immunofluorescence	29
5.	Fluoro-JadeB staining	30
6.	Electron microscopy	30
7.	DiOlistics and morphological analysis	31
8.	Synaptic junction preparation	32
9.	Western Blot analysis	33
10.	RT-PCR analysis	35
11.	Proteomic analysis	36
11.1.	Protein digest	36
11.2.	iTRAQ labelling and SCX chromatography	36
11.3.	LC-MS/MS and data analyses	37

Results	38
1. Experimental design	38
2. Distribution of <i>T. gondii</i> induced lesions: MRI vs. histopathological investigations	39
3. Chronic <i>T. gondii</i> infection alters the brain connectivity microstructure: <i>in vivo</i> qualitative and quantitative DT-MRI	41
4. Neuroinfection is associated with white matter microstructural abnormalities	46
5. Chronic infection is negatively influencing the dendritic morphology of noninfected cortical neurons	48
6. Dendritic spine density and morphology is affected in the cortex of infected mice	50
7. Chronic infection with <i>T. gondii</i> alters the structure of hippocampal neurons	53
8. Synaptophysin and PSD95 protein expression level is reduced in the cortex and the hippocampus of mice chronically infected with <i>T. gondii</i>	56
9. Latent infection with <i>T. gondii</i> alters the proteome of adult mouse cortical and hippocampal synaptosomes	57
10. Glutamate receptor abnormalities in the synapses of infected mice	65
11. Akt/GSK3 β signaling defects in the cortex of chronically infected mice	68
Discussion	71
References	80
Annex	95
Selbständigkeitserklärung	101
Curriculum vitae	102

List of abbreviations

%	percent
°C	degree Celsius
<D>	mean diffusivity
D^{\perp}	radial (perpendicular) diffusivity
D_{\parallel}	axial (parallel) diffusivity
μg	microgram
μm	micrometer
μL	microliter
Akt	protein kinase B
AMPA	α-amino-3-hydroxy-5-methyl-4-isoxazolepropionic acid
AMPA R	α-amino-3-hydroxy-5-methyl-4-isoxazolepropionic acid receptor
BBB	blood brain barrier
CA1	cornu ammonis1
CNS	Central Nervous System
DG	dentate gyrus
DT-MRI	Diffusion-Tensor Magnetic Resonance Imaging
FA	fractional anisotropy
FD	fiber density
g	gravitational constant
GAPDH	Glycerinaldehyd-3-phosphat-Dehydrogenase
GBP	p67 guanylate-binding proteins
GM	grey matter
GSK3β	Glycogen synthase kinase 3 beta
hrFM	high resolution fiber maps
HPRT	hypoxanthine-guanine phosphoribosyltransferase
IFN-γ	interferon gamma
IgG	immunoglobulin G
IL	interleukin

iNOS	inducible nitric oxide synthase
i.p	intraperitoneal
iTRAQ	isobaric tags for relative and absolute quantitation
Kg	kilogram
LC-MS/MS	Liquid chromatography–mass spectrometry
MAP2	Microtubule Associated Protein 2
min	minutes
mg	milligram
mm	millimeters
MRI	magnetic Resonance Imaging
NK cells	natural killer cells
NO	nitric oxide
NMDA	N-Methyl-D-aspartic acid or N-Methyl-D-aspartate
NMDAR	N-Methyl-D-aspartic acid or N-Methyl-D-aspartate receptor
NR1	Glutamate (NMDA) receptor subunit zeta-1
NR2A	Glutamate (NMDA) receptor subunit epsilon-1
NR2B	Glutamate (NMDA) receptor subunit epsilon-2
OCD	obsessive compulsive disorder
pAkt	phosphorylated protein kinase B
PBS	phosphate buffered saline
pGSK3 β	phosphorylated Glycogen synthase kinase 3 beta
p.i.	post infection
PSD95	post synaptic density 95
ROI	reactive oxygen intermediates
ROP	rhodopsin protein
rpm	rotations per minute
RT	room temperature
RT-PCR	real time polymerase chain reaction
SSC	somatosensory cortex
TLR	toll-like receptor
TNF	tumor necrosis factor
WB	western blot
WM	white matter

List of figures and tables

Figure 1. Schematic drawings of a tachyzoite (left) and a bradyzoite (right) of <i>T. gondii</i> (15).	3
Figure 2. <i>T. gondii</i> tissue cyst	4
Figure 3. The complex life cycle of <i>Toxoplasma gondii</i> (29).....	5
Figure 4. Schematic description of a neuron and a synapse.....	20
Figure 5. Schematic illustration of the brain-periphery crosstalk pathway in the regulation of neuroplasticity (232)	22
Figure 6. Pathological changes identified by MRI and histopathological examination of the murine brain chronically infected with <i>T. gondii</i>	40
Figure 7. <i>In vivo</i> appraisal, by DT-MRI, of cortical injuries induced upon chronic <i>T. gondii</i> infection.....	42
Figure 8. Structural abnormalities in axons and dendrites were observed within the cortex of <i>T. gondii</i> infected mice.....	43
Figure 9. <i>In vivo</i> DT-MRI based quantitative evaluation of brain microstructural alterations induced by chronic <i>T. gondii</i> infection.....	45
Figure 10. Quantitative assessment of modifications induced by <i>T. gondii</i> infection on brain parametric maps generated from <i>in vivo</i> DT-MRI data	47
Figure 11. Morphological analysis of Layer II/III pyramidal neurons within the cortices of <i>T. gondii</i> infected and control mice.....	49
Figure 12. Spine density deficits in pyramidal neurons within the cortex of <i>T. gondii</i> infected mice	51
Figure 13. Effect of infection with <i>T. gondii</i> on cortical dendrites spine length and spine head width.....	52
Figure 14. Morphological investigation of granule neurons within dentate gyrus of <i>T. gondii</i> infected and control mice	54

Figure 15. Morphological analysis of neurons within CA1 pyramidal neurons of *T. gondii* infected and control mice 55

Figure 16. Impaired expression of synaptic related proteins in *T. gondii* infected brains 56

Figure 17. Canonical pathway with reduced activity implicates glutamatergic signaling 60

Figure 18. Statistical evaluation of synaptosome protein data 62

Figure 19. The expression of glutamate receptor subunits AMPA1 and AMPA2 is not altered by chronic infection with *T. gondii* 66

Figure 20. Chronic infection with *T. gondii* is associated with NMDA receptor subunit abnormalities 67

Figure 21. Effects of *T. gondii* induced neuroinflammation on Akt expression and phosphorylation 69

Figure 22. Effects of *T. gondii* induced neuroinflammation on GSK3 β expression and phosphorylation 70

Table 1. Summary of primary antibodies used for western blot experiments..... 34

Table 2. Behavioral dysfunctions associated with altered proteins in chronically infected mice synaptosomes. P-values were determined by Fisher's exact test..... 58

Table 3. Neurological dysfunctions associated with altered proteins in chronically infected mice synaptosomes. P-values were determined by Fisher's exact test..... 59

Table 4. Summary of proteins strongly downregulated during chronic cerebral infection with *T. gondii* 64

Introduction

Toxoplasma gondii (*T. gondii*) is one of the most studied protozoan parasites world-wide due to its importance for human and veterinary medicine. Its versatility to infect a broad range of host cells and to successfully evade the host's immune control makes *T. gondii* an intriguing model to study different aspects of immunology, molecular biology as well as neuro-immunology. Moreover, its preferential tropism for the nervous system, in line with the recent studies correlating chronic toxoplasmosis with behavioral alterations in several host species, has turned attention towards potential neurobiological mechanisms by which *T. gondii* may alter brain functions.

1. Brief description of *T. gondii* - basic morphology and life cycle

T. gondii is a heteroxenous (requiring more than one host to complete its life cycle), polyxenous (capable of infecting more than one species), and obligate intracellular protozoan. It belongs to phylum *Apicomplexa*, class *Conoidasida*, order *Eucoccidiorida*. Like all members of *Apicomplexa* such as *Plasmodium* spec., *Babesia* spec. and others, *T. gondii* is a unicellular, spore-forming parasite and able to infect all warm-blooded animals including humans (1,2).

The first identification of the parasite was done in 1908 by Nicolle and Manceaux at the Pasteur Institute in Tunis (Tunisia) and in the same period by Splendore in Brazil. The name *Toxoplasma gondii* was proposed by Nicolle and Manceaux based on the morphology of the infectious stage (modern Latin. *toxos* = arc, bow; *plasma* = shape, form) and the host in which it was initially found, the rodent *Ctenodactylus gundi* (3,4). In the years following its discovery, the interest of the scientific community for *T. gondii* increased, *T. gondii*-like organisms were isolated from several hosts and culminated with the first isolate of viable *T. gondii* from a 3 day old infant presented with encephalomyelitis and retinitis (5–7).

The 1990s/2000s were marked by an increased volume of *Toxoplasma* research and a move further from basic parasitology into specialist areas such as immunology, genetics and molecular biology. Progressively, detailed reports on infections acquired during adulthood have called awareness on the susceptibility to toxoplasmosis of immunocompromised patients but also on the association between seropositivity and behavioral, personality and neuropsychiatric disorders in immunocompetent individuals (8–14).

There are three infectious stages of *T. gondii*: the tachyzoites, the bradyzoites (in tissue cysts) and the sporozoites (in oocysts) (15).

1.1. Tachyzoites

The term “tachyzoite” (Greek. *tachys*, fast; *zōon*, animal) describes the stage that rapidly replicates in any cell of the intermediate host and in the intestinal epithelial cells of the definitive host. The tachyzoite is approximately 2-6 µm long and 2-4 µm wide, with a pointed anterior (apical) end and a rounded posterior end (Figure 1) (15). The apical end is dominated by the conoid and the presence of complex organelles such as rhoptries and micronemes. Rhoptries are eight to ten club-shaped, unique secretory/excretory organelles found only in the *Apicomplexa*. The secreted proteins called rhoptry proteins (ROPs) have been shown to be the key molecules responsible for the virulence of different *T. gondii* strains (16–18). Tachyzoites invade host cells either actively by penetrating the host cell plasmalemma or passively by phagocytosis, and form a cytoplasmic vacuole where they start to replicate (15,19). Tachyzoites multiply asexually within the host cell by repeated endodyogeny, a specialized form of reproduction in which two progeny form within the parent parasite (15). The host cell ruptures when it can no longer support the growth of tachyzoites. The newly released tachyzoites will infect new host cells, spreading this way the infection.

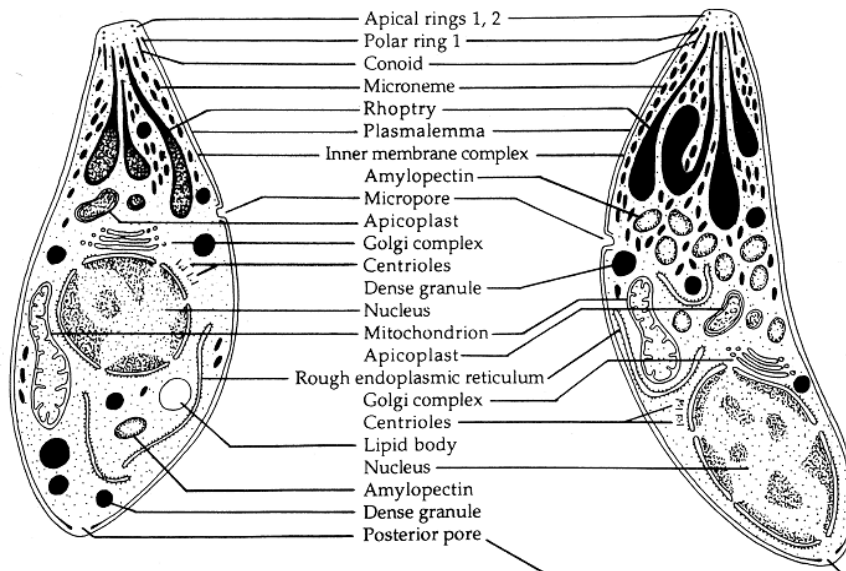


Figure 1. Schematic drawings of a tachyzoite (left) and a bradyzoite (right) of *T. gondii* (15)

1.2. Bradyzoites

The term bradyzoite (Greek. *brady*, slow; *zōon*, animal) was coined to describe the infectious stage in which *T. gondii* is multiplying slowly within a tissue cyst. The bradyzoite is crescentic or oval, each measuring approximately 7 by 1.5 μm in size. Structurally, bradyzoites differ only slightly from the tachyzoites. The nucleus is located towards the posterior end. The number of rhoptries is lower, as well as their secretory properties, in line with the less challenging survival needs of the bradyzoites (Figure 1) (15). Under the pressure of the host's immune response, tachyzoites are transformed into bradyzoites which are surrounded by a protective wall and give rise to tissue cyst (Figure 2) (20–22). The newly formed wall around the bradyzoites protects them from environmental conditions and the host's immune system allowing the slow multiplication by endodyogeny (15,21,23).

In the central nervous system (CNS), tissue cysts can be found in any cell type of brain and spinal cord parenchyma, are round-shaped and can reach a diameter of 50-70 μm (Figure 2) (15). In healthy, immunocompetent hosts, it is presumed that tissue cysts can survive life-long inside the host cells or it can be destroyed by the host's immune system. In immunocompromised individuals the cyst can rupture, the bradyzoites transform back into tachyzoites and cause recrudescence of infection (2,15,21).

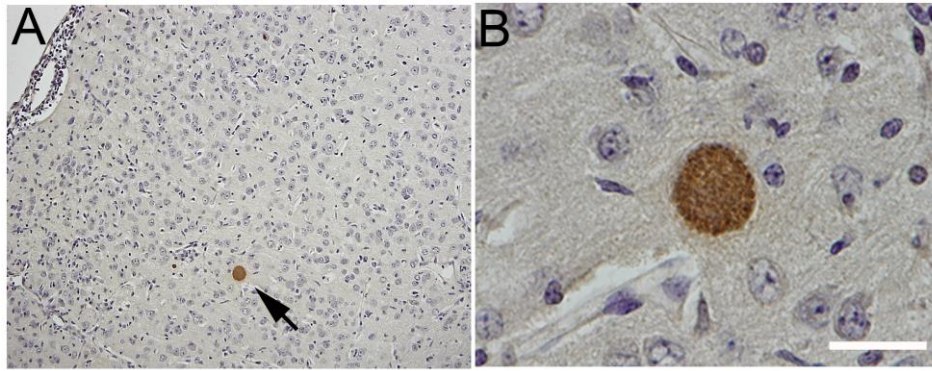


Figure 2. *T. gondii* tissue cyst

A) Immunohistological staining of a mouse brain chronically infected, depicting a *T. gondii* cyst (indicated by arrow) located in the cortex. B) Magnified view of the *T. gondii* cyst from A. Scale bar 100 μm .

1.3. Sporozoites

Sporozoites develop over the course of several days inside the oocysts that are shed by felids into the external environment. Moreover, sporozoites are morphologically similar to tachyzoites, 2 μm wide and 6-8 μm long, with a subterminal nucleus (15) and show the same infective capacity as tachyzoites being able to actively invade host cells (24,25).

1.4. Life cycle of *T. gondii*

Felids are the definitive host of *T. gondii* in which asexual reproduction (merogony) and sexual reproduction occur in the epithelial cells of the small intestine, leading to the production of unsporulated oocysts which are eliminated from the gut together with the feces. The maturation of the unsporulated oocysts towards infectious sporulated oocysts takes place in the environment, one to five days after being shed (Figure 3) (15,23,26). Infectious oocysts can contaminate soil, water or food sources and can remain infective for more than one year in unfrozen, moist soil (15,27). Intermediate hosts can be represented by any warm-blooded animal; however the first line is usually constituted by small prey like rodents and birds. The transmission is mainly horizontal, intermediary hosts become infected after ingestion of food or water containing the sporulated oocysts. After ingestion, the wall of the oocysts ruptures and the sporozoites invade the host's intestinal epithelial cells (24,25). Following the invasion of the epithelium the sporozoites transform into tachyzoites, which multiply and disseminate mostly via immune cells in all organs of the host, with a preferential tropism for the muscles,

the eye and the CNS. Once the tachyzoites reached their final destination tissues, under the pressure host's immune system, they go through stage conversion to become bradyzoites and give rise to tissue cysts (Figure 3) (21,23,28,29). Humans are considered to be accidental dead-end hosts with no significant contribution to the direct life cycle of the parasite. Nevertheless, they become readily infected by consuming oocysts contaminated water and vegetables or by eating raw/undercooked meat from previously contaminated farm animals (Figure 3) (2,28–30).

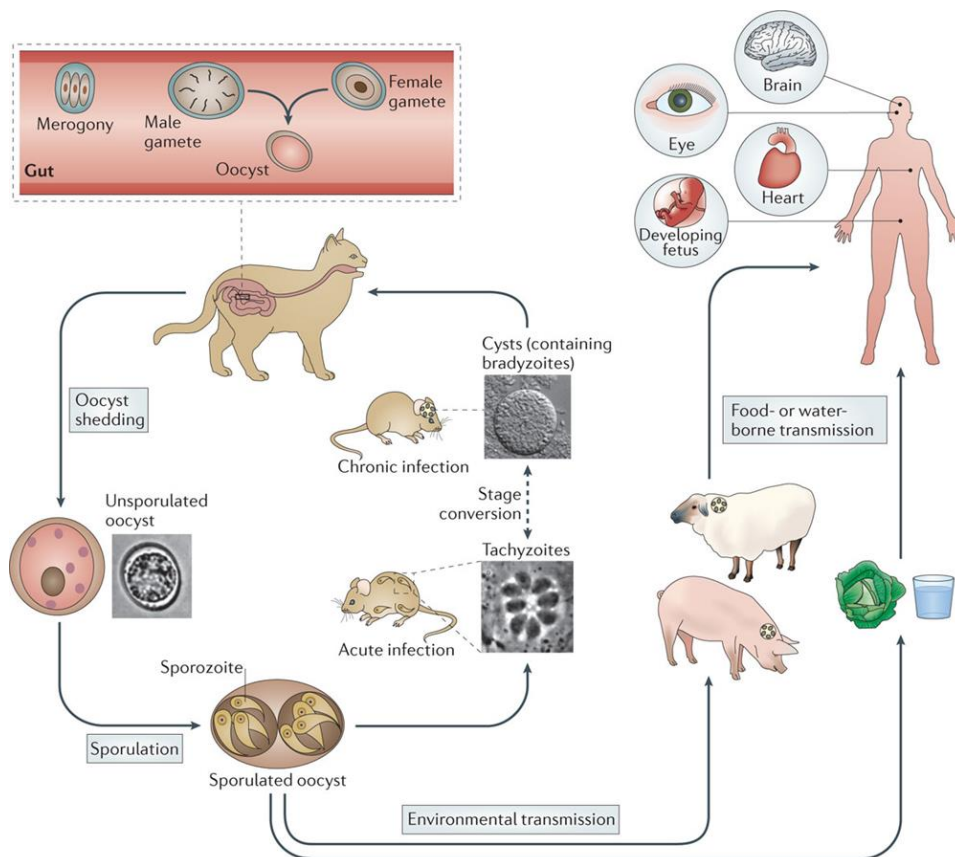


Figure 3. The complex life cycle of *Toxoplasma gondii* (29)

Cats are the definitive hosts in which sexual replication of *T. gondii* takes place. The fusion of gametes leads to the formation of sporozoites containing oocysts that are shed in cat faeces. Sporulated oocysts can contaminate food and water, providing a route of infection for intermediate hosts. In the intermediate host acute infection is characterized by tachyzoites that disseminate throughout the body. Differentiation to bradyzoites within tissue cysts leads to chronic infection. Humans become infected by eating undercooked meat containing tissue cysts or by ingesting sporulated oocysts in contaminated water or food.

2. Immune response and pathogenesis of *Toxoplasma gondii* infection

In immunocompetent individuals the protection against *T. gondii* infection is mainly controlled by complex mechanisms involving an intimate collaboration between innate and adaptive cell mediated immunity through the production of inflammatory cytokines and less by humoral immunity (29,31,32). In the natural parasitic life cycle, *T. gondii* infects its intermediary hosts by entering the small intestine epithelium following the ingestion of the tissue cysts or oocysts.

2.1. Immunopathogenesis of cerebral toxoplasmosis

Within the first 3-5 days post infection, in response to parasite recognition and invasion, enterocytes produce a set of chemoattractant and activating molecules, but also molecules with a direct antiparasitic activity, like nitric oxide (NO) (33–36).

Up to 7-10 days post infection, a massive infiltration of pro-inflammatory immune cells can be observed in the gut (37,38). Several lines of evidence indicate that neutrophils, macrophages, dendritic cells (DCs), CD11c⁺ and CD11b⁺ monocytes, and natural killer (NK) cells migrate in the intestinal parenchyma, attracted by chemokines and cytokines (38–41).

Although toxoplasmosis can be associated with multiorgan involvement (liver, heart, lung, lymph nodes, eye) the immune privileged brain is the most frequently affected organ. All cases of toxoplasmic encephalitis develop as a result of hematogenous spread. Several reports indicate that the parasite is able to home in the brain parenchyma as early as 7 days post infection, after crossing the blood-brain barrier (BBB) by a Trojan horse mechanism (39,42). This is achieved by actively infecting various types of immune cells such as neutrophils, monocytes and dendritic cells (39,43,44). Infected leukocytes are able to transport the parasites throughout the body as well as to provide protection against host immune defense (45,46). In return, the parasite has evolved a way to manipulate host apoptotic pathways, thus promoting the survival of both the parasite and the shuttle leukocyte (47,48). To favor dissemination to the brain, the parasite-host cell interaction not only allows the survival of both cells but may also alter the trafficking of the infected leukocytes as well as the expression of specific receptors and/or adhesion molecules to support the diapedesis (49–51).

A fundamental process in CNS toxoplasmosis is the activation of resident microglia and astrocytes in response to the early invasion of the brain extravascular space by tachyzoites

along with the infection of astrocytes, microglia and neurons. First signs of glia activation can be observed between 7-10 days post infection (52,53). Stimulation of resident glia is intimately associated with the recruitment of peripheral T cells and mononuclear cells resulting in the development of a T-cell mediated immune response during which interferon- γ (IFN- γ) is the key molecule in the control and elimination of the parasite (54–56).

T. gondii displays a differential invasive and developmental preference in neural cells in relation with the course of infection. Several studies have highlighted the ability of the parasite to infect a large number of astrocytes and microglia during the acute stage, in contrast with the low number of infected neurons (57–62). However, cysts were found to occur almost exclusively in neurons throughout chronic infection (63).

Early activation of microglia and astrocytes is a mandatory step in the initiation and development of immune defense mechanisms necessary for further effective control of the parasite multiplication. *In vitro* and *in vivo* experiments have shown that following infection glia cells can produce a plethora of chemokines and cytokines. For example, astrocytes and microglia produce monocyte chemoattractant protein-1 (MCP-1), inducible protein-10 (IP-10), macrophage inflammatory protein-1 (MIP-1 α and MIP-1 β) which are involved in recruiting peripheral leukocytes to the brain (64). Infection of neurons is also characterized by the production of chemokines and cytokines. *In vitro* experiments using neuron cell cultures have demonstrated that cells infected by *T. gondii* are able to produce interleukin-1 (IL-1), IL-6, MIP-1 α and MIP-1 β and thus, contribute to parasite control (65,66).

As previously mentioned, the recruitment of T cells and peripheral inflammatory leukocytes and activation of these cells towards the production of IFN- γ and tumor necrosis factor (TNF) is critical for triggering the effective control of the cerebral toxoplasmosis (54–56,67,68). The importance of a vigorous adaptive immune response directed against *T. gondii* during human infection is highlighted by the increased susceptibility of patients with primary or acquired defects in T cell function (14). Initiation of T cells responses requires that naïve CD4⁺ or CD8⁺ cells encounter antigen-presenting cells in conjunction with co-stimulatory and cytokine signals. During the early stages of infection CD4⁺ T cells initiate optimal B and CD8⁺ T cell responses, whereas the ability to control the later course of infection is mainly attributed to IFN- γ , or expression of CD40L which can activate effector mechanisms in other immune cells (69–76). CD8⁺ T cells are specialized to recognize and destroy infected cells,

thus manifesting an essential role in the initiation and regulation of parasite burden during the acute stages of infection (69). CD8⁺ T cells can control the disease through the perforin-mediated cytotoxicity of infected cells or by the production of IFN- γ (69,77).

IFN- γ conveys a signal through a surface IFN- γ receptor to activate signal transducer and activator of transcription 1 (STAT1). In response to STAT1 activity effector cells will enhance their microbicidal and microbistatic capacities by upregulation of nitric oxide (NO), reactive oxygen intermediates (ROIs), immunity-related p47 GTPases (IRGs) and p67 guanylate-binding proteins (GBPs) which are involved in parasite clearance (29,78–81). IRGs constitute a family of hydrolase enzymes which are able to attach to different membranes of the intracellular compartments, including the parasite vacuole, and can hydrolyze guanosine triphosphate, thus leading to rupture of the vacuole, and subsequent digestion of the parasite within the cytosol (78,82–84). Moreover, IFN- γ can induce the expression of certain genes implicated in the activation and maturation of several populations of immune cells (80).

One way for IFN- γ to mediate protective effects to control *T. gondii* is by inducing increased synthesis of nitric oxide (NO) (85,86). NO is produced by numerous cell types implicated in the immune response, especially by macrophages (87). Increased NO production is mediated by upregulated expression of the inducible NO synthase (iNOS) in response to secretion of pro-inflammatory cytokines during infection (85). Although during the early stages of infection, NO may limit parasite growth, it is mostly involved in the development of pathology (88,89). The specific mechanisms through which NO can interfere with parasite survival and replication includes inhibition of the parasite enzymatic activity and direct damage of the DNA (90). A second way for IFN- γ to mediate protection against *T. gondii* invasion is by stimulating the synthesis of toxic oxygen radicals by the DCs and macrophages (72,91). Involvement of ROIs in their antimicrobial activity was suggested since impairing the ability of the cells to generate oxygen intermediates inhibited toxoplasmaicidal activity by greater than 80% (92).

Other mechanisms triggered by IFN- γ additionally contributing to the control of the parasite replication and burden in the infected hosts are represented by intracellular iron deprivation (93) and tryptophan degradation (94). The production, by the infected host cell, of both iron and tryptophan is essential for the development of *T. gondii*, as the parasite is a natural iron and tryptophan auxotroph (93,95).

TNF is also required for an appropriate immune reaction against *T. gondii* infection. Several studies demonstrated that the blockage of this cytokine results in increased mortality approximately 3-4 weeks post infection and higher parasite burden despite having a functional IFN- γ response (96–98). TNF synergizes with IFN- γ to promote an anti-parasitic mechanisms in macrophages, mediated through the production of reactive oxygen and nitrogen intermediates (29,72,73,91,99). Macrophages are professional phagocytes and mediators of the host innate response. IFN- γ activated mouse macrophages acquire antimicrobial activity that is largely dependent on the production of TNF, reactive oxygen and nitrogen intermediates, which consequently leads to parasite damage (29,72,73,91,92,99). Monocytes are also required for resistance during toxoplasmosis. Recruited monocytes expressing CCR2, after emerging from the bone marrow, home to sites of inflammation in response to CCL2 enterocytes-produced chemokine. Monocytes exert their role to control the infection directly by the secretion of TNF and inducible NO synthase (iNOS) and indirectly by enhancing IFN- γ production of the CD4⁺ and CD8⁺ cells (29,40,41,100).

In humans, as well as in animal species the outcome of cerebral infection depends on the mode of infection, parasite strain, host's immune system status and host's genes (101). Primary toxoplasmosis with neurological symptoms in immunocompetent individuals is rare, and still rare is the presence of neuropathological changes. Microglial nodules containing the parasite or encysted forms are occasionally found in the brain of individuals deceased of other causes (102).

In rodents, the development of pathology is not caused by the replication of the parasite but rather by the overproduction of IL-12, IFN- γ , TNF and NO leading to a strong Th1 immune response (55,101,103). Histopathological features of toxoplasmic encephalitis associated with persistent neuroinflammation are widespread astrogliosis and the formation of microglial nodules. Moreover, high cellularity, due to peripheral inflammatory cells transmigration to the brain, the presence of single or paired cysts, parenchymal hemorrhage, edema and areas of necrosis can be observed. The inflammatory cells are organized in foci, not always surrounding the cysts, suggesting the involvement of soluble factors produced by the parasite (103–107).

3. Toxoplasmosis in Humans

The world-wide prevalence of *T. gondii* infection is estimated to 30-70% in human populations, although the seroprevalence varies markedly across different geographical regions and ethnic groups (1,2,108). Transmission incidence in the human population is mostly linked to hygiene and culinary habits, since the contamination may occur via ingestion of infectious oocysts from the environment, or tachyzoites and tissue cysts which are contained in animal tissues (1,2).

Toxoplasma infection can be categorized as congenital, acute, or chronic and each may be active or asymptomatic.

3.1. Congenital toxoplasmosis

Congenital toxoplasmosis implicates materno-fetal transmission via transplacental dissemination of the parasite. Early infection of the fetus results in fatal disease comprising hydrocephalus, retinal damage and intracranial calcifications. Infection at later stages of pregnancy might have long-term effects such as retino-choroiditis and impaired intellectual functions (2,109–112). Several lines of evidence indicated congenital exposure to *T. gondii* as a risk factor for developing schizophrenia spectrum disorders or other psychiatric abnormalities in young adults (113–115).

3.2. Acute toxoplasmosis

In individuals with intact immune systems, acute infection acquired after birth is usually asymptomatic or presents with mild flu-like symptoms. Rare complications associated with infection in the normal immune host include pneumonia, myocarditis, encephalopathy, pericarditis, polymyositis and ophthalmological lesions (116). Few cases of disorientation, anxiety and depression have been noted in patients with acute toxoplasmosis (117).

3.3. Chronic toxoplasmosis

Long-standing infection with *T. gondii* has generally been considered of little clinical consequence, however in the last years this dogma has been questioned by findings which raised awareness on the possible roles played by chronic toxoplasmosis in the etiology of different mental disorders ranging from behavioral and personality alterations to severe psychiatric disorders.

3.3.1. Cognitive, motor and personality alterations associated with *T. gondii* infection

First investigations into the potential effect of *T. gondii* on human behavior were performed in 1950s/1960s. Several groups reported a high prevalence of *T. gondii* infection in patients from institutions for mental disorders or in children manifesting changes of personality, slow learning capacities and low intelligence quotient (118). Although the authors could not confirm that altered mental and cognitive performance is definitely attributed to infection with *T. gondii*, these initial studies opened a venue for further investigations on the potential association between cognitive performance and parasitism.

In 2001, the first report on the potential impact of *T. gondii* on psychomotor performance was published (119). Using a standard computerized test on volunteer blood donors, infected and uninfected, the authors conclude that individuals with latent infection exhibited increased reaction times, scored more poorly at a standard computerized test and appeared to lose their concentration more quickly (119).

More recently, Beste *et al.* investigated the possible modulatory role of latent *T. gondii* infection on cognitive functions in elderly individuals (120). Based on a test measuring the goal-directed behavior differences between humans with latent toxoplasmosis and uninfected controls were detected. When confronted with an auditory deviant stimulus elderly individuals with positive immunoglobulin G (IgG) *T. gondii* serum concentrations revealed delaying processes of attentional allocation and disengagement (120).

Furthermore, the implications of the subtle alterations in psychomotor performance on the human behaviour were assessed. Association of *T. gondii* infection with delayed reaction and the impaired ability for long-term concentration may account for the observations from three independent groups indicating that individuals chronically infected with *T. gondii* had a two times higher risk of traffic accidents (10,12,121–123).

However, a recent study by Stock *et al.* revealed a paradoxical improvement of cognitive control processes in *T. gondii* infected healthy individuals, arguing therefore for a rather positive effect of infection on cognitive capacities than the commonly held view that latent infection is detrimental for the host (124,125).

Also of interest is the hypothesis that chronic toxoplasmosis can alter human personality profiles. Throughout various studies, Flegr *et al.* have administered personality questionnaires on several cohorts of university staff and students, military servicemen, blood donors, both men and women, and compared individuals with or without antibodies to *T. gondii* in order to identify correlations between chronic infection and personality traits (10,126–128).

Interestingly, the results revealed prominent gender differences in personality shift. Men were more likely to disregard rules, were more expedient, jealous, suspecting, loyal, stoic, low novelty seeking and dogmatic. By contrast, infected women were more rules bound, dutiful, warm, easy-going and out-going, conforming and moralistic. Both, men and women had higher guilt proneness (self-doubting, worried, self-blaming) than the uninfected individuals (10,126–128).

3.3.2. Association of latent *T. gondii* infection and psychiatric disorders

Perhaps of greatest interest is the proposal that chronic infection with *T. gondii* could exert a role in the etiology of certain psychiatric disorders in humans.

The most substantial body of evidence gathered to date relates to the potential association between *T. gondii* and some cases of schizophrenia. Schizophrenia is a chronic, neuropsychiatric disorder with a complex etiology and clinical symptomatology, that affects approximately 1% of the adult population (129). Several studies emphasized that schizophrenic patients have an increased incidence of *T. gondii* infection compared with control volunteers (114,130–133). The result of two independent meta-analyses of 38 and 42 studies, carried out in several countries, revealed that *T. gondii* seroprevalence was 2.7 times greater in schizophrenic individuals than in the general population (134,135). Moreover, other studies suggested that individuals with increased levels of *T. gondii* IgG antibodies (indicative of chronic infection) are at high risk of developing more severe symptoms of psychoses (136,137). Further evidence supporting a possible association between *T. gondii* and

schizophrenia/psychosis is shown by the ability of antipsychotic drugs (i.e haloperidol) to inhibit the growth of tachyzoites *in vitro* (138,139).

Increased incidence of seropositivity for *T. gondii* has also been reported in cases of major depression, bipolar disorders, obsessive-compulsive disorder (OCD), anxiety and panic disorders (140–143). Interestingly, OCD symptoms in individuals infected with *T. gondii* have been reduced by treatment of the infection alone (144). Depression is associated with self-directed violence and suicide. It is estimated that more than half of the individuals suffering from depression had a suicide attempt, making suicide the 10th leading cause of death worldwide (145,146). Several studies have identified a positive correlation between *T. gondii* infection and suicidal behavior. The first reports of a relationship between *T. gondii* infection and suicidal behavior were published in 2009 by Arling *et al.* and in 2010 by Yagmur *et al.*, which confirmed the association between *T. gondii* IgG, but not IgM antibodies (indicative of acute infection), and suicide attempts (146,147).

In addition to the links of *T. gondii* to schizophrenia, mood disorders and OCD, chronic infection with *T. gondii* has been suggested to be associated with Alzheimer's (148) and Parkinson's disease (149,150), autism spectrum disorders (151), Tourette's syndrome (152), epilepsy (153) and headaches (154,155).

Importantly, all reports mentioned above demonstrate that only a certain percent of the patients suffering from a neuropsychiatric disease have a chronic infection with *T. gondii* and not all immunocompetent individuals infected with *T. gondii* are at risk of presenting neurologic involvement. Therefore, no direct causal relation between the infection and psychiatric disorders could be established. Different theories discuss the genetic susceptibility, route of infection (tissue or oocytes), number of ingested parasites, and/or timing of infection (congenital, childhood or adulthood) as important factors in the development of neurological manifestations (13,125).

Overall, these studies suggest that *T. gondii* infection in humans may result in deviating behaviour and could have substantial health implications.

4. *Toxoplasma gondii* infection and animal behavior

Infection with *T. gondii* is highly prevalent in the rodent population, up to 35% of wild rats show serological evidence of exposure to the parasite (156). A number of studies have demonstrated that long-standing infection is associated with significant alteration in rodent behaviour. In 1980, Hutchinson *et al.* reported that infection with *T. gondii* in mice is associated with an increased amount of general movement but decreased rearing and digging (157). Similar results have been observed in wild or laboratory rats chronically infected with *T. gondii* (158–160). In addition to increased locomotor activity, infected rats display reduced neophobic behavior compared to uninfected ones (158). The definitive hosts of *T. gondii*, cats, are major predators of mice and rats. They show little interest in stationary objects, but are easily attracted to movement (161,162). It is presumed that increased exploratory activity and mobility of infected rodents will lead to increased predation thus, allowing the parasite to complete its life cycle.

Interestingly, new data indicate a more complex ability of *T. gondii* to manipulate the behavior of rodents in relation to predator-prey interactions. The infection not only reduced the instinctive aversion of rodents to cat odor, but instead attracted them (160,163–165). Furthermore, this behavioral adaptation might not be an epiphenomenon as it seems to be highly specific towards cat odour and not due to destruction of the olfactory regions of the brain or to altered anxiety-like behavior, learned fear and nonaverse learning (166,167).

Another recent study, which used an identical murine model of toxoplasmosis as implemented in our study, reported motor coordination and sensory deficits but normal cognition in infected mice which was associated with widespread parasite cysts and no specific tropism to a certain brain region (168). Contrary to previous findings, experiments conducted by Gatkowska *et al.* described reduced exploratory activity in *T. gondii* infected mice, however these behavioral changes were mainly pronounced in the acute stage (169).

In conclusion, all studies conducted in different experimental models indicate that certain behavioral changes occur upon acute and chronic *T. gondii* infection. However, the underlying neurobiological mechanisms by which *T. gondii* alters brain functions remain largely unclear.

5. Hypotheses for specific behavior changes in intermediate hosts

Research performed in the last years, mainly with animal models, has provided several hypotheses which may explain the behavioral and neuropsychiatric deficits. These rationales are mostly centered on the ability of the parasite to interfere with the survival and activity of the neurons it infects.

5.1. Cyst location in the CNS

The location of the cysts has been suggested to play an important role in the behavioral changes of the host. In rodents, parasite cysts were found to persist in many areas of the CNS, such as the olfactory bulbs, forebrain, cortex, striatum, amygdala, cerebellum and spinal cord (104,164,166,170–172). One report indicated a higher density of cysts in the amygdala of infected mice, proposing a possible explanation for the instinctual fear loss towards feline odor (166). Amygdala is a brain structure, which is part of the limbic system and involved in fear, memory and reward modulation (173,174). However, up to date most of the studies argue against the tropism of the cysts towards a specific brain region and question the effective manipulation of the host behaviour without a well targeted tropism of the parasite (172,175).

In humans, less information is available on the presence and location of cysts in individuals chronically infected with *T. gondii*. These studies mainly focused on immunocompromised hosts that suffered from reactivated toxoplasmosis (176–178). Conejero-Goldberg *et al.* have investigated the presence of *T. gondii* in the frontal cortex of postmortem specimens from 14 individuals with schizophrenia, 11 with other psychiatric diagnoses and 26 normal individuals. All specimens, from all individuals, were negative (179). The limited number of information could be due to the complications of accessing postmortem material as well as the effect of the methods used to process postmortem brain samples, which may destroy the *T. gondii* cysts.

5.2. *T. gondii* modulates dopamine production

One of the most appealing hypotheses to explain neuromodulatory effects of *T. gondii* infection is based on the capacity of the parasite cysts to disturb dopamine metabolism. In 2009, Gaskell *et al.* found two genes in the genome of *T. gondii*, which encode tyrosine hydroxylase, the rate-limiting molecule for dopamine synthesis (180). Interestingly, in 2011

Prandovszky *et al.* reported, using *in vitro* as well as *in vivo* approaches, that parasite cysts harbored inside neurons express tyrosine hydroxylase as well as dopamine (181). Moreover, there was a threefold increase in the amount of dopamine released in infected cells, compared to uninfected ones (181). These results lead to the hypothesis that excess of dopamine produced by the parasite could interfere with crucial brain functions (i.e. locomotion, cognition, memory, mood, learning, reward) directly influencing the behaviour of the intermediary host (182). In humans, dopamine and dopamine signaling pathway dysregulations have been associated with several neurodegenerative and psychiatric disorders like schizophrenia and Parkinson's disease (183–186). However, the information provided by the limited number of animal studies on this topic, are not conclusive and even contradictory (187,188).

5.3. *T. gondii* can functionally “silence” neurons

Recently, Haroon *et al.* reported that *T. gondii* tachyzoites directly modulate neuronal function by active manipulation of Ca^{2+} signaling upon glutamate stimulation, thus, leading to either hyper- or hypo-responsive neurons (164). Moreover, activity-dependent uptake of the potassium analogue thallium was decreased in neurons containing the cysts, implying an inhibited function of the neurons. All major structures of the neurons contained parasite antigens, thus the enlargement of the neurons itself may further contribute to the impaired neuronal activity. Importantly, both bradyzoites and tachyzoites functionally silenced infected neurons, which may contribute to the host's behavior changes (164).

5.4. Proteins injected by *T. gondii* can manipulate host cell

Two different studies described the capacity of *T. gondii* to inject ROPs into the cell it invades in order to intersect different host cell transcription factors and thus, impairing the capacity of the host to produce defensive molecules (189,190). Recently, another study presented evidence that *T. gondii* can actually inject ROPs in a large number of host cells without effectively invading the respective cells (191). Koshy *et al.* found that ROPs can manipulate the uninfected cells in a similar manner to infected cells. However, it is not clear if these proteins remain active for long term within the injected neurons. Although the study reveals a net effect of the injected effector proteins on host cell transcription factors (i.e STAT6) involved in immune response, no evidence of other functional and/or morphological dysregulations are provided. Nevertheless, these studies open a new direction for research

suggesting that cyst persistence in different brain regions is not mandatory to interfere with host behavior.

5.5. Persistent behavioral changes after parasite clearance

More recently, Ingram *et al.* (165) in a quest for unraveling the underlying mechanisms of the pathogen-mediated behavioral changes have explored the contribution of the three major clonal lineages of *T. gondii* to the loss of innate aversion of cat urine. Interestingly, they have used an attenuated Type I strain and provided evidence of sustained loss of aversion at times post infection when neither parasite nor ongoing brain inflammation were detectable (165). This suggests that the behavioral change could be due to a specific, hard-wired alteration in brain structure, which is generated early during infection and is independent of parasite presence. This finding casts doubt on hypotheses discussed above that cysts or dopamine can cause the behavioral changes associated with *T. gondii* infections.

It is worthy to highlight that behavioral alterations, in rodents as well as in humans, were also detected upon other parasitic infections, such as *Heligmosomoides polygyrus*, *Toxocara canis* or *Eimeria vermiformis* (192–195). Importantly, these parasites do not directly infect the CNS, suggesting an even more complex peripheral or apparently global, indirect, neuromodulatory effect rather than direct alterations of neuronal function.

6. Neuroplasticity and neuroinflammation

Expression of behavior or mental illness is directly regulated by biological functions of the brain. Physiologically, the function of the brain is to exert centralized control over the other organs of the body and to adaptively integrate the body to the broad environmental conditions.

6.1. Overview on neuronal anatomy and plasticity

Neurons represent the morphological and functional units of the brain. The brain contains between one billion and one trillion neurons, depending on the species. The functional property that makes neurons unique is their ability to send high-speed electrical signals to specific target cells over long distances (196). The neuron consists of a cell body containing the nucleus, cytoplasm, and an electrically excitable output fiber, the axon, which projects to variable distances to other neurons (i.e. from a cortical pyramidal neuron to adjacent cortical neurons, or to spinal cord motoneurons) (Figure 4, left panel) (196). Many axons are covered with a layered insulating myelin sheath, made of specialized glia cells, which speeds the transmission of electrical signals along the axon. Most of the space in the brain is occupied by axons, which are bundled together in what are called nerve fiber tracts. All nerve fiber tracts create a complex map of neural connections or the brain wiring diagram (196).

Additionally, neurons have a number of other, generally shorter projections like the branches of a tree, called dendrites. Their function is associated with the reception of signals from other neurons. The interneuronal communication takes place at the level of dendritic spines, which are membranous protrusions from the neuronal surface located mostly on dendrites. The spine is a structure specialized for synaptic transmission (Figure 4, middle panel) (196,197). Synapses (Greek. *synaptein*, to clasp together) are key functional contact points where one neuron communicates with another. Synapses can be of two types: chemical or electrical. In a chemical synapse, the electrical signal of the presynaptic neuron is converted into the release chemicals called neurotransmitter (such as glutamate, γ -aminobutyric acid (GABA), dopamine, serotonin), which further bind to receptors located on the postsynaptic neuron (like α -amino-3-hydroxy-5-methyl-4-isoxazolepropionic acid (AMPA) or N-methyl-D-aspartate (NMDA) receptor). In turn, this triggers an electrical response or a second messenger pathway that may inhibit or activate the postsynaptic cell. In an electric synapse, the presynaptic and postsynaptic cell membranes are connected by special channels called gap junctions that are capable of passing electric current (196). As mentioned, a synapse has a pre- and a post-

synaptic compartment. The presynaptic site contains complex molecular machinery dedicated to neurotransmitter transport, packing into vesicles, release and re-uptake. The postsynaptic element is represented by the postsynaptic density (PSD), a membrane associated disc of electron dense material consisting of receptors, channels and signaling systems (Figure 4, right panel) (196,197).

Any alterations in the synaptic compartments trigger changes of the strength or efficacy of synaptic transmission at preexisting synapses, a concept termed synaptic plasticity (198). This is a dynamic and continuous process, which takes place in response to experiences (like learning, thinking, emotions) or environment. Long-term, persistent experiences or bodily injury can have an impact not only at the cellular level, but can lead to large-scale neuroplasticity changes, involved in brain remapping of neural connections (199,200).

The study of structural connectivity and neuroplasticity originates from the fact that function and structure of the brain are intricately linked (196,197). Investigation of the brain structural changes to better understand the functional output can be achieved at different levels of scale. At the macroscopical level the only methodology providing a global *in vivo* noninvasive window into the brain is Magnetic Resonance Imaging (MRI), and especially diffusion tensor (DT)-MRI and consecutive fiber tractography (201–205). Mapping of the neuroplasticity on a neuron-by-neuron level, currently, cannot be accomplished with noninvasive imaging techniques, requiring post-mortem microscopic analysis of limited portions of brain tissue (206,207).

6.2. The impact of neuroinflammation on neuroconnectivity

Inflammation is a response of the immune system that aims to protect and defend living tissues. Triggers can be represented by aseptic (i.e. traumatic injury) or septic (such as bacterial, viral or parasite pathogens) insults. The attribute of inflammation is the mobilization and interaction of several cell types and molecules, resulting in a response that is both local and systemic (208,209). Classically, the CNS has been considered to be immune-privileged, because, within its boundaries, there is an absence of the typical immune response as seen in the periphery (210). However, recent evidence indicates a complex neuroimmune crosstalk which is essential for brain homeostasis (211,212). Several hypotheses have proposed that CNS injury is associated with abnormal expression of immune mediators, thus

neuroinflammation, which might result in synaptic impairment and in subsequent destabilization of neuronal networks (213,214).

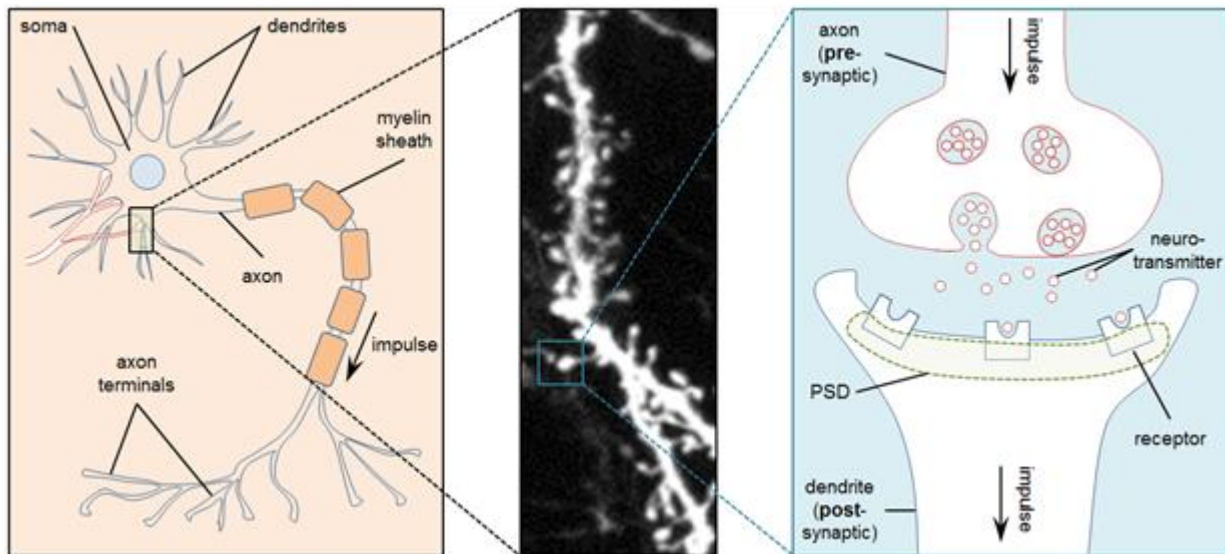


Figure 4. Schematic description of a neuron and a synapse

Illustration of a neuron showing the major structural components (left panel), a detailed view of a dendrite and dendritic spines (middle panel) and the diagram of a synapse (right panel). When electrical signals reach the end of the axon, they trigger the release of neurotransmitters that are stored in vesicles. Neurotransmitters bind to receptor molecules that are present on the dendrites of adjacent neurons. These receptors act as on and off switches for the next cell. Abbreviation: PSD, postsynaptic density.

6.2.1. Central neuroinflammation

In addition to the local, relatively limited functional effects of *T. gondii* cysts on neurons, as discussed above, the hallmark of chronic infection is the permanent activation of resident glia cells throughout the whole CNS and the recruitment of peripheral immune cells (53,74,215). This prolonged neuroinflammation is able to directly influence a large number of neurons located in various neuroanatomical areas (213,216,217). Data obtained from studies using animal models indicate that, once the CNS is invaded by *T. gondii*, resident cells as well as recruited immune cells induce a chronic neuroinflammatory milieu characterized by the predominance of Th1-type (IFN- γ , IL-12, IL-1, IL-6, TNF) immune responses (55,101,103). In the last years, research focused on the impact of the broad range of immune responses of the CNS on human behavior and neuropsychiatric morbi has received increasing attention

(209,214,218). These studies have revealed that patients diagnosed with major depression, obsessive-compulsive disorders, and schizophrenia show increased biomarkers of inflammation such as IFN- γ , IL-12, IL-1, IL-6 and TNF (218–221).

Chronic neuroinflammation following acquired infection with *T. gondii* in immunocompetent intermediate hosts can potentially elicit behavioral alterations and neurological disorders by triggering subtle alterations in the morphology and functionality of neurons. A considerable body of evidence indicates that neuropsychiatric disorders, such as schizophrenia, might not be the result of focal brain abnormalities but rather the consequence of pathological interactions between several brain regions leading to abnormal integration of brain functions (222–225). Deficits in interregional functional coupling can arise from impairments of neuroconnectivity due to changes in morphology/distribution of dendritic spines, alterations of the synaptic plasticity (i.e. composition of some receptors and their subunits) or white matter structural abnormalities (222,226–229).

Interestingly, in a recent study, Horacek *et al.* have assessed by voxel-based morphometry MRI the changes in the volume of the brain cortex of schizophrenic individuals, with or without IgG against *T. gondii* (230). They report that schizophrenic patients chronically infected with *T. gondii* had significant reductions in grey matter volume of several cortical regions as compared with the noninfected patients (230). The anatomic substrate of the grey matter volume reduction indicated impairments of neuropil and structural connectivity; however, the precise nature of the impairments was not investigated, representing a significant omission.

6.2.2. Neuroinflammation via peripheral mediators

Immune signals from the systemic milieu are able to initiate neuroinflammatory processes, which in turn can cause or accelerate dysfunctions in synaptic plasticity, neurotransmitters and their receptors, and neuronal circuitry (Figure 5) (214,231,232). The importance of peripheral immune mediators in the pathophysiology of brain disorders has been documented for schizophrenia, major depression, Alzheimer's disease, Huntington's disease, stroke and traumatic brain injury (214,232,233). Similarly to the case of other pathogens known to alter host's behavior (192,193,195), it is likely that neuroinflammation can be induced not only following the invasion of the neural parenchyma by the parasite but also by peripheral immune stimuli. Before reaching the CNS, within the first 3-5 days post infection, *T. gondii*

triggers systemic inflammation, in response to parasite recognition and invasion, which is initiated in the intestine. Thus, the systemic inflammatory milieu also can lead to local or global disruptions of neuronal physiology and neuroconnectivity (29,35,234–236).

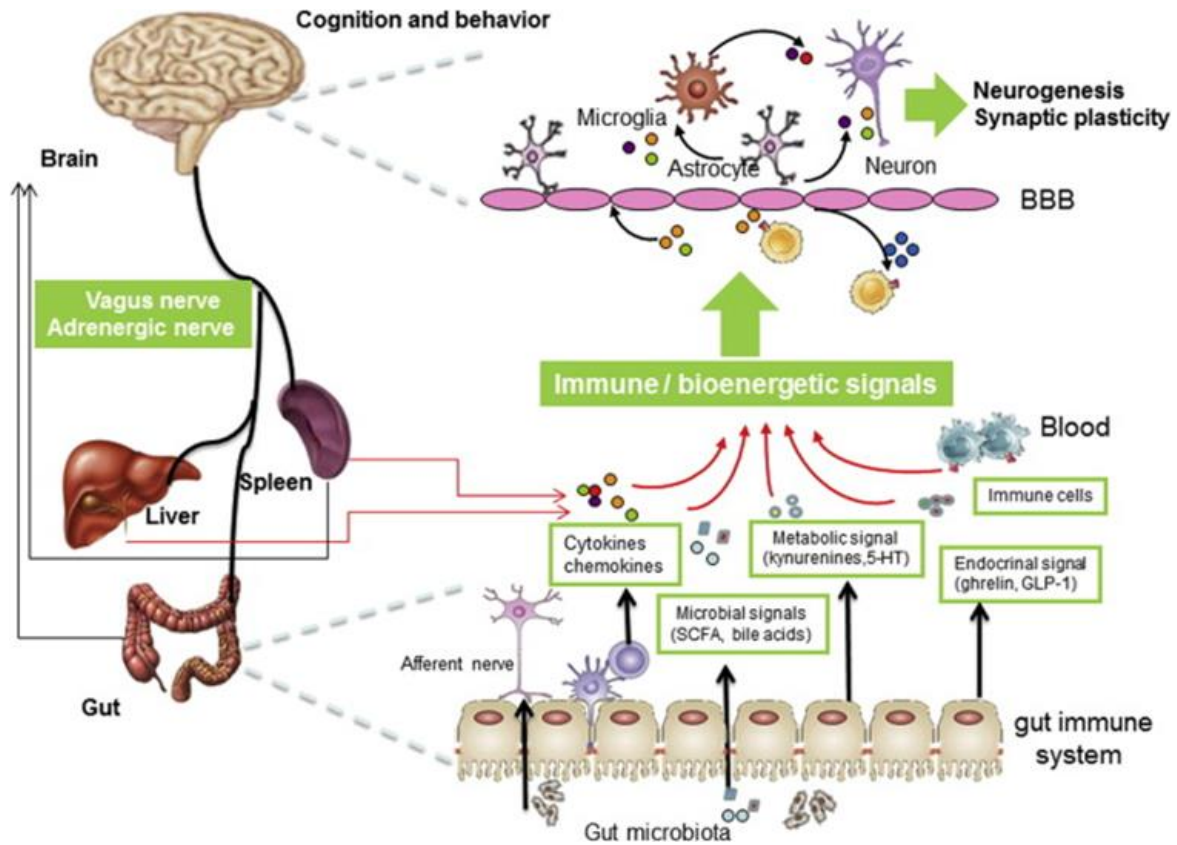


Figure 5. Schematic illustration of the brain-periphery crosstalk pathway in the regulation of neuroplasticity (232)

One essential pathway is the neural route, which is achieved through the vagal or adrenergic innervation of distant organs. Another important pathway is via the blood, where circulating immune signals (e.g., cytokines, chemokines and immune cells) and bioenergetic signals (e.g., endogenous metabolites, microbial products and hormones) cross the BBB and exert a systemic impact on the brain microenvironment. These intricate links play a profound role in the regulation of neurogenesis and synaptic plasticity. Abbreviations: BBB, blood–brain barrier; 5-HT, serotonin; SCFA, short chain fatty acid; GLP-1, glucocan-like peptide 1.

Aims

Studies carried out in recent years emphasized a possible association between chronic infection with *T. gondii* and certain psychiatric disorders and behavioral perturbations (10,125,133,146,166). However, little is known about the underlying neurobiological mechanisms by which *T. gondii* might trigger certain neuropsychiatric illnesses.

Evidence is accumulating for neuro-immune mediated interactions that could contribute to psychiatric disorders (218,237). Furthermore, recent data indicates that psychiatric disorders might be the consequence of abnormal integration of brain functions (222–225). Deficits in functional coupling can arise from impairments of neuroplasticity due to changes in morphology/distribution of dendritic spines, alterations of the synaptic plasticity or white matter abnormalities (222,226–229).

The hallmark of persistent *T. gondii* infection is permanent resident glia cell activation in the CNS and production of a plethora of chemokines and cytokines (55,56). Neuroinflammation can distinctively influence neuronal morphology and functions (216–218,238). Therefore, it is tempting to speculate that *T. gondii* infection could trigger such impairments of neuroplasticity.

The aim of this thesis was to address the hypothesis that latent *T. gondii* infection leads to defective neuroplasticity in a murine model of toxoplasmosis. The detailed objectives were:

1) To study the impact of chronic infection with *T. gondii* on murine brain connectivity blueprints. To this end, we first investigated the distribution of *T. gondii*-induced lesions by MRI. *In vivo* imaging analysis, using diffusion-tensor MRI and a fiber-tracking methodology, corroborated with histopathological investigations, allowed us to investigate neuronal fiber density and fiber connectivity alterations.

2) To examine the effect of chronic infection with *T. gondii* on the structure of individual, noninfected neurons. Therefore, by using DiOlistic labeling on fixed acute brain slices, we performed detailed analysis of the dendritic morphology of mature pyramidal neurons. Additionally, we investigated if dendritic spine density and morphology in noninfected neurons were impacted by infection.

3) To investigate the role of chronic infection with *T. gondii* on the integrity and functionality of synapses. Dendritic spines abnormalities predict changes in the information trafficking between neurons. To reveal the biology associated with synaptic plasticity, we explored the synaptoproteome by mass spectrometry analysis. Additionally, we measured, by western blot, the expression level of several proteins that regulate key synaptic functions.

Materials and Methods

1. Animals and *T. gondii* infection

All animal experiments were approved, according to German and European legislation by the Landesverwaltungsamt Halle (Sachsen-Anhalt, Germany, approval number IMMB/G/01-1089/11). Experiments were conducted with adult C57BL/6 female mice (8 weeks old, purchased from Janvier). Mice were housed in standard lighting conditions (12:12 h light-dark cycle) and temperature (21-23°C), 4 to 5 animals per cage, with food and water *ad libitum*.

T. gondii cysts of the ME49 type II strain were used for this study. Parasites were harvested from mice of NMRI strain, infected with *T. gondii* cysts 4 to 5 months earlier. Brains were isolated from infected mice and dispersed in 1 mL sterile phosphate buffered saline (PBS) by mechanically disrupting the tissue followed by several passages through needles with regressing diameter.

Cysts were counted using a light microscope in 10 µl of the brain suspension and the total number of cysts per brain was calculated. Three cysts were administered intra peritoneal (i.p.) into mice in a total volume of 200 µL/mouse. Control (noninfected) mice were mock infected with sterile PBS.

2. *In vivo* Magnetic Resonance Imaging

This work was done in collaboration with Dr. Laura Adela Harsan and Dr. Dominik von Elverfeldt from Department of Radiology, Medical Physics, Animal Molecular Imaging Research Center, University Medical Center, Freiburg, Germany (201,203,239).

Mouse brain MR Imaging was performed on seven infected mice (week 8 p.i.) and nine control mice using a 9.4 T (Tesla) small bore animal scanner, equipped with a BGA12S gradient system capable of 675mT/m (Biospec 94/20, Bruker, Germany). A transmit/receive 1H mouse quadrature birdcage resonator (35 mm inner diameter) and the ParaVision 5 software interface were also used for the acquisition of the MR signal. All imaging procedures were carried-out under isoflurane (3% for induction and ~1.5% for maintenance) mixed with oxygen (1l/min) anesthesia and using respiratory gating.

2.1. Data acquisition

Prior any brain imaging, the magnetic field homogeneity was optimized by performing a localized shimming procedure on a volume of interest ($4.8 \times 5.3 \times 9 \text{ mm}^3$), selected inside the mouse brain on the localizer images. This step of the MRI protocol was designed to correct the distortions and signal intensity dropout caused by local susceptibility differences between adjacent structures (particularly observed in border regions). For this optimization, we used the press waterline spectroscopy protocol as well as FastMap procedures provided with the Bruker ParaVision 5 system.

Morphological T2*- and T2-weighted imaging

A FLASH 2D sequence was used for T2*-weighted imaging of the whole mouse brain in 31 contiguous axial slices, acquired with a $78 \times 78 \times 500 \text{ }\mu\text{m}^3$ imaging resolution (TR/TE = 920/12 ms, flip angle = 60° , 2 signal averages). Acquisition time: 7m52s. RARE T2-weighted imaging was performed with the same slice geometry and resolution as described for T2*-imaging, using the following parameters: TR/TE = 3675/20 ms, RARE factor = 4 and 4 signal averages, acquisition time: 15m40s.

Diffusion Tensor-MRI (DT-MRI)

Diffusion MRI data was acquired in 31 axial 500- μm slices, with the same orientation as for the previous T2*- and T2-weighted scans, using a 4-shot DT-EPI sequence [repetition time,

7750 ms; echo time, 20 ms; time (Δ) between the application of diffusion gradient pulses, 14 ms; diffusion gradient duration (\square), 7 ms]. The acquisition protocol was adapted for using diffusion-sensitizing gradients applied along 45 isotropic directions of three-dimensional space, with a b factor of 1000 s/mm². Six averages were acquired to increase the signal to noise ratio (SNR). The in-plane image resolution was 156 x 156 μm at a field of view (FOV) of 20 x 20 mm and an acquisition matrix of 128 x 92. Partial Fourier with an acceleration factor of 1.35 and 31 over scan lines were used. Off resonance artifacts were eliminated by using a fat suppression module (1.9 ms Gaussian pulse, 1400 Hz bandwidth, 2 ms spoiler). The resulting total imaging time for the T2*-weighted, T2-weighted and DT-MRI was ~2h20m for each animal (~24 min for T2*- and T2-weighted images, ~ 115 min for DT-MRI acquisition – with respiratory gating) slightly varying depending on the respiratory rhythm of each animal.

2.2. Data post-processing

DT-MRI data post-processing including tensor calculation, generation of parametric maps (fractional anisotropy - FA, mean diffusivity $\langle D \rangle$, radial - D^\perp and axial - D^\parallel diffusivities) and fiber tracking was performed using a FiberTool package developed in-house. (http://www.uniklinik-freiburg.de/mr/live/arbeitsgruppen/diffusion/fibertools_en.html).

A global fiber tracking approach was employed to define the large scale mouse brain connectivity networks (201). The global tracking algorithm reconstructed all fiber bundles simultaneously, for the whole brain, without the requirement of defining seed or target regions (203). The results were used for generating mouse brain fiber density maps (FD) as well as highly resolved spatial histograms of diffusion orientations – here named high resolution fiber maps (hrFM). hrFM were tailored to increase eight times the native imaging resolution of the diffusion data, reaching a spatial resolution of 19.5 x 19.5 x 62.5 μm^3 . We used a reconstruction approach previously described by Harsan *et al.* (201) and another group (240).

Quantitative comparison of *T. gondii* vs. control group

Spatial normalization of the mouse brain parametric maps generated from the diffusion data (including FA and FD maps) and the morphological T2*- and T2-weighted images was performed using Matlab-script that registered the brain maps from all investigated animals on a previously created mouse brain template. Group (toxoplasma vs. control group) averaged

maps of FA, FD, $\langle D \rangle$, D^\perp and D^\parallel were created and used for quantitative group comparison. White matter (WM), gray matter (GM) and cerebro-spinal fluid (CSF) masks were generated using the T2-weighted images and used as regions of interest. An additional region of interest, the somatosensory cortex (SSC) was included in the quantification and was manually selected based on mouse brain atlas guidelines (241).

3. Histopathological analysis

Mice were initially anesthetized by intra peritoneal injection of Ketamine-Xylazine (100 mg/kg ketamine, 5 mg/kg xylazine) and then perfused transcardially with ice cold 4% paraformaldehyde (PFA). For histopathological investigation control and *T. gondii* infected brains were immediately removed from the skull and placed in 4% PFA at 4°C. Brain samples were then dehydrated in xylol, embedded in paraffin and sectioned coronally at 5 μm with a Leica microtome. To evaluate the lesions observed by T2*-weighted MRI sequence, a classical examination was performed with hematoxylin and eosin (H&E).

Moreover, immunohistochemical analysis was performed using primary antibodies against ionized calcium binding adaptor molecule 1 (Iba1, 1: 250 Dako, Denmark) to label microglia, CD3 (1:150, Dako, Denmark) to label infiltrating T lymphocytes, CD11b (1: 200, Abcam, UK) to label infiltrating monocyte derived macrophages, glial-fibrillary acidic protein (GFAP, 1: 200, Abcam, UK) to label astrocytes, Cleaved Caspase-3 (Asp175, 1:200, Cell Signaling, USA) to label apoptotic cells and anti-Toxo (1:200, Dianova, Germany) to label *T. gondii* cysts.

A Zeiss (Carl Zeiss, Germany) microscope equipped with an AxioCam HRc 3 digital camera and AxioVision 4 Software were used to obtain images. A minimum of 6 region-matched coronal slices were analysed for each brain. In the anatomical brain regions where the parasite was found the following pathological processes were analysed: necrosis, hemorrhage, edema, astrogliosis, cellular death and inflammation.

4. Immunofluorescence

For immunofluorescence and Fluoro-Jade B, control and *T. gondii* infected brains were immediately removed from the skull and placed in 4% PFA at 4°C for several days. Each brain was sectioned coronally (18µm) using a Leica cryostat (C 3050, Wetzlar, Germany). Free floating tissue sections were stored in cryoprotection medium (30% glycerol and 30% ethylene glycol) at -20°C until required. The immunofluorescence procedure followed similar steps for all tested markers. Coronal sections were routinely prepared and rinsed in 0.1 M PBS, pH 7.4.

Brain slices were first treated with 0.25% Triton X-100 in PBS for 30 minutes at room temperature (RT), followed by incubation in 10% normal goat serum (100µl/mL, Vector Laboratories, USA) and 0.25% Triton X-100 in PBS for 30 minutes. Immunolabeling with a mouse anti-pan-neuronal neurofilament (1:800, clone SMI311, Millipore, Calbiochem, USA) and rabbit anti-microtubule associated protein (1:50, MAP2, Cell Signaling, USA) antibodies was performed overnight at 4°C, to detect alterations in dendritic and axonal structure.

Tissue sections were incubated with appropriate (anti-rabbit/anti-mouse) AlexaFluor 488/594 secondary antibody (1:200, Invitrogen, Germany), for 1.5 hours at RT and protected from light. Sections were rinsed in PBS (two times for 20 minutes), and mounted on 1% gelatin coated glass slides with ProLong Gold antifade medium with DAPI (Invitrogen, Germany). A Zeiss (Carl Zeiss, Germany) microscope equipped with an AxioCam HRc 3 digital camera and AxioVision 4 Software were used to obtain images. A minimum of 6 region-matched coronal slices were analysed for each brain. Brain areas were assigned according to a mouse stereotaxic atlas (241).

5. Fluoro-JadeB staining

To specifically assess neurodegeneration induced by chronic *T. gondii* infection, Fluoro-Jade B (Millipore, Chemicon, USA) staining was performed according to the manufacturer's indications with slight modifications. Sections were immersed in 100% ethanol for 5 minutes followed by 70% ethanol (2 minutes) and distilled water (2 minutes). The rehydration step was followed by incubation in 0.06% potassium permanganate (15 minutes), then rinsed in dH₂O (1 minute) and transferred for 30 minutes in 0.0004% FluoroJade B solution in the dark. Finally, the sections were rinsed three times in distilled water for 1 minute per change, air dried, cleared by immersion in Roti-Histol (Roth, Germany), (2 minutes) before coverslipping with DPX (Fluka, Milwaukee WI). On average 4 region-matched coronal sections were analysed for each brain.

6. Electron microscopy

This work was done in collaboration with Prof. Dr. Christian Mawrin from the Institute of Neuropathology, Otto-von-Guericke University, Magdeburg, Germany (242,243).

Coronal brain slides (150-200 μ m), corresponding to middle third of the cerebrum, including SSC, were cut immediately after perfusion and fixed in phosphate-buffered glutaraldehyde (3%), followed by embedding in epon. Prior to trimming, toluidine-blue stained sections (500 nm thickness) were evaluated for the optimum area for electron microscopic examination. Ultrathin section (50 nm) were cut using a Leica Ultracut device, mounted on copper grids and stained with lead citrate solution for contrast enhancement. Sections were evaluated on a Zeiss-EM 900 electron microscope.

7. DiOlistics and morphological analysis

This work was done in collaboration with Prof. Dr. Martin Korte, Dr. Marta Zagrebelsky and Marianna Weller from Zoological Institute, Division of Cellular Neurobiology, University of Braunschweig, Germany (206,207).

Hippocampal neurons from C57Bl/6 control and *T. gondii* infected mice were labeled, 8 weeks post-infection, using DiOlistic on fixed acute slices (206,207). Briefly, the mice were anesthetized and perfused transcardially with 30 ml of 4% paraformaldehyde and 4% sucrose in 0.1 M PBS. The brains were immediately dissected and postfixed in the same solution for 30 minutes at 4°C. Further, the brains were embedded into 2% agar in phosphate buffered saline, cut in 400 µm thick coronal sections with a vibratome (Leica VT 1000 S).

Tungsten particles (50 mg; 1.7 µm in diameter; Bio-Rad) were mixed with 100 µl of dye solution (3 mg DiI, Invitrogen in 100 µl of methylene-chloride, Sigma-Aldrich), dried and suspended in 3 ml distilled water. The dye solution was sonicated, diluted 1:80 and used to coat the inside of a TEZFEFEL tubing (Bio-Rad). Dye-coated particles were delivered to the acute slices using a hand-held gene gun (Bio-Rad; Helios Gene Gun System) with a pressure of 120 psi. A membrane filter (3 µm; Millipore) was inserted between the gene gun and the slice to prevent clusters of particles from landing on the tissue. After shooting, the slices were kept in PBS for 6 hours at room temperature (RT) to allow dye diffusion. The slices were stained with DAPI (4',6-diamidino-2-phenylindole, AppliChem), washed, and mounted using an antifading water-based mounting medium (Biomeda).

The neurons were imaged with an Axioplan 2 imaging microscope (Zeiss) equipped with an ApoTome module (Zeiss). Each neuron was first imaged with a 20x objective (0.8 N.A., Zeiss) with a z-sectioning of 1 µm. Morphological reconstruction of the neurons and their process was achieved with the NeuroLucida software (MicroBrightField). Dendritic complexity and length of the dendrites were analysed with the Neuroexplorer software (MicroBrightField). The cells were analysed up to a distance of 160 µm for DG, 200 µm for apical CA1 apical and Cortex Layer II/III and 150 µm for basal CA1 and Cortex Layer II/III, to ensure that only completely labeled dendrites were included in the analysis. Moreover, spine density, length and spine head width were measured separately for apical and basal dendrites. For that, the images of dendrite stretches, from the apical and basal compartments,

were acquired using a Leica SP2 confocal microscope with a 63× objective. The number of spines was normalized per micrometer of dendritic length.

The data obtained were compared between the two different experimental conditions using a two-tailed Student t test. Asterisks indicate the significance levels as follows: *p <0.05; **p <0.01.

8. Synaptic junction preparation

Highly purified synaptic junction proteins fractions were prepared according to a previously published protocol by Smalla *et al.* (244). Briefly, 8 weeks post-infection, animals were sacrificed by transcardially perfusion with ice cold PBS. For each individual mouse both, left and right, hippocampi together with somatosensory cortices were dissected on ice and stored at -80°C until further used.

For subcellular fractionation, samples were homogenized in buffer A (10 mL/g tissue) containing 5 mM HEPES buffer pH 7.4 in a 0.32 M sucrose solution and protease inhibitor cocktail (Complete Mini, Roche, Germany). All centrifugation steps were performed at 4°C. Homogenates were centrifuged two times at 1000 g for 10 min. Supernatants were collected and subjected to another two additional centrifugation steps at 12000 g for 20 min to obtain the P2' pellet (crude membrane fraction). The P2' pellet was homogenized in buffer B (1.5 mL/g tissue; containing 0.32 M sucrose, 5 mM Tris pH 8.1, supplemented with protease inhibitors), loaded on a 0.85 M/1.0 M/1.2 M sucrose step gradient and centrifuged at 85000 g for 2 hours. Synaptosomes fraction was collected at the 1.0 M/1.2 M sucrose interphase, subjected to hypo-osmotic shock by adding 5 volumes of 1 mM Tris/HCl pH 8.1 for 30 minutes and then spun down at 32000 g for another 30 minutes. After centrifugation, solubilized P3 pellets (synaptosomal membranes) were applied to a discontinuous sucrose gradient (1.0M/1.2 M) and subjected to ultracentrifugation at 85000 g for 2 h.

The synaptic junctions were collected at the interphase between 1.0 and 1.2 M sucrose and stored at -80°C until further used for western blot experiments. Protein content was determined using the Bicinchoninic Acid protein assay kit (Pierce, Rockford) (according to manufacturer's indications). Briefly, samples were mixed with the BCA working reagents and incubated for 30 min at 37°C. Absorbance was measured at 562 nm, for each sample the

protein concentration was determined by comparison with a bovine serum albumin standard curve.

9. Western Blot analysis

Except the subcellular fractionation to obtain the synaptic junction proteins the rest of the western blot analysis was performed with whole brain homogenates. The protein extraction procedure is described further.

For each individual brain, the hippocampus and the ipsilateral cortex from control and *T. gondii* infected mice were dissected as previously described (245,246) and stored at -80°C until further required. Prior to use, samples were mechanically homogenized at 4°C in TBS/TX buffer (150mM NaCl, 1% Triton X, 50mM Tris, pH 8.0) containing a protease inhibitor (Complete Mini, Roche, Germany) and a phosphatase inhibitor cocktail (PhosSTOP, Roche, Germany). The homogenates were subsequently centrifuged (18000 rpm, 15 min, 4°C) and the supernatant was removed and stored at -80°C until further use. Protein content was determined using the Bicinchoninic Acid protein assay kit (Pierce, Rockford) (according to manufacturer's indications).

Samples containing equal amounts of total protein (10.0 µg), were separated on 10% SDS-polyacrylamide gels and transferred to polyvinylidene fluoride membranes using a semi-dry blotting system (detail). The membranes were soaked in TBS-T solution (0.1% Tween-20, 0.8% NaCl, 20mM Tris, pH 7.5) containing 5% nonfat dry milk or 5% bovine serum albumin, for 1 h at RT, followed by incubation with appropriate primary antibodies. The detailed list of primary antibodies used for immunoblotting is presented in Table 1.

After incubation with the primary antibodies, membranes were washed with TBS-T and incubated with horseradish peroxidase (HRP)-conjugated swine anti-rabbit secondary antibody (1:1700; Dako, Denmark). Blots were developed using a Pierce ECL 2 kit (Thermo Scientific, USA). For semiquantitative studies the chemiluminescence signals were captured using a ChemoCam Imager (Intas, Germany) and converted into a digital format. The immunostained band densities were normalized with respect to the loading control (GAPDH) and analysed using LabImage software (Kapelan Bio-Imaging, Germany).

All data were analyzed with GraphPad Prism 6 and are shown as mean \pm SEM. Statistical significance was determined using the unpaired two-tailed Student t test. p values of ≤ 0.05 were considered significant.

Antibody (clone)	Mol. Wt (kDa)	Antigen	Type	Reference	Conc (%)
Akt (pan) (C67E7)	60	Human peptide	Monoclonal (rabbit)	Cell Signaling #4691	1:1000
pAkt (Thr308) (D25E6)	60	Human peptide	Monoclonal (rabbit)	Cell Signaling #13038	1:1000
pAkt (Ser473) (D9E)	60	Human peptide	Monoclonal (rabbit)	Cell Signaling #4060	1:1000
GAPDH (14C10)	37	Human peptide	Monoclonal (rabbit)	Cell Signaling #2118	1:10000
AMPA1 (D4N9V)	100	Human peptide	Monoclonal (rabbit)	Cell Signaling #13185	1:1000
AMPA2 (E1L8U)	100	Human peptide	Monoclonal (rabbit)	Cell Signaling #13607	1:1000
GSK3β (27C10)	46	Human peptide	Monoclonal (rabbit)	Cell Signaling #9315	1 :1000
pGSK3β (Ser9) (D85E12)	46	Human peptide	Monoclonal (rabbit)	Cell Signaling #5558	1 :1000
MAP2 (D5G1)	280	Human peptide	Monoclonal (rabbit)	Cell Signaling #8707	1:1000
NMDAR1 (D65B7)	120	Human peptide	Monoclonal (rabbit)	Cell Signaling #5704	1 :1000
NMDAR2A	180	Human peptide	Polyclonal (rabbit)	Cell Signaling #4205	1 :800
NMDAR2B (D15B3)	190	Human peptide	Monoclonal (rabbit)	Cell Signaling #4212	1 :1000
PSD-95 (D27E11)	95	Human peptide	Monoclonal (rabbit)	Cell Signaling #3450	1:1000
Synaptophysin (D35E4)	38	Human peptide	Monoclonal (rabbit)	Cell Signaling #5461	1:5000

Table 1. Summary of primary antibodies used for western blot experiments

Primary antibodies were diluted in TBS-T solution (0.1% Tween-20, 0.8% NaCl, 20mM Tris, pH 7.5) containing 5% nonfat dry milk or 5% bovine serum albumin, and incubated overnight at 4°C, following manufacturer's indications.

10. RT-PCR analysis

After removal, tissue samples from brains were immediately transferred to RNA later (QIAGEN, Hilden, Germany). They were kept at 4°C for at least 24 h and then stored at -20°C until RNA isolation. For RNA isolation, the tissue was removed from RNA later and homogenized with 1mL of TriFast (peqGOLD, Erlangen, Germany) in BashingBeads tubes (Zymo Research, Freiburg, Germany). PeqGOLD HP Total RNA Kit was used for purification and manufacturer's instructions were followed. On-membrane DNase I digestion (peqGOLD, Erlangen, Germany) was performed and RNA purity and concentration was determined by absorbance at 230, 260 and 280 nm in a NanoDrop (Fisher Scientific, Germany).

For qPCR, TaqMan® RNA-to-Ct 1-Step Kit (Life Technologies, Darmstadt, Germany) was used with 300ng total RNA in a reaction volume of 10µL. Triplicate reactions were developed in a LightCycler® 480 Instrument II (Roche, Grenzach-Wyhlen, Germany). Reverse transcription was performed for 15 min at 48°C followed by 10 min at 95°C. Subsequently, 45 amplification cycles were run, comprising of denaturation at 95°C for 15 sec and annealing/elongation at 60°C for 1 min. TaqMan® Gene Expression Assays (Life Technologies, Darmstadt, Germany) were used for amplification of Hprt (Mm01545399_m1) and Gsk3b (Mm00444911_m1). Hprt expression was chosen as reference for normalization and target/reference ratios were calculated with the LightCycler® 480 Software release 1.5.0 (Roche, Grenzach-Wyhlen, Germany).

Resulting data were further normalized on values of control groups and statistically analyzed with GraphPad Prism version 6 (GraphPad Software, Inc., San Diego, CA, USA). All data are shown as mean ± SEM. p values of ≤0.05 were considered statistically significant.

11. Proteomic analysis

This work was done in collaboration with Prof. Dr. Lothar Jänsch and Dr. Marco van Ham from Cellular Proteome Research Group, Helmholtz Centre for Infection Research, Braunschweig, Germany (247,248).

11.1. Protein digest

Cortical and hippocampal synaptosomes were pulled together and digested, with trypsin, in 50 mM triethylammonium bicarbonate (TEAB) containing 10 % acetonitrile (ACN) and phosphatase inhibitors. A protein/protease ratio of no more than 50:1 was applied and digestion was performed at 37°C overnight. Peptides were vacuum dried, resolved in 0.2 % trifluoroacetic acid (TFA) in water, desalted on self-packed Lichroprep RP18 (10 µl, Merck), eluted in 0.2 % TFA in 60 % ACN and dried again.

11.2. iTRAQ labelling and SCX chromatography

Isobaric tags for relative and absolute quantitation (iTRAQ) labelling was performed according to the manufacturer's protocol (Applied Biosystems). Briefly, 150 µg dried peptides was redissolved in iTRAQ dissolution buffer at a ratio of no more than 50 µg peptide/20 µl buffer and incubated with three vials of label for 2 h followed by vacuum drying. A small aliquot was used to confirm the minimum percentage of peptide labelling using a 30 min RP18 gradient and the OrbitrapVelos mass spectrometer. Labeled fractions were combined and employed for Strong Cation Exchange (SCX) chromatography to reduce the complexity. The following iTRAQ reporter combinations were used: Toxoplasma-infected mice 114; noninfected mice 116.

The complex peptide mixtures were then subfractionated according to Reinl *et al.* (249). In short, up to 100 µg peptide were separated on a Mono S PC 1.6/5 column (GE Healthcare) via an Ettan micro-LC system (GE Healthcare) using a 30 min gradient from 0 to 35 % SCX buffer B (0.065 % formic acid, 25 % ACN supplemented with 0.5 M KCl) at a flow rate of 150 µl/min. Up to twenty 150 µl fractions were collected, desalted and used for LC-MS/MS.

11.3. LC-MS/MS and data analyses

LC-MS/MS analyses were performed on a DionexUltiMate 3000 n-RSLC system connected to an Orbitrap Fusion mass spectrometer (Thermo Scientific). Peptides were loaded onto a C18 pre-column (3 μ m, Acclaim, 75 μ m x 20 mm, Dionex), washed for 3 min at a flow rate of 6 μ l/min. Subsequently, peptides were separated on a C₁₈ analytical column (2 μ m, Acclaim PepMap RSLC, 75 μ m x 25 cm, Dionex) at 350 μ l/min via a linear 120-min gradient with UPLC buffer A (0.1 % FA in water) and 25% UPLC buffer B (0.1 % formic acid in ACN), followed by a 60 min Gradient from 25 to 50 % of buffer B. The LC system was operated with Chromeleon Software (version 6.8, Dionex) embedded in Xcalibur software (version 2.1, Thermo Scientific). The effluent from the column was electro-sprayed (Pico Tip Emitter Needles, New Objectives) into the mass spectrometer.

The mass spectrometer was controlled by Xcalibur software and operated in the data-dependent mode allowing the automatic selection of a maximum of 10 doubly and triply charged peptides and their subsequent fragmentation. A dynamic exclusion allowed up to 3 repeats. Peptide fragmentation was carried out using High Collision Dissociation settings optimized for iTRAQ-labeled peptides.

MS/MS raw data files were processed via Proteome Discoverer 1.3.0.339 mediated searches against UniProtKB/Swiss-Prot protein database (release 2013_01, with 538,849 entries; taxonomy *Mus musculus* with 16589 entries on a Mascot server (V. 2.4, Matrix Science). The following search parameters were used: enzyme, trypsin; maximum missed cleavages, 1; fixed modifications, iTRAQ 4-plex (K), iTRAQ (N terminus), Methylthio (C), oxidation (M); peptide tolerance, 5 ppm; MS/MS tolerance, 0.2 Da.

The knowledge-based Ingenuity Pathway Analysis (IPA, Ingenuity Systems, Redwood City, CA) was employed to identify networks, canonical pathways, molecular and cellular functions, and behavioral and neurological dysfunctions using proteins from iTRAQ data set.

Results

1. Experimental design

All the experiments were performed 8 weeks after infection. This time point was chosen because active parasite levels in critical peripheral organs are absent by this time and the parasite load in the brain is stable in chronically infected mice (168).

Initially, mouse brain T2- and T2*-weighted images were acquired at different time points. The development and the localization of *T. gondii*-induced brain lesions were monitored starting one week prior to infection, to chronic stages [week 8 post infection (p.i.)] and validated by histopathological examination.

Additionally, at the chronic stage (week 8 p.i.), *in vivo* mouse brain DT-MRI analyses were performed in *T. gondii* infected and control (noninfected) mice.

To reveal different aspects of *T. gondii*-CNS interactions, we also performed:

- immunofluorescent and electron microscopy experiments
- investigation of neuronal dendritic and spine morphology
- synaptosome/synaptic junction preparation and proteomic analysis
- western blotting (WB) and real time polymerase chain reaction (RT-PCR) experiments

2. Distribution of *T. gondii* induced lesions: MRI vs. histopathological investigations

To determine the pattern of brain microstructural alterations induced by chronic *T. gondii* infection in a murine model, *in vivo* non-invasive MRI was performed at high magnetic field (9.4 T). T2*-weighted imaging was used to identify and anatomically localize the preferential lesion sites of parasite induced brain pathology. Multiple foci of hypointensity were visualized with T2*-based contrast in various cortical and subcortical brain areas (Figure 6A). A pattern of high density of hypointense lesions was evident in the somatosensory (SSC) and motor cortices, hippocampus and striatal brain structures of all the infected mice. Interestingly, in T2-weighted imaging such regions appeared generally unaffected, demonstrating the superiority of T2*-weighted imaging for assessing the *T. gondii* induced brain pathology. To further define the composition of microstructural alterations leading to the changed T2*-contrast in the infected mice, brains of mice used for MRI studies were analyzed *ex vivo* using various neuropathological markers (Figure 6B). Scattered inflammatory infiltrates were detected throughout the whole brain, as well as only minor meningeal alterations and edemas (hematoxylin-eosin staining). We focused our analysis on the somatosensory cortex (regions between bregma + 0.14 mm and bregma -1.82 mm), where we observed a high density of hypointense lesions on T2* - weighted images of the infected mice. The number of *T. gondii* cysts was randomly distributed with no preference to a specific brain area. In each slide, 6 to 10 parasite cysts were detected within the cortex, 1 to 2 cysts within the hippocampus and 4 to 6 cysts in the other remaining brain areas. The cyst wall around the bradyzoites remained intact and extracellular parasites were not present, indicating latent rather than active *T. gondii* infection (Figure 6B). Interestingly, clusters of activated immune cells were not exclusively surrounding the cysts. Activated resident microglia cells were distributed ubiquitously in the whole brain with preference for the developing cortical inflammatory nodules (Iba1-positive). Activated astrocytes manifested evenly throughout the brain parenchyma (GFAP-positive). Moreover, perivascular cuffs were constituted mainly by recruited mononuclear cells with few neutrophil granulocytes (CD11b-positive) and lymphocytes (CD3-positive) (Figure 6B). Cell apoptosis (indicated by caspase-3 (Casp-3) staining) was observed demonstrating cell death as a consequence of chronic *T. gondii* infection. To clarify whether neurons were affected we employed a specific staining (Fluoro-Jade B) which only detects degenerating neurons. Fluoro-Jade B-labeled cells were observed

only sporadically in the inflammatory foci within the cortex and hippocampus, indicating that the majority of neurons in those regions did not die (Figure 6B).

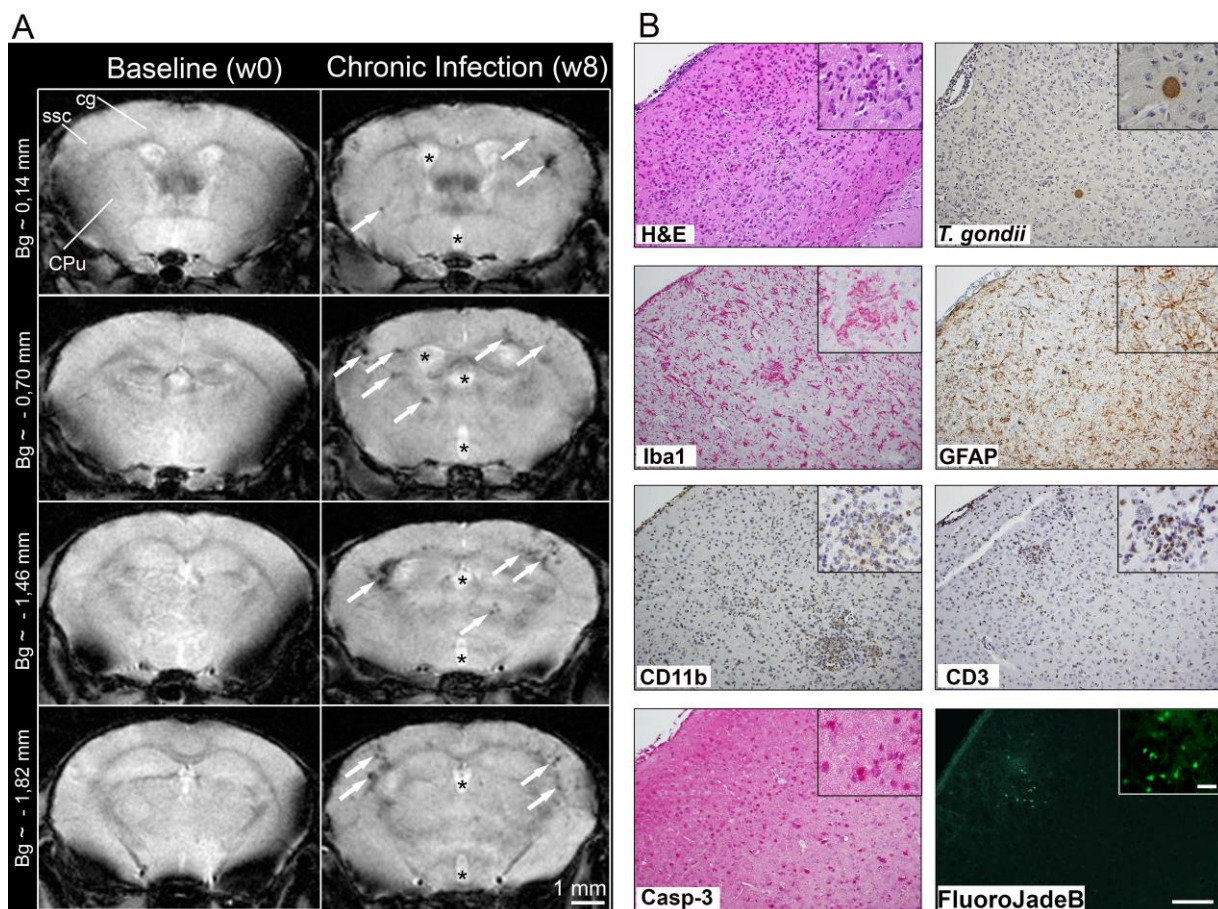


Figure 6. Pathological changes identified by MRI and histopathological examination of the murine brain chronically infected with *T. gondii*

(A) Representative T2*-weighted MR images, acquired before infection (baseline) and at 8 weeks post infection (chronic), depicting *T. gondii* induced brain microlesions throughout four coronal brain slices. Note the changes in the lateral and third ventricle size (asterisks) and the localization of the lesions (arrows) within the cortex but also in the striatum and along the white matter fiber tracks (ssc, somatosensory cortex; cg, cingulum; CPu, caudate putamen, Bg, bregma).

(B) In the cortical regions where hypointense T2*-weighted lesions were observed, H&E and anti-*T. gondii* staining revealed a higher density of cells, parenchymal micro-hemorrhage, and the presence of intact *T. gondii* cysts. Closer examination using anti-Iba-1 and anti-GFAP antibodies indicated diffuse activation of microglia and astrocytes. This was followed by recruitment of CD11b positive cells, indicating microglia cells as well as brain recruited macrophages. Numerous recruited T cells were detected by anti-CD3 antibody. Apoptotic cells, highlighted by an anti-Caspase-3 staining, were scattered throughout cortical areas. Fluoro-Jade B staining revealed a low number of degenerating neurons limited to the inflammatory foci (*T. gondii* infected mice n= 7; four to six coronal slides per mouse were analyzed). Scale bars in B: 100 μm, 20 μm in insets.

3. Chronic *T. gondii* infection alters the brain connectivity microstructure: *in vivo* qualitative and quantitative DT-MRI

To investigate the impact of *T. gondii* infection on the mouse brain neuronal wiring we performed a detailed qualitative and quantitative analysis of brain microstructural connections using *in vivo* DT-MRI and high resolution fiber mapping (hrFM). We adopted a novel fiber tracking and mapping methodology (201), which provided fine-grained maps of the living mouse brain structural connectivity (Figure 7A, B, hrFM). At first, we focused our investigation on the SSC showing the highest density of hypointense lesions on T2*-weighted images of the infected mice (Figure 7).

High resolution fiber maps revealed an altered connectivity pattern with a loss in fiber coherence and density at the lesion sites (Figure 7B, arrows). Using a special reconstruction algorithm (203,240) the resolution of the final fiber maps was increased by eight times (final resolution of 19.2 x 19.2 x 62 μm^3) vs. the scale of the original DT-MRI data. This allows a close comparison with the cortical pattern of axonal cytoskeletal proteins evaluated *ex vivo* with immunofluorescence.

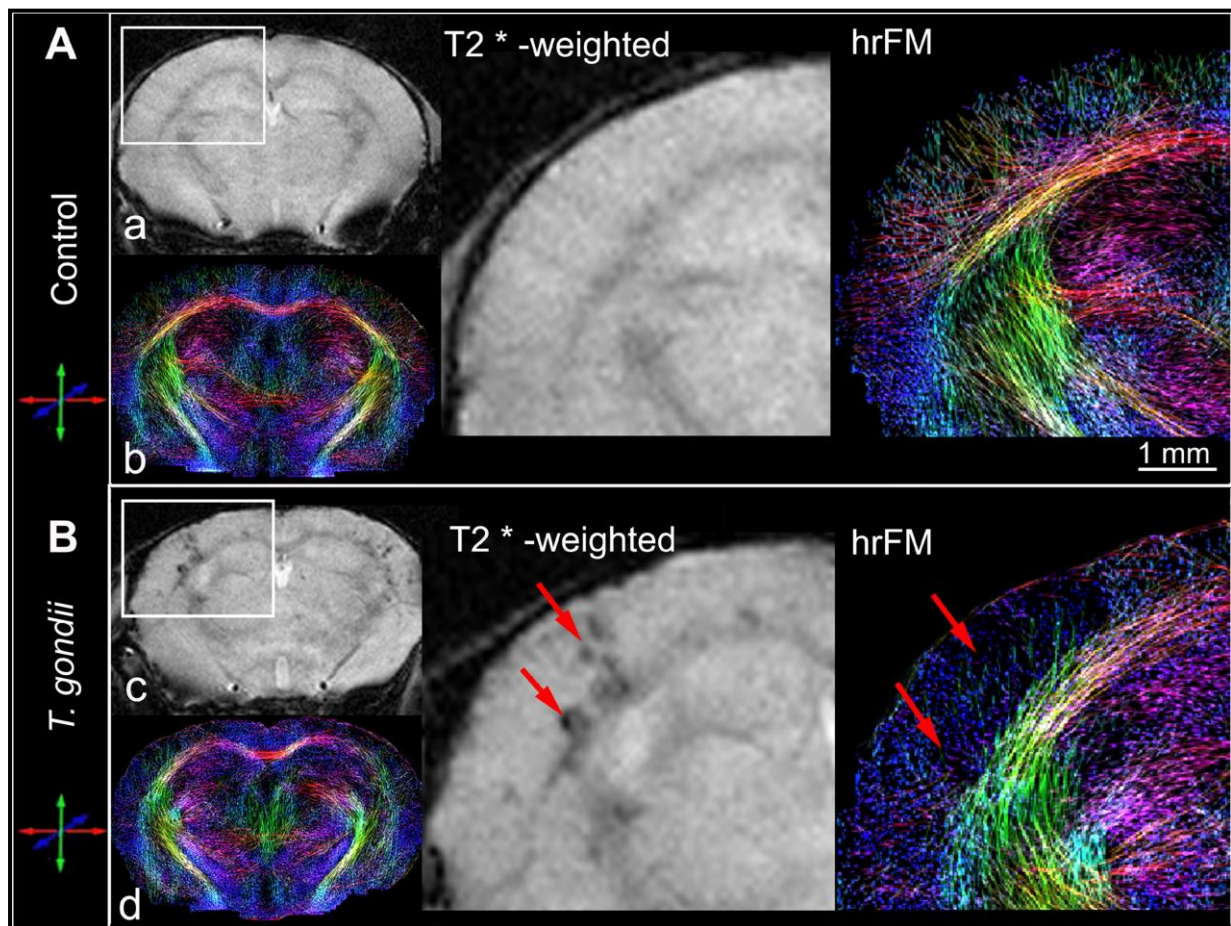


Figure 7. *In vivo* appraisal, by DT-MRI, of cortical injuries induced upon chronic *T. gondii* infection

Comparative visualization of T2*-weighted images (a, c) and high resolution fiber maps (hrFM) (b, d) of control (A) and *T. gondii* infected (B) mouse brains. Magnified views show the localization of *T. gondii* induced injuries (arrows) in the somatosensory cortex. Note the changed cortical connectivity pattern (vs. control) and the loss of fiber density in infected cortical areas. Brain connectivity maps were generated using a global optimization fiber tracking algorithm on data acquired at 9.4 Tesla. Control mice n=9, infected mice n=7.

The impaired cortical connectivity blueprints depicted *in vivo* in *T. gondii* infected brains (Figure 7B, hrFM) were paralleled by the observation of an abnormal expression pattern of the axonal and dendritic cytoskeleton markers Pan-Neuronal Neurofilament (clone SMI311) (Figure 8E, F, G) and Microtubule Associated Protein-2 (MAP2) (Figure 8H) in the same cortical areas. Clear reductions of the SMI311 and MAP2 immunofluorescence signals were detected, unraveling structural abnormalities along the cortical dendritic arbor of infected mice (Figure 8). Further analysis by western blot revealed a significant reduction in MAP2 content in the cortical extracts of *T. gondii* infected mice (Figure 8I) (relative intensities

normalized to GAPDH: control animals, 0.74 ± 0.12 ; *T. gondii* infected mice, 0.32 ± 0.08 ; $p=0.02$; unpaired Student's t test). Such modifications might not only involve the local cortical connectivity, but could influence the overall brain fiber microstructure and wiring.

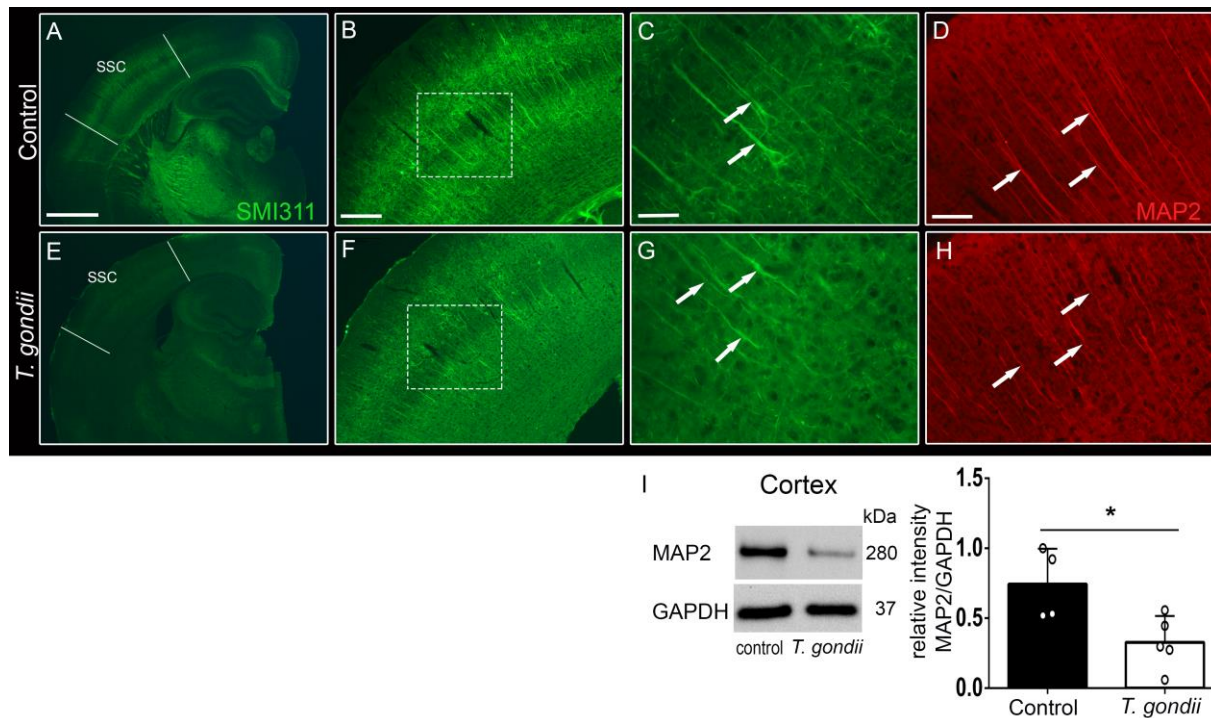


Figure 8. Structural abnormalities in axons and dendrites were observed within the cortex of *T. gondii* infected mice

Immunofluorescence stainings with the neuronal cytoskeleton marker, anti-Pan-Neuronal Neurofilament (SMI311) revealed structural abnormalities in the axons and dendritic trees within the SSC of *T. gondii* infected (E-F) vs. control mice (A-B). Detailed examination of the cortical layers (dashed squares) demonstrated defective morphology of noninfected pyramidal neurons of chronically infected mice (G, arrows) as indicated by reduced expression of SMI311 in contrast to normal expression in control animals (C, arrows).

Parallel immunofluorescence stainings against Microtubule Associated Protein-2 (MAP2) confirmed the structural alterations of the dendrites within the SSC of *T. gondii* infected mice (H, arrows) vs. control mice (D, arrows). Five to six coronal slides per mouse were analyzed, $n=3-4$ mice per group. (Scale bars, 1 mm in A and E, 200 μm in B and F, 50 μm in C and G, and 100 μm in D and H).

(I) Western blot analysis of MAP2 content in cortical extracts from control and infected mice, alongside GAPDH loading controls. Graph indicates densitometric analysis of blots, expressed as mean \pm SEM. Analysis was performed in three independent experiments. The circles show individual values, from one representative experiment. $*p < 0.05$

To obtain quantitative insights about the whole brain structural modifications upon *T. gondii* infection, we performed group statistical analysis (control vs. *T. gondii* infected animals) using the brain parametric maps derived after the calculation of the diffusion tensor as well as the fiber density (FD) maps generated with our global fiber tracking approach.

After spatial normalization to a mouse brain template, the brain parametric maps of fractional anisotropy (FA), mean diffusivity ($\langle D \rangle$), radial (D^\perp) and axial (D^\parallel) diffusivities and FD from each individual were group averaged and used for quantitative group comparison. Several studies have demonstrated the usefulness of FA, $\langle D \rangle$, D^\perp and D^\parallel to describe directional diffusivity of water molecules within the brain, along and across axonal tracts, providing meaningful biological information related to axonal and myelin pathology (239,250,251).

Figure 9 illustrates the overall impact of chronic infection with *T. gondii* on the FD and FA values. A general pattern of fiber loss could be noted in the infected group upon comparative inspection of group averaged FD maps (Figure 9A). Using a brain mask approach we separately assessed the FD modifications in areas of white matter (WM) and grey matter (GM) (Figure 9C) that were previously segmented from spatially normalized and averaged T2-weighted images. An additional region of interest was manually selected, covering the SSC.

Statistically significant decreases of the FD values were quantified on the WM area (17.8% reduction: see Figure 9B; control 0.74 ± 0.07 , infected 0.61 ± 0.08 ; normalized values ranging from 0 to 1) as well as on the SSC (23% reduction: see Figure 9B; control 0.39 ± 0.03 , infected 0.30 ± 0.055 ; normalized values ranging from 0 to 1). Despite the general tendency of a decrease in FD values over the whole GM brain area, the difference did not reach the level of statistical significance, mostly because of a high variability across the *T. gondii* infected mouse population.

Moreover, a comparable pattern of pathologically induced FA alterations (Figure 10A) were quantified along the segmented WM tracts of infected animals (17.6% reduction vs. control group: see Figure 9C; control 0.69 ± 0.07 , infected 0.57 ± 0.05 ; normalized values ranging from 0 to 1) and in the SSC (36% reduction vs. control group: see Figure 9C; control 0.25 ± 0.03 , infected 0.16 ± 0.04 ; normalized values ranging from 0 to 1). Within the entire GM area no significant FA reduction could be assessed.

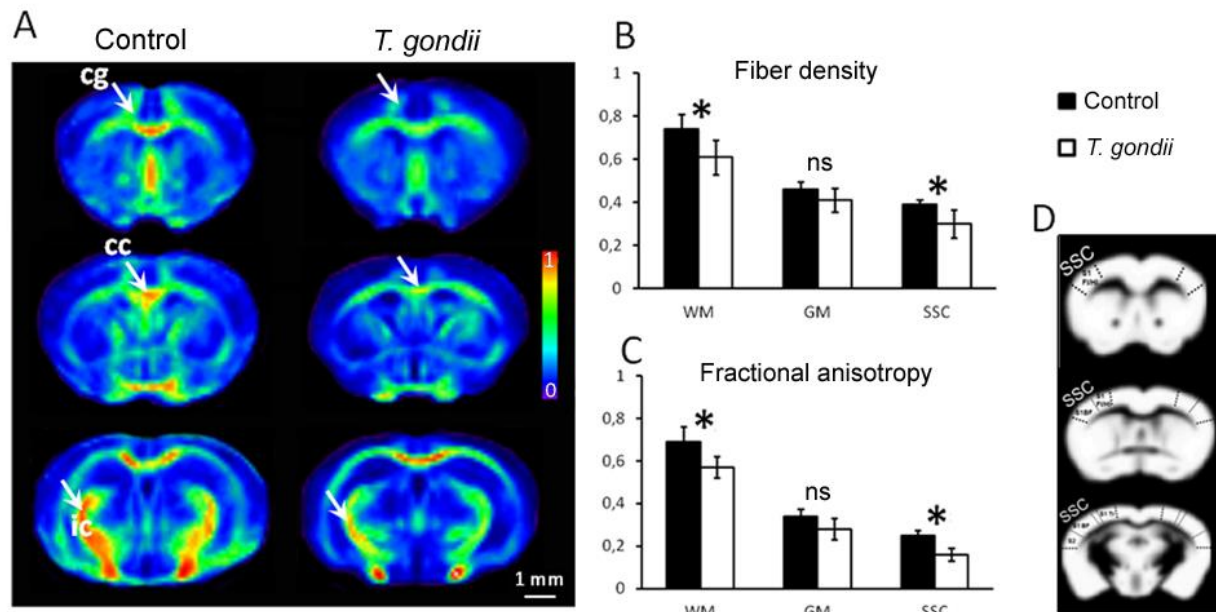


Figure 9. *In vivo* DT-MRI based quantitative evaluation of brain microstructural alterations induced by chronic *T. gondii* infection

(A) Group averaged (control vs. *T. gondii*) coronal fiber density (FD) maps, generated after spatial normalization to a mouse brain template, show a general pattern of fiber loss particularly evident in white matter areas (arrows, cg - cingulum; cc – corpus callosum; ic – internal capsule) of *T. gondii* infected mice. The FD values were normalized from 0 (no fibers mapped) to 1 (maximum density of fibers depicted in averaged FD maps across the whole population of investigated animals).

(B, C) Quantitative comparison of the FD and fractional anisotropy (FA) values in white matter (WM), gray matter (GM) and the somatosensory cortex (SSC) of control and *T. gondii* infected animals. Note the significant reduction of FD and FA in WM and SSC brain areas upon chronic *T. gondii* infection. Lower FD and FA values were quantified within the GM brain area, without reaching the threshold of statistical significance.

(D) Maps illustrate the brain masks (WM – dark area; GM – white area; and SSC) used for the quantitative analysis presented in B and C. The WM and GM masks were generated after segmentation of spatially normalized and averaged T2-weighted images. All data are expressed as mean±SEM, *T. gondii* infected mice n=7, control mice n=9. *p<0.05; ns, not significant.

4. Neuroinfection is associated with white matter microstructural abnormalities

Interestingly, probing the WM microstructure with electron microscopy revealed myelin abnormalities in the *T. gondii* infected brains (Figure 10B). Particularly, we could identify numerous axons displaying clear decompaction and degeneration of the myelin lamellae (Figure 10B, arrows, against the normal myelination pattern indicated by arrowheads). Such features are generally considered specific hallmarks of the WM pathology.

Moreover, quantification of D^{\perp} values in the WM of infected mice evidenced a statistically significant elevation of the water diffusivity perpendicular to the fiber tracts (Figure 10C; control 0.47 ± 0.08 mm²/s, infected 0.58 ± 0.07 mm²/s). Increased values of D^{\perp} were previously associated with myelin degeneration (239,250,251), suggesting that chronic *T. gondii* infection could elicit pathological processes leading to myelin sheath alterations and consequently, disrupted structural connectivity. Although subtle modifications of the $\langle D \rangle$ and D_{\parallel} were also noticed in the WM, GM and the SSC of *T. gondii* infected brains (Figure 10C), these parameters do not show enough sensitivity for discriminating the structural modifications induced by the pathology.

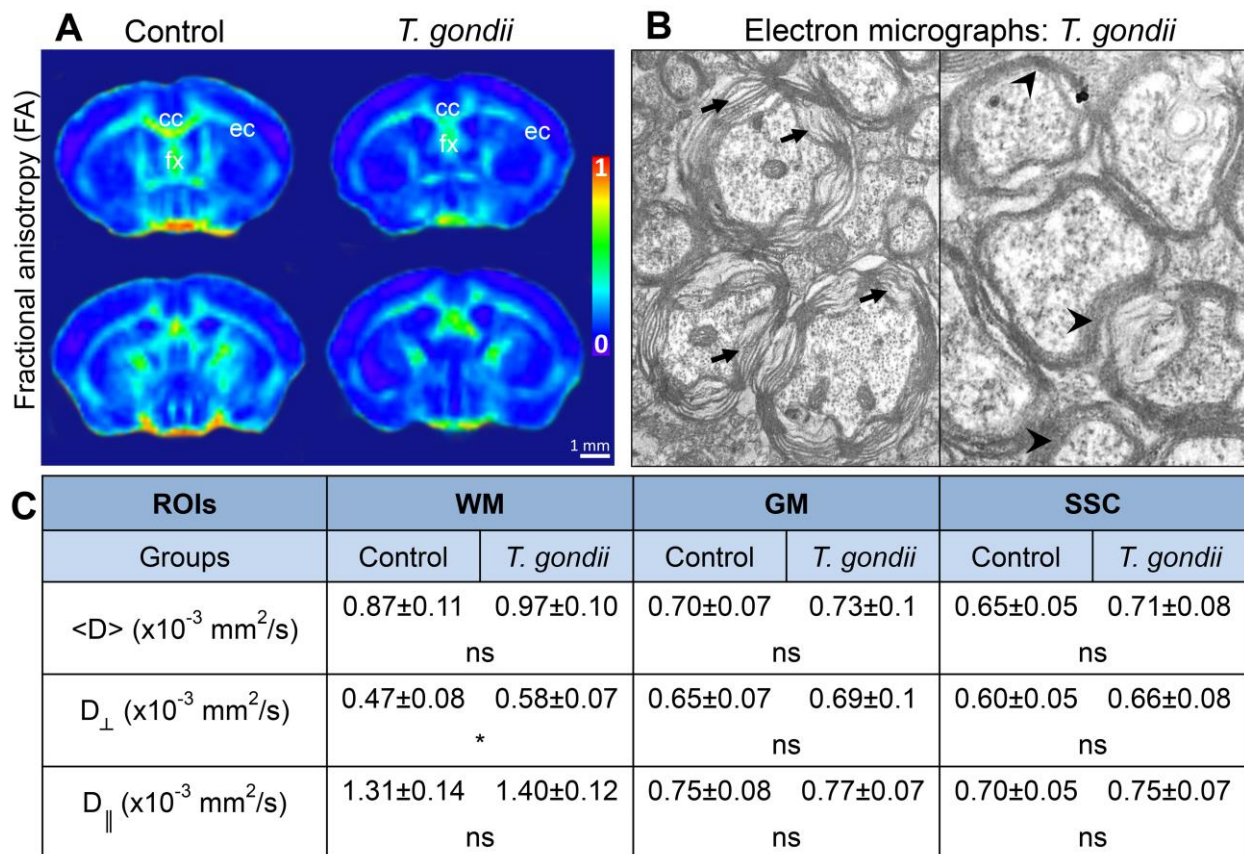


Figure 10. Quantitative assessment of modifications induced by *T. gondii* infection on brain parametric maps generated from *in vivo* DT-MRI data

(A) Comparison of group averaged coronal FA maps (control vs. *T. gondii* infected groups) within two different brain locations, showing decreased FA values along the WM tracts (i.e. cc – corpus callosum; ec – external capsule; fx – fornix).

(B) Electron micrographs from *T. gondii* infected brain, depicting axons with myelin lamellae decompaction (left panel – arrows). Intact myelin sheath surrounding healthy axons are comparatively shown in the right panel – arrowheads.

(C) Detailed quantitative comparison of mean (<D>), radial (D_⊥) and axial (D_∥) diffusivities in white matter (WM), gray matter (GM) and somatosensory cortex (SSC) of control and *T. gondii* infected animals. D_⊥ is the only parameter showing statistically significant increase in the WM of infected brains. Note also the general trend of elevated mean diffusivity <D> in all investigated regions of interest (ROIs). All data are expressed as mean±SEM, *T. gondii* infected mice n=7, control mice n=9. *p<0.05; ns, not significant

5. Chronic infection is negatively influencing the dendritic morphology of noninfected cortical neurons

In view of the alterations observed throughout the brains of mice infected with *T. gondii*, we next performed a detailed analysis of the dendritic morphology of individual neurons within different brain regions. Specifically, we selected Layer II/III pyramidal neurons from the cortex, a brain region where we have previously identified microstructural alterations. When qualitatively compared to control Layer II/III pyramidal neurons, the cells derived from infected mice showed a very simplified dendritic tree (Figure 11A). This pattern was confirmed by comparing the total dendritic length (Figure 11B, B') and total dendritic complexity (Figure 11D, D') using the Sholl analysis.

In view of their different morphology and connectivity, we analyzed the complexity of apical and basal dendrites separately. Total dendritic length of layer II/III neurons of *T. gondii* infected mice was reduced both for the apical and the basal dendrites (Figure 11B: control basal n=16, 1872.45 ± 167.95 μm , infected basal n=16, 1357.41 ± 104.17 μm , 27.5% reduction; Figure 11B': control apical n=20, 1228.36 ± 102.84 μm , infected apical n=20, 1059.74 ± 92.42 μm , 13.72% reduction).

Moreover, a statistically significant reduction in total dendritic complexity for the basal dendritic compartment was observed in infected vs. control mice (Figure 11D: control basal n=16, 161.38 ± 15.11 intersections, infected basal n=16, 124.31 ± 8.99 intersections, 22.97% reduction; Figure 11D': control apical n=20, 99.15 ± 8.2 intersections, infected apical n=20, 86.5 ± 8 intersections, 12.75% reduction).

A more detailed Sholl analysis performed by plotting the number of intersections against the distance from the cell body confirmed these results (Figure 11C) and revealed a significant decrease in complexity of the basal [110 μm radius (control, 9.63 ± 1.39 ; infected 6.19 ± 0.83 ; $p=0.04$), 120 μm radius (control, 8.19 ± 1.3 ; infected 4.75 ± 0.82 ; $p=0.03$), 130 μm radius (control, 6.69 ± 1.31 ; infected 3.38 ± 0.6 ; $p=0.02$), 140 μm radius (control, 5.25 ± 1.09 ; infected 2.5 ± 0.56 ; $p=0.03$)] but not for the apical dendrites in layer II/III cells of *T. gondii* infected mice.

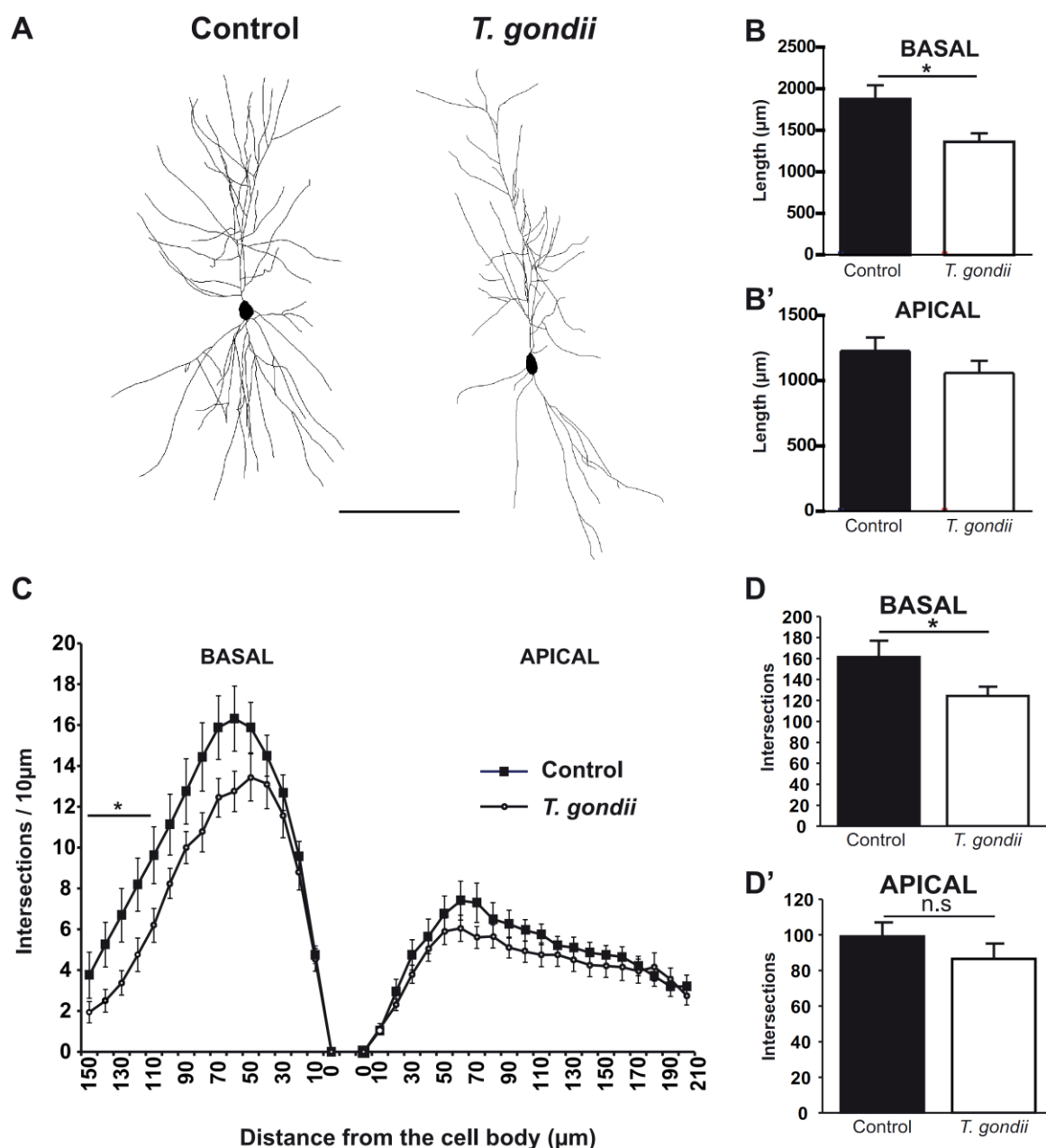


Figure 11. Morphological analysis of Layer II/III pyramidal neurons within the cortices of *T. gondii* infected and control mice

(A) Shows two examples of rendered pyramidal neurons, consisting of stacks of multiple optical sections from control and *T. gondii* infected mice. Note the simplified dendritic architecture of the neuron from the *T. gondii* infected brain. Scale bar is $100\mu\text{m}$. (B, B'), the graphs compare total dendritic length for the basal (B) and apical (B') dendritic tree in neurons of control vs. infected mouse brain. (C), Sholl analysis, plotting dendritic complexity in relation to the distance from the cell body for the basal (left) and apical (right) dendrites of Layer II/III neurons of control and infected mouse brain. (D, D'), the graphs show the total dendritic complexity for the basal (D) and apical (D') dendritic tree of Layer II/III neurons of control and infected mouse brain. Analysis was performed in three independent experiments. All data are expressed as mean \pm SEM, n=3-4 mice per group. *p<0.05; ns, not significant

6. Dendritic spine density and morphology is affected in the cortex of infected mice

Changes in dendritic morphology indicate changes in the number and morphology of dendritic spines, which are responsible for the inter-neuronal information exchange. Apical and basal dendrites were visualized by the expression of Dil stain in a random population of cortical pyramidal neurons of infected and noninfected brains. When Dil dye-expressing dendrites were qualitatively compared, a clear alteration in the number of dendritic spines could be detected (Figure 12A-D). Additionally, the density of dendritic spines was quantitatively analyzed both for the apical and basal dendrites in layer II/III neurons of infected mice and showed a significant reduction when compared to neurons from the same area of control mice (Figure 12E: control apical n=24, 1.47 ± 0.06 spines/ μm , infected apical n=20, 1.16 ± 0.11 spines/ μm ; Figure 12F: control basal n=23, 1.53 ± 0.04 spines/ μm , infected basal n=19, 1.15 ± 0.09 spines/ μm).

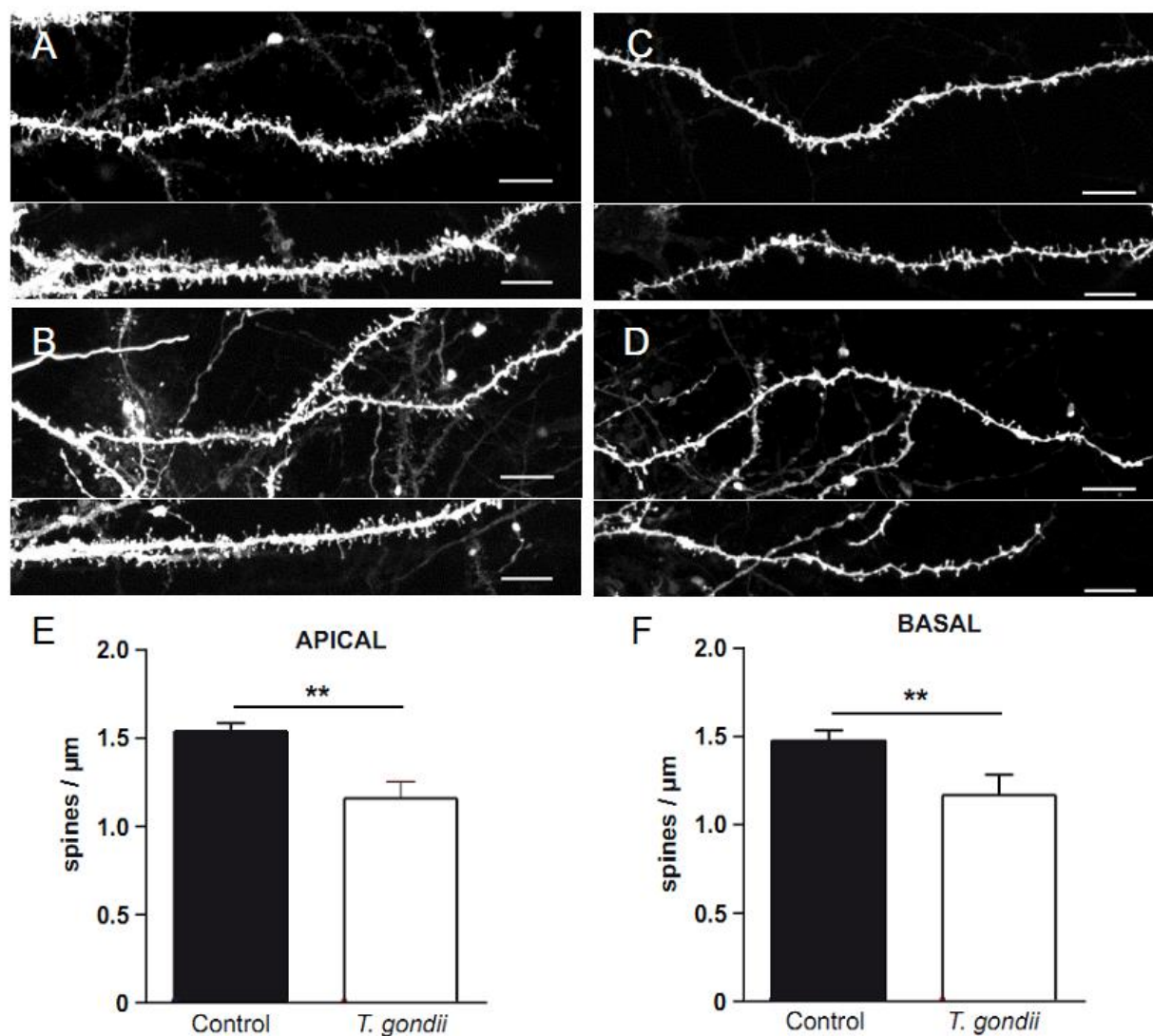


Figure 12. Spine density deficits in pyramidal neurons within the cortex of *T. gondii* infected mice

(A and B) Representative confocal high-magnification images of apical (A) and basal (B) dendrite branches from pyramidal neurons of noninfected mouse brain. (C and D) Representative high-magnification images of apical (C) and basal (D) dendrite branches from pyramidal neurons of infected mouse brain. Note the reduced density of dendritic spines. Scale bar is 10 μm . (E and F) Spine density counts showing a significantly lower spine density in both apical (E) and basal (F) dendritic compartments from cortical pyramidal neurons of *T. gondii* infected mouse brain. Analysis was performed in three independent experiments. All data are expressed as mean \pm SEM, n=3-4 mice per group. **p<0.01

Finally, in order to detect possible changes in the morphology of dendritic spines their length and head width were compared in pyramidal neurons of control vs. infected mice. The length was measured from their base at the dendrite to the tip of their head. Interestingly, spine length and spine head width showed a significant reduction for the apical dendrites (Figure 13A: control apical n=11, $1.53\pm 0.01\ \mu\text{m}$, infected apical n=8, $1.27\pm 0.08\ \mu\text{m}$; p=0.002; Figure 13C: control apical n=11, $0.85\pm 0.02\ \mu\text{m}$, infected apical n=8, $0.76\pm 0.02\ \mu\text{m}$; p=0.03) while the morphology of the spines on the basal dendrites was not altered (Figure 13B: control basal n=7, $1.436\pm 0.126\ \mu\text{m}$, infected basal n=6, $1.204\pm 0.08\ \mu\text{m}$; p=0.1; Figure 13D: control basal n=7, $0.84\pm 0.05\ \mu\text{m}$, infected basal n=6, $0.79\pm 0.07\ \mu\text{m}$; p=0.5).

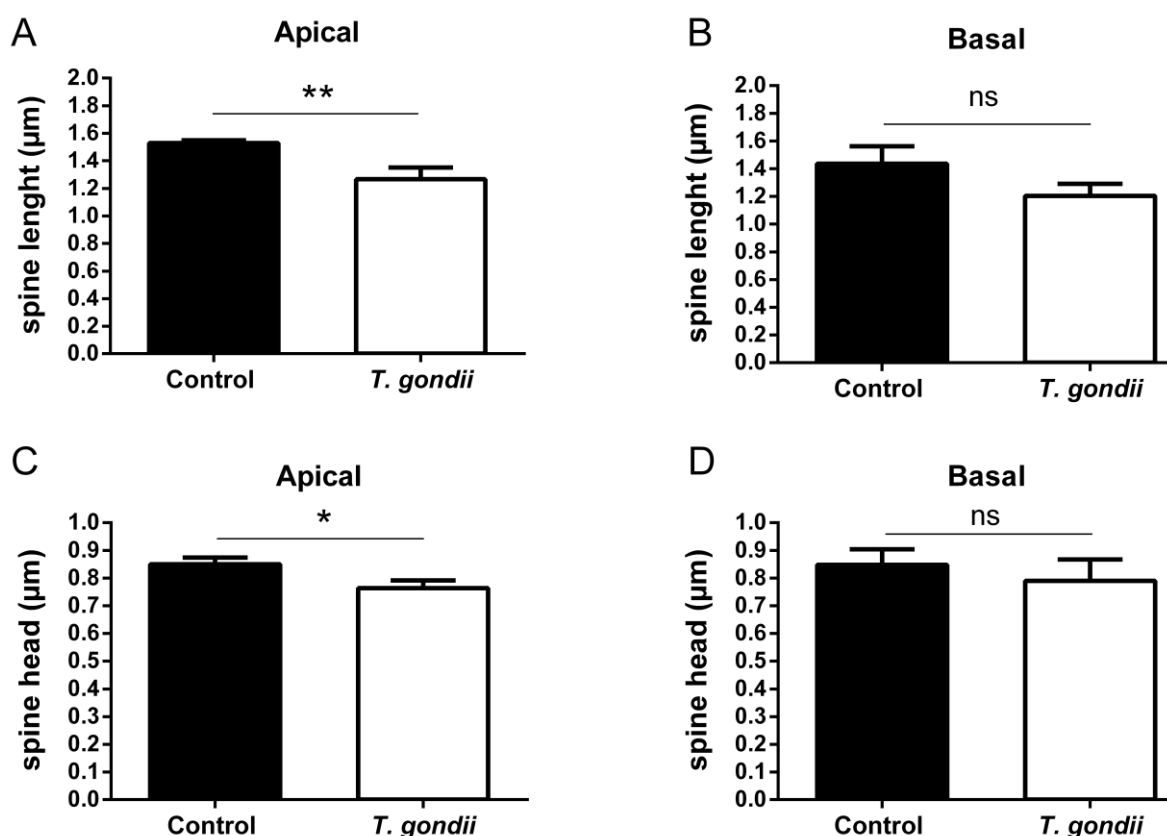


Figure 13. Effect of infection with *T. gondii* on cortical dendrites spine length and spine head width

Comparative analysis of dendritic spine length and spine head morphology of apical (A, C) and basal (B, D) dendrites from pyramidal neurons of control and *T. gondii* infected mouse brain is shown. Chronic infection triggers a significant reduction in the spine length and spine head width for the apical dendrites, but not for the basal dendrites. The length was measured from the base of the dendrite to the tip of their head. Analysis was performed in three independent experiments. All data are expressed as mean±SEM, n=3-4 mice per group. **p<0.01; ns, not significant

7. Chronic infection with *T. gondii* alters the structure of hippocampal neurons

In addition to the Layer II/III pyramidal neurons from the cortex, we next focused our analysis on hippocampus, a key neuroanatomical structure highly relevant to normal behavior, cognition and memory. Thus, we performed a detailed analysis of the dendritic morphology of individual granule cells of the dentate gyrus (DG) as well as CA1 pyramidal neurons from the hippocampus. Qualitative comparison between DG granule neurons revealed that the cells derived from infected mice showed a subtle reduction in the dendritic tree (Figure 14A). The reduction was further confirmed by comparing the total dendritic length (Figure 14B; control n=35, 890.7±46 µm, infected n=30, 742.5±42 µm, 16.6% reduction). Moreover, detailed Sholl analysis, performed in the DG granule cells of infected mice showed a clear reduction in dendritic complexity (intersections) (Figure 14C) throughout the entire dendritic length (160 µm from the cell body) with statistical significance for the 20 µm (control, 2.72±0.75; infected, 2.0±0.21; p=0.02), 70 µm (control, 6.67±0.91; infected, 5.27±0.31; p=0.006), 150 µm (control, 5.31±0.84; infected, 4.0±0.46; p=0.03) and 160 µm (control, 4.69±0.86; infected, 3.5±0.43; p=0.04) radius. Total dendritic complexity (intersections) indicated a significant reduction of dendritic arbor in granule cells of the DG (Figure 14D; control n=35, 84.81±4.39 intersections; infected n=30, 70.03±4.36 intersections, 17.42% reduction).

Once more, given their different structure and connectivity, we analyzed the complexity of CA1 apical and basal dendrites separately. Total dendritic length of CA1 neurons of *T. gondii* infected mice was reduced both for the apical and the basal dendrites (Figure 15A, B; control apical n=15, 1744.5±169.1 µm, infected apical n=12, 1359.1±119.1 µm; control basal n=12, 1514.7±172.9 µm, infected basal n=11, 1111.2±148.3 µm). Similarly, the Sholl analysis revealed a decrease in complexity of the apical and basal dendrites of CA1 pyramidal neurons of infected vs. control mice, throughout the analyzed length (Figure 15C) with the following statistical significances for apical [50 µm radius (control, 6.93±0.91; infected 4.25±0.57; p=0.03), 100 µm radius (control, 10.4±0.93; infected 7.83±0.6; p=0.04), 110 µm radius (control, 10.73±0.95; infected 7.5±0.52; p=0.01), 120 µm radius (control, 10.13±0.79; infected 7.5±0.78; p=0.03), 140 µm radius (control, 9±0.94; infected 5.92±0.75; p=0.02), 150 µm radius (control, 8.47±1.05; infected 5.42±0.79; p=0.04)] and basal [50 µm radius (control, 14.08±1.05; infected 9.36±1.25; p=0.008), 60 µm radius (control, 14.58±1.36; infected 9.45±0.99; p=0.007), 70 µm radius (control, 14.17±1.72; infected 9.18±0.98; p=0.02), 80 µm

radius (control, 13.92 ± 1.72 ; infected 8.73 ± 1.32 ; $p=0.02$), 90 μm radius (control, 13 ± 1.82 ; infected 8.09 ± 1.44 ; $p=0.04$) dendrites. Comparing total dendritic complexity of CA1 pyramidal neurons showed a clear reduction upon *T. gondii* infection for both apical and basal dendritic branches (Figure 15D, E; basal, control $n=13$, 141.58 ± 14.53 intersections; infected $n=15$, 99.45 ± 12.97 intersections, 29.76% reduction; apical, control $n=13$, 128.53 ± 11.21 intersections; infected $n=15$, 95.17 ± 0.8 intersections, 25.96% reduction).

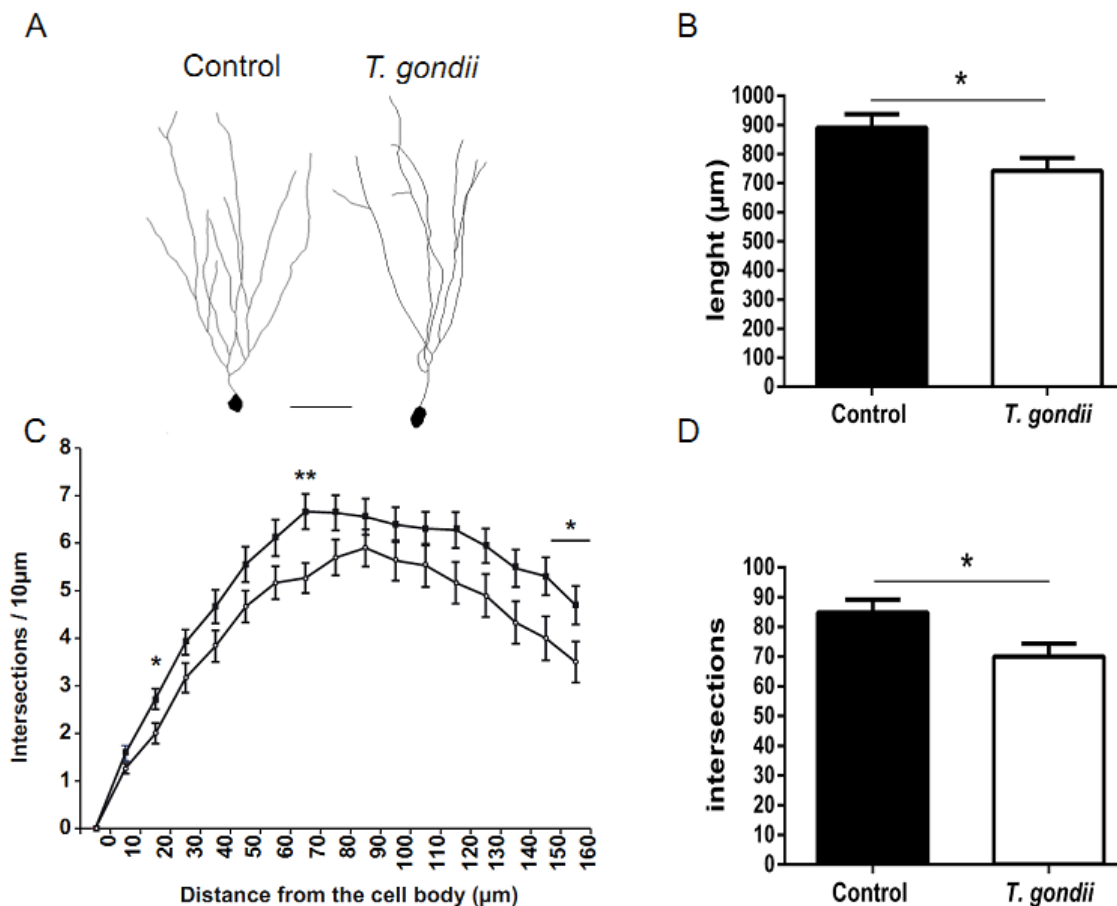


Figure 14. Morphological investigation of granule neurons within dentate gyrus of *T. gondii* infected and control mice

(A) Neurolucida reconstruction of DG neurons, consisting of stacks of multiple optical sections from control and *T. gondii* infected mice. Note the simplified dendritic architecture of the neuron from the *T. gondii* infected brain. Scale bar is 50 μm . (B) The graph compares total dendritic length of the dendritic tree in neurons of control vs. infected mouse brain. (C) Sholl analysis, plotting the distribution of dendritic complexity in relation to the distance from the cell body of neurons from the dentate gyrus of control and *T. gondii* infected mice. (D) The graph shows the total dendritic complexity (intersections) for the dendritic tree of granule neurons in the dentate gyrus of control and infected brains. Analysis was performed in three independent experiments. All data are expressed as mean \pm SEM, $n=3-4$ mice per group. * $p<0.05$; ** $p<0.01$

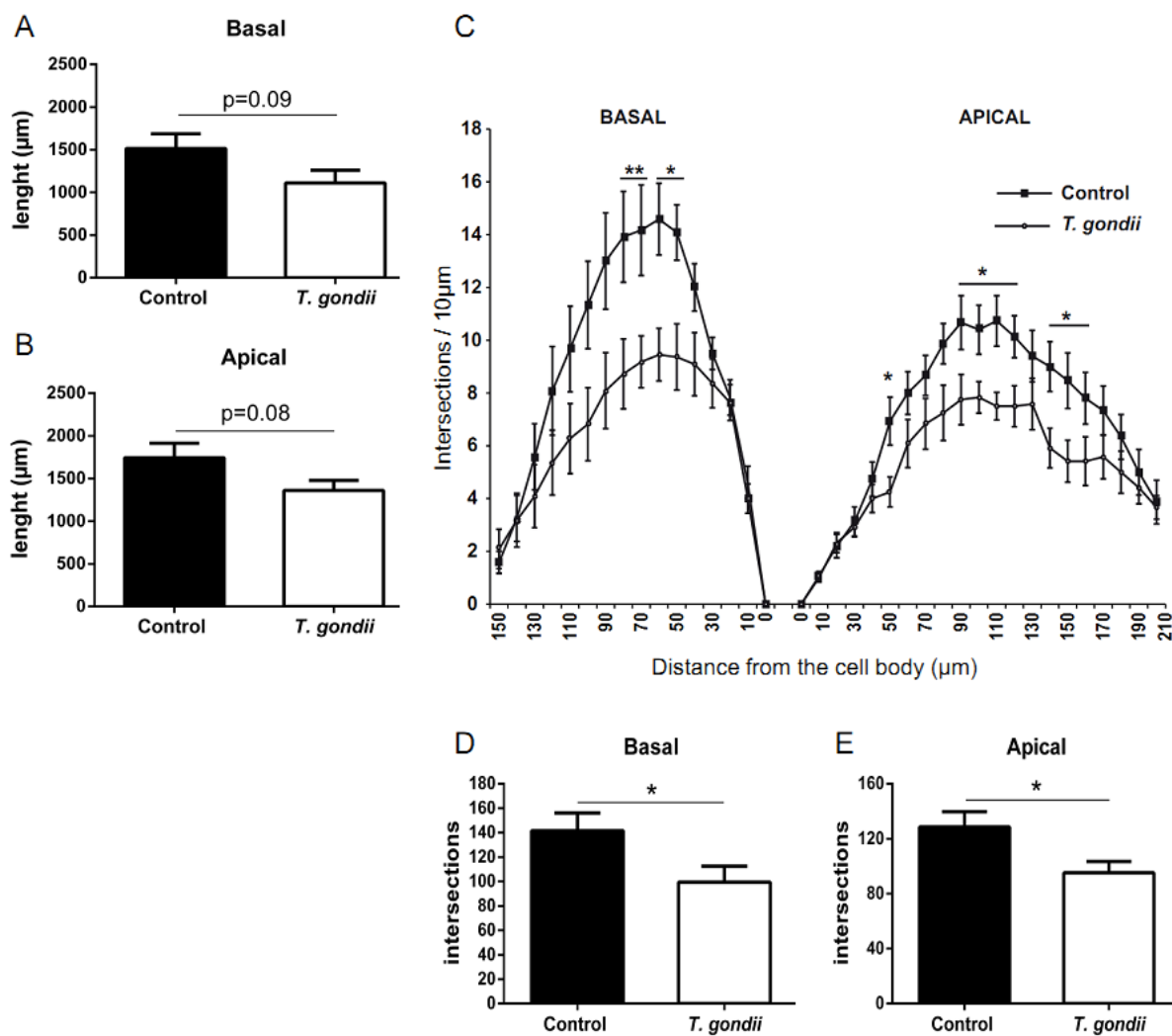


Figure 15. Morphological analysis of neurons within CA1 pyramidal neurons of *T. gondii* infected and control mice

(A and B) The graph shows the total dendritic length for the basal (A) and apical (B) dendritic tree of CA1 neurons of control and infected mouse brain. (C) Sholl analysis, plotting the distribution of dendritic complexity in relation to the distance from the cell body for the basal (left) and apical (right) dendrites of CA1 pyramidal neurons of control and *T. gondii* infected brain. (D and E) the graphs show the total dendritic complexity (intersections) for the basal (D) and apical (E) dendritic tree of CA1 pyramidal neurons of control and *T. gondii* infected brain. Analysis was performed in three independent experiments. All data are expressed as mean \pm SEM, n=3-4 mice per group. *p<0.05; **p<0.01.

8. Synaptophysin and PSD95 protein expression level is reduced in the cortex and the hippocampus of mice chronically infected with *T. gondii*

To determine whether the observed changes in neuronal architecture might be reflected in altered expression of key molecules involved in synaptic signaling, we investigated the expression of presynaptic synaptophysin as well as the postsynaptic density protein (PSD95) by western immunoblotting. Semi-quantitative protein expression revealed significantly lower protein levels of these two molecules between *T. gondii* infected and noninfected animals, in both cortex and hippocampus (Figure 16A, B; relative intensities normalized to GAPDH: PSD95, cortex: control animals, 0.88 ± 0.05 ; infected mice, 0.69 ± 0.03 ; $p=0.01$; PSD95, hippocampus: control animals, 0.91 ± 0.03 ; infected mice, 0.73 ± 0.02 ; $p=0.005$; Synaptophysin, cortex: control animals, 1.06 ± 0.04 ; infected mice, 0.69 ± 0.12 ; $p=0.03$; Synaptophysin, hippocampus: control animals, 1.11 ± 0.07 ; infected mice, 0.73 ± 0.07 ; $p=0.01$; unpaired Student's t test). Our findings provide evidence that chronic *T. gondii* infection can interfere with the normal activity of mature synapses in key brain structures.

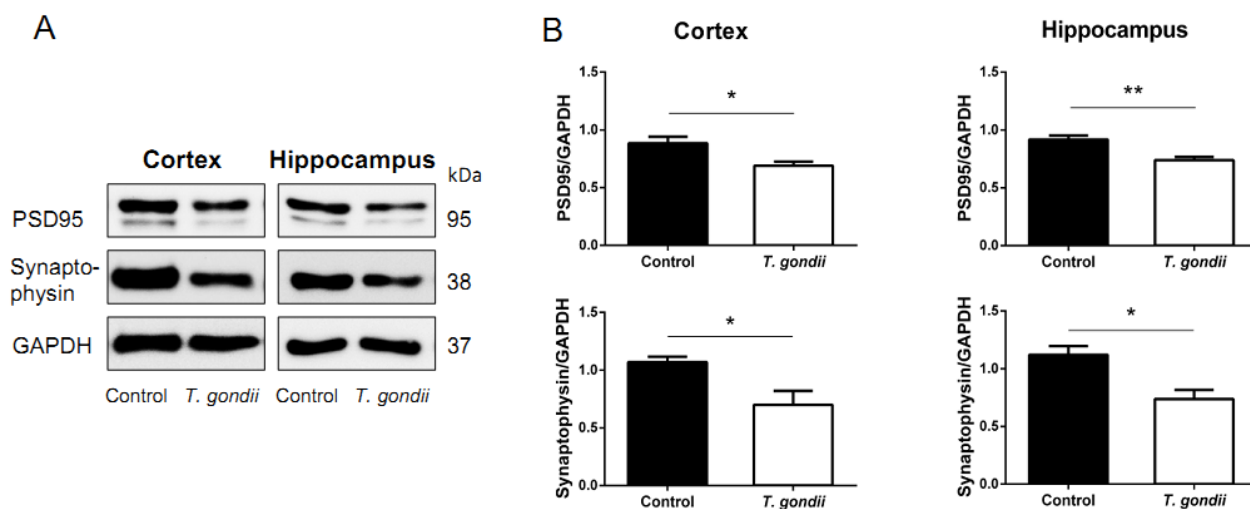


Figure 16. Impaired expression of synaptic related proteins in *T. gondii* infected brains

(A) Representative blots from the cortex and hippocampus whole tissue extracts of control and *T. gondii* infected mice, used for PSD95 and Synaptophysin protein semi-quantification. (B) Densitometric analysis of PSD95 and Synaptophysin protein levels revealed statistically significant reductions in *T. gondii* infected mice, suggesting deficits of the synaptic cleft physiology. Analysis was performed in three independent experiments. Data are expressed as mean ± SEM, n=3-4 mice per group. * $p<0.05$ and ** $p<0.01$.

9. Latent infection with *T. gondii* alters the proteome of adult mouse cortical and hippocampal synaptosomes

Synapses provide the physical basis for communication within the brain, and the ability for synapses to maintain their integrity and functionality is critical to maintaining proper CNS function. Quantitative proteomic analysis is a useful heuristic tool to analyze global changes in expression of synaptic proteins in several animal models of neurological and neuropsychiatric illness (252–255). In the present study we employed this approach to demonstrate differentially expressed proteins critical for signaling at synapses of mice chronically infected with *T. gondii*. For that, we performed a subcellular fractionation protocol (244) to obtain synaptosomes which contain both pre- and post-synaptic compartments, from cortex and hippocampus of control and infected mice.

The results presented here are preliminary, obtained from a limited number of biological replicates, and ongoing experiments will confirm and further expand these findings.

Two biological replicates of control and infected mice were used in iTRAQ experiments (254), in which we identified more than 800 unique proteins. Further analysis focused on characterization of strongly deviating protein levels and resulted in 120 identified proteins differentially regulated (see annex), which were functionally mapped by IPA software. Initially, we used IPA to identify behavioral and neurological disorders associated with differentially expressed synaptic proteins in infected mice. Among these, the main neurobehavioral disorders include memory, learning, locomotion, social interactions, cognitive impairment, schizophrenia, Alzheimer's disease, mental retardation (Table 2 and Table 3).

	Function	p-Value	Molecules	#
Behavior	working memory	3.82E-03	HOMER1, SYNGAP1	2
	spatial memory	3.41E-04	APOD, GRIA2, HOMER1, LRRC7, SYNGAP1	5
	short-term memory	4.53E-04	HOMER1, LRRC7, SYNGAP1	3
	spatial learning	1.25E-04	APOD, APOE, GRIN1, PLCB1, PPP1R1B, Ptpd, SYNGAP1	7
	learning	9.97E-08	APOD, APOE, DLG4, GABBR2, GABRA1, GRIA2, GRIN1, HOMER1, LRRC7, PLCB1, PPP1R1B, PPT1, SLC12A5, SYNGAP1	14
	exploratory behavior	2.05E-03	APOE, GRIA2, RIMS1, SYNGAP1	4
	locomotion	4.77E-08	APOE, DLG4, GABRA1, GRIA2, GRIA3, GRIN1, HOMER1, LRRC7, PCSK1N, PPP1R1B, PPT1, RIMS1, RTN4, SLC17A6	14
	hyper locomotion	2.51E-03	DLG4, SLC17A6	2
	social behavior	8.68E-05	GRIN1, GSTM5, RIMS1, RTN4, SYNGAP1	5
	social withdrawal	2.51E-03	RTN4, SYNGAP1	2
	anxiety	1.22E-03	APOE, GABBR2, HOMER1, LRRC7, PCSK1N, SYNGAP1	6

Table 2. Behavioral dysfunctions associated with altered proteins in chronically infected mice synaptosomes. P-values were determined by Fisher's exact test

Function	p-Value	Molecules	#	
Neurological Disorders	movement disorders	1.93E-15	APOD, APOE, ARHGDB, ATCAY, B2M, BCAS1, C4A/C4B, CHGA, CHGB, CLU, CTSD, DLG2, DNAJC5, GABBR2, GABRA1, GFAP, GRIA2, GRIA3, GRIN1, HOMER1, LAMP2, MAL2, NDUFB5, PFN1, PLCB1, PPP1R1B, PPT1, PRDX6, PVALB, RAB3A, RHOG, RTN4, SCG2, SLC1A2, SV2A, SYNGAP1, TPM3	37
	seizure disorder	1.86E-12	CHGB, CLU, CTSD, GABBR2, GABRA1, GFAP, GRIA2, GRIN1, HOMER1, LGII, NAMPT, PLCB1, PPP1R1B, PPT1, RIMS1, SG, SLC12A5, SLC1A2, SLC6A11, SV2A, SV2B, SYNGAP1	22
	Alzheimer's disease	5.54E-12	ACLY, ALB, APOD, APOE, C4A/C4B, CLU, CST3, CTSD, GABBR2, GABRA1, GFAP, GRIA2, GRIA3, GRIN1, HOMER1, LGAS, PRDX1, PRKACA, RIMS1, SLC1A2, SV2A, SYP, TF	23
	schizophrenia	1.57E-11	APOD, APOE, C4A/C4B, CHGB, DLG2, DLG4, GABRA1, GFAP, GRIN1, HOMER1, LGALS1, LGI1, PPP1R1B, PRDX6, PVALB, RTN4, S100A6, SCG2, SLC12A5, SLC1A2, SYP, TF	22
	Huntington's Disease	4.42E-11	APOD, APOE, B2M, C4A/C4B, CHGB, CLU, GABRA1, GFAP, GRIN1, HOMER1, LAMP2, MAL2, NDUFB5, PFN1, PLCB1, PPP1R1B, PRDX6, PVALB, RAB3A, RHOG, SCG2, SLC1A2, TPM3	23
	epilepsy	1.85E-09	CHGB, CLU, GABRA1, GFAP, GRIN1, HOMER1, LGI1, NAMPT, PLCB1, PPP1R1B, SCG2, SLC12A5, SLC1A2, SLC6A11, SV2A	15
	major depression	2.60E-05	APOE, CHGA, GABRA1, GFAP, GRIA3, GRIN1, KRT17, WFS1	8
	cognitive impairment	3.59E-05	APOE, CST3, GABBR2, GABRA1, GRIA3, GRIN1, HOMER1, SLC1A2, SYNGAP1, SYP	10
	bipolar disorder	4.67E-05	APOD, APOE, DLG4, GABRA1, GRIA2, GRIA3, GRIN1, HSP90B1, PRDX1, WFS1	10
	Neuroinflamm. of brain	4.96E-04	GFAP, PPT1	2
mental retardation	2.10E-03	GABBR2, GRIA3, GRIN1, SLC1A2, SYNGAP1, SYP	6	

Table 3. Neurological dysfunctions associated with altered proteins in chronically infected mice synaptosomes. P-values were determined by Fisher's exact test

Next, we could categorically organize proteins into functional pathways. Comparison analysis revealed alterations of the glutamate signaling canonical pathway, which is relevant for normal functioning of the synapse (Figure 17).

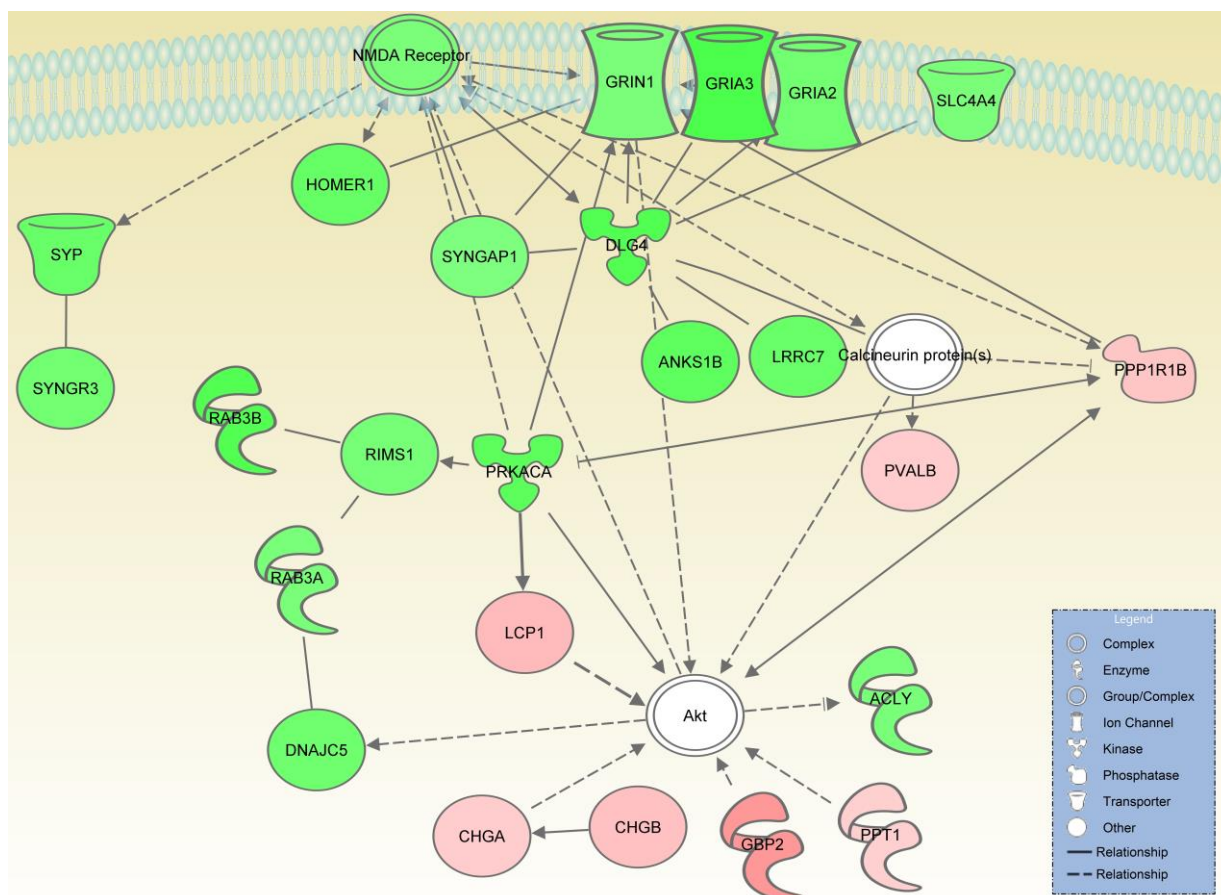


Figure 17. Canonical pathway with reduced activity implicates glutamatergic signaling

Protein clustering was performed with Ingenuity Pathway Analysis (IPA, Ingenuity Systems) based on molecular functions, cellular functions and functional group. Data show proteins with decreased level (green) and increased level (red). Straight lines indicate direct interactions while dashed lined stand for regulatory effects. Abbreviations: ACLY, ATP citrate lyase; Akt, protein kinase B; ANKS1B, ankyrin repeat and sterile alpha motif domain containing 1B; CHGA, chromogranin A; CHGB, chromogranin B; DLG4, disks, large homolog 4 (PSD95); DNAJC5, DnaJ homolog, subfamily C, member 5; GBP2, guanylate binding protein 2, interferon-inducible; GRIN1, glutamate receptor, ionotropic (NR1); GRIA2, glutamate receptor, ionotropic (AMPA2); GRIA3, glutamate receptor, ionotropic (AMPA3); HOMER1, homer homolog 1; LCP1, lymphocyte cytosolic protein 1; LRR7, leucine rich repeat containing 7; PPP1R1B, protein phosphatase 1, regulatory subunit 1B; PPT1, palmitoyl-protein thioesterase 1; PRKACA, protein kinase, cAMP-dependent, catalytic, alpha; PVALB, parvalbumin; RAB3A, member RAS oncogene family; RAB3B, member RAS oncogene family; RIMS1, regulating synaptic membrane exocytosis 1; SLC4A4, solute carrier family 4, member 4; SYNGAP1, synaptic Ras GTPase activating protein 1; SYNGR3, synaptogyrin 3; SYP, synaptophysin;

A global inspection of regulatory data from control and infected samples was performed by box plot analysis (Figure 18A). Protein regulation factors in assessed samples indicated a wide regulation range from +2.9 to -1.3 ($\log_2\text{RF} = \log_2$ regulation factor) (Figure 18A). Moreover, from the 120 proteins differentially regulated we have selected and focused our analysis on 25 proteins strongly deviating upon infection with *T. gondii*, and which might be of clinical interest for future studies (Table 4). The regulation factors of a selection of proteins that might be of clinical interest are presented as heat maps (Figure 18B).

In conclusion, synaptosomes isolated from infected mice show altered expression of synaptic proteins-mediated cellular signaling, supporting the hypothesis that persistent infection with *T. gondii* impacts on the synaptic efficacy, which likely cause neurobehavioral abnormalities. Importantly, it is an exploratory study that forms the bases for further targeted investigations.

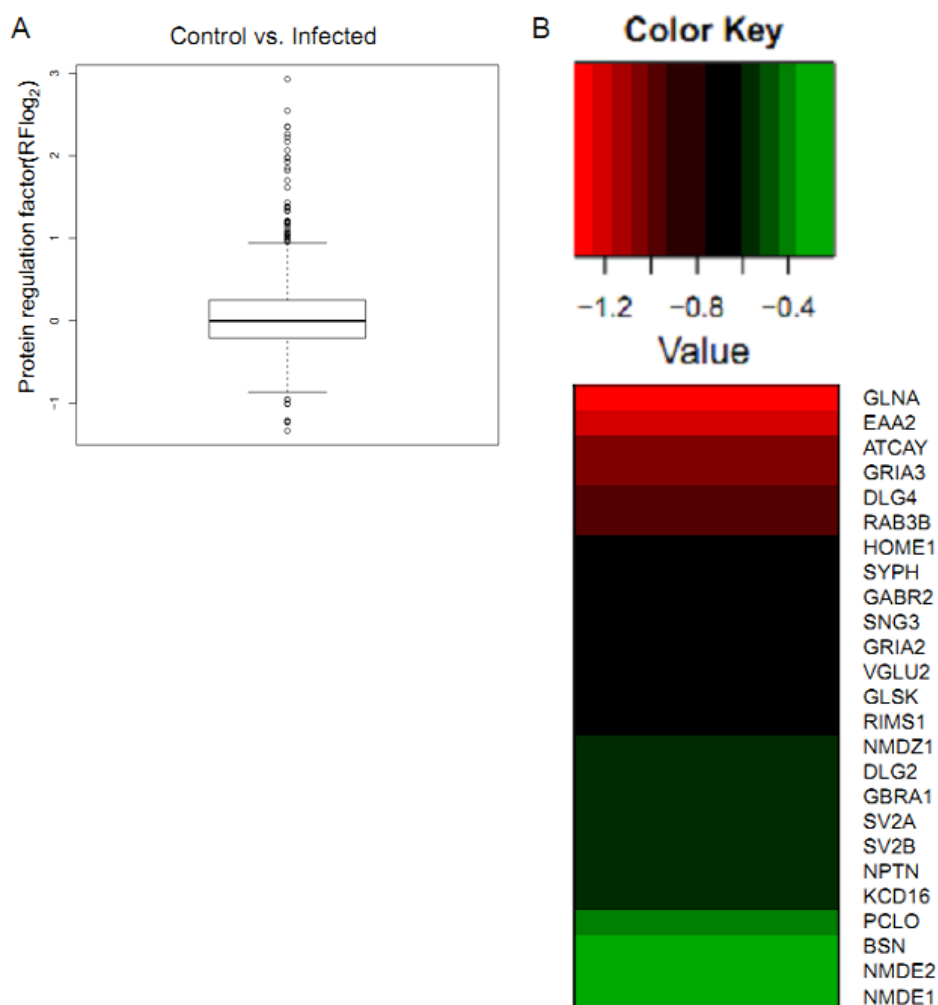


Figure 18. Statistical evaluation of synaptosome protein data

(A) Box plot of protein regulation factors in control and infected cortical and hippocampal synaptosomes determined by iTRAQ-based LC-MS/MS quantitation. Each box displays 50% of all determined protein regulation factors, the box height depicts their spreading and the black line within the boxes indicated the median. The restricting lines (high and low whiskers) display 1.5 X height of the box. All protein regulation factors above or beneath the whiskers are categorized as strongly regulated and are shown as open dots. (B) Heat map of \log_2 -protein regulation factors of 25 selected candidates, with significant reduced levels. Heat maps were generated by loading the list of selected proteins into the statistical program R. Colored boxes display the regulation factors corresponding to the indicated color code (top).

UniProt accession name	UniProt accession number	Protein name	Biological functions	Pathology	References
ATCAY	Q8BHE3	Caytaxin	Regulates glutaminase, the enzyme responsible for glutamate production by neurons	Jittery phenotype, which is characterized by severe truncal and limb ataxia	(256)
BSN	O88737	Protein Bassoon	Neurotransmitter release in brain glutamatergic synapses	Altered excitability attributed to inactivation of brain glutamatergic synapses.	(257)
DLG2	Q91XM9	Disk large homolog 2	Part of the postsynaptic protein scaffold of excitatory synapses, regulates surface expression of NMDA receptors	Reduced response to persistent pain. Postsynaptic surface expression of NMDA receptors and NMDA receptor-mediated synaptic function are reduced.	(258)
DLG4	Q62108	Disk large homolog 4 (PSD-95)	Required for synaptic plasticity associated with NMDA receptor signaling.	Impaired spatial learning, altered NMDA-mediated synaptic plasticity.	(259)
EAA2	P43006	Excitatory amino-acid transporter 2	Transport of L-glutamate, glutamate re-uptake from the synaptic cleft.	-	-
GABR2	Q80T41	γ -aminobutyric acid type B receptor subunit 2	Component of G-protein coupled receptor for GABA, implicated in synaptic inhibition but also in hippocampal long-term potentiation	-	-
GBRA1	P62812	γ -aminobutyric acid receptor subunit alpha-1	Component of the receptor for GABA.	-	-
GLNA	P15105	Glutamine synthetase	Catalyzes the production of glutamine and γ -aminobutyric acid.	-	-
GLSK	D3Z7P3	Glutaminase kidney isoform, mitochondrial	Regulates the levels of the neurotransmitter glutamate in the brain.	Normal levels of activity but disorganized.	(260)
GRIA2	P23819	Glutamate receptor 2 (AMPA2)	Receptor for glutamate that functions as ligand-gated ion channel in the CNS, key role in excitatory synaptic transmission.	-	-
GRIA3	Q9Z2W9	Glutamate receptor 3 (AMPA3)	Receptor for glutamate that functions as ligand-gated ion channel in the CNS, key role in excitatory synaptic transmission.	-	-
HOME1	Q9Z2Y3	Homer protein homolog 1	Postsynaptic density scaffolding protein.	-	-
KCD16	Q5DTY9	BTB/POZ domain-containing protein KCTD16	Auxiliary subunit of GABA-B receptors that determine the pharmacology and kinetics of the receptor response.	-	(261)
NMDE1	P35436	Glutamate receptor ionotropic, NMDA 2A	NMDA receptor subtype of glutamate-gated ion channels.	-	-
NMDE2	Q01097	Glutamate receptor ionotropic, NMDA 2B	NMDA receptor subtype of glutamate-gated ion channels.	-	(262)
NMDZ1	P35438	Glutamate receptor ionotropic, NMDA 1	NMDA receptor subtype of glutamate-gated ion channels. Key role in synaptic plasticity, synaptogenesis, excitotoxicity, memory acquisition and learning.	-	-
NPTN	P97300	Neuroplastin	Cell adhesion molecule involved in long term potentiation at hippocampal excitatory synapses, role in synaptic plasticity	-	-
PCLO	Q9QYX7	Protein piccolo	Scaffolding protein involved in the organization of synaptic active zones and in synaptic vesicle trafficking	-	(263)
RAB3B	Q9CZT8	Ras-related protein Rab-3B	Protein transport. Probably involved in vesicular traffic	-	-

UniProt accession name	UniProt accession number	Protein name	Biological functions	Pathology	References
RIMS1	Q99NE5	Regulating synaptic membrane exocytosis protein 1	Essential for maintaining normal neurotransmitter release and for regulating release during short-term synaptic plasticity.	-	-
SNG3	Q8R191	Synaptogyrin-3	Positive regulation of dopamine transporter activity	-	-
SV2A	Q9JIS5	Synaptic vesicle glycoprotein 2A	Regulates neurotransmitter vesicle fusion by maintaining the readily releasable pool of secretory vesicles	Severe epileptic seizures	(264)
SV2B	Q8BG39	Synaptic vesicle glycoprotein 2B	Role in the control of regulated secretion in neural and endocrine cells.	Severe epileptic seizures	(265)
SYPH	Q62277	Synaptophysin	Regulation of short-term and long-term synaptic plasticity	Impaired short-term and long-term synaptic plasticity	(266)
VGLU2	Q8BLE7	Vesicular glutamate transporter 2	Mediates the uptake of glutamate into synaptic vesicles at presynaptic nerve terminals of excitatory neural cells.	Reduction in evoked glutamergic responses	(267)

Table 4. Summary of proteins strongly downregulated during chronic cerebral infection with *T. gondii*

List of 25 identified proteins with decreased level in the synaptosomes. Included are the UniProt (<http://www.uniprot.org/>) accession names and numbers, protein names as well as the biological functions and reported involvement in pathology.

10. Glutamate receptor abnormalities in the synapses of infected mice

Previous reports have shown that synaptic dysfunction can be a consequence of prolonged neuroinflammation, suggesting that inflammatory processes modulate the changes from physiological synaptic transmission to impaired functioning (213,214,218). In the CNS, glutamate receptors are synaptic receptors important for neural communication, memory formation, learning, and regulation (268,269). Altered glutamate AMPA and NMDA ionotropic receptor function/presence have been showed to contribute to a variety of neurological and neuropsychiatric conditions (270–272). To determine whether *T. gondii* infection induces synaptic dysfunctions due to glutamate subunit expression alterations, we compared the expression level of the NMDA receptor subunits NR1, NR2A and NR2B, as well as AMPA receptor subunits AMPA1 and AMPA2, in cortical and hippocampal synaptic junction fractions of chronically infected mice and noninfected littermates.

Western blot analysis revealed that protein expression levels of AMPA 1 and 2 subunits was not significantly altered between groups (Figure 19A, B; relative intensities normalized to GAPDH: AMPA1, cortex: control animals, 1.328 ± 0.18 ; infected mice, 1.605 ± 0.16 ; $p=0.2$; AMPA1, hippocampus: control animals, 0.915 ± 0.05 ; infected mice, 0.856 ± 0.06 ; $p=0.5$; AMPA2, cortex: control animals, 0.98 ± 0.16 ; infected mice, 0.702 ± 0.06 ; $p=0.1$; AMPA2, hippocampus: control animals, 1.258 ± 0.2 ; infected mice, 1.439 ± 0.29 ; $p=0.6$; unpaired Student's t test).

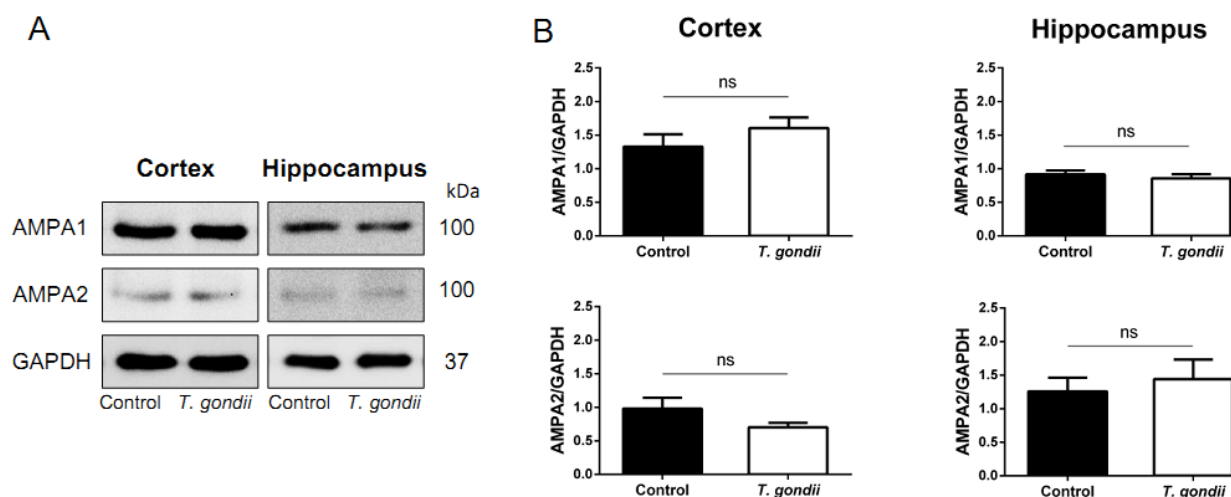


Figure 19. The expression of glutamate receptor subunits AMPA1 and AMPA2 is not altered by chronic infection with *T. gondii*

(A) Representative blots from the cortex and hippocampus synaptic junction fractions of control and *T. gondii* infected mice, used for the quantification of glutamatergic receptor subunits AMPA1 and AMPA2 protein level. (B) Densitometric analysis of AMPA1 and AMPA2 protein levels revealed no significant change in *T. gondii* infected mice when compared with controls. Analysis was performed in two independent experiments. Data are expressed as mean±SEM, n=3-4 mice per group. n.s., not significant

Interestingly, in contrast to AMPA receptor subunits, protein expression levels of NMDA subunits NR1, NR2A and the NR2B were significantly decreased in the synaptic junction fraction of infected mice (Figure 20A, B; relative intensities normalized to GAPDH: NR1, cortex: control animals, 1.195 ± 0.07 ; infected mice, 0.664 ± 0.06 ; $p=0.0002$; NR1, hippocampus: control animals, 1.215 ± 0.10 ; infected mice, 0.695 ± 0.09 ; $p=0.003$; NR2A, cortex: control animals, 0.938 ± 0.05 ; infected mice, 0.323 ± 0.04 ; $p<0.0001$; NR2A, hippocampus: control animals, 1.015 ± 0.03 ; infected mice, 0.3688 ± 0.07 ; $p<0.0001$; NR2B, cortex: control animals, 1.055 ± 0.09 ; infected mice, 0.665 ± 0.06 ; $p=0.005$; NR2B, hippocampus: control animals, 0.969 ± 0.04 ; infected mice, 0.608 ± 0.08 ; $p=0.004$; unpaired Student's t test), although the effect on NR2A levels appeared to be greater.

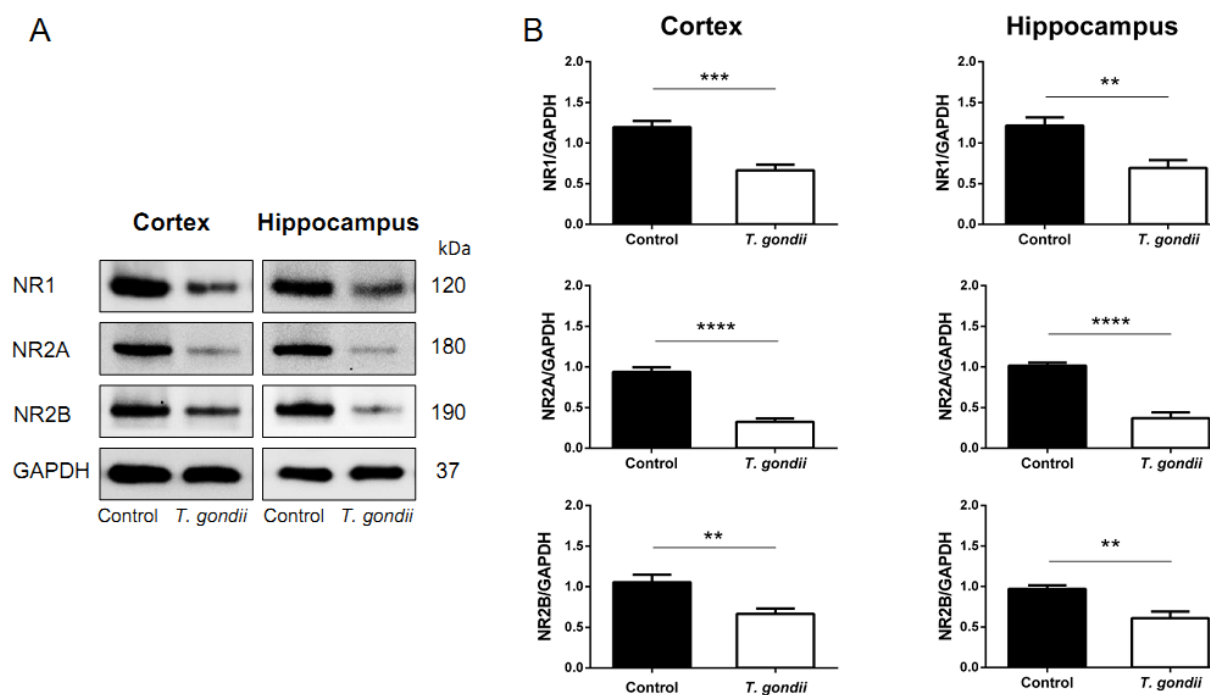


Figure 20. Chronic infection with *T. gondii* is associated with NMDA receptor subunit abnormalities

(A) Representative blots from the cortex and hippocampus synaptic junction fractions of control and *T. gondii* infected mice, used for the quantification of glutamatergic receptor subunits NR1, NR2A and NR2B protein level. Particularly, the levels of NR2A appear highly reduced in synaptic junctions of infected mice, in both cortex and hippocampus. (B) Quantification of NR1, NR2A and NR2B protein levels confirmed the significant reduction in mice infected with *T. gondii*, suggesting synapse dysfunction. Analysis was performed in two independent experiments. Data are expressed as mean±SEM, n=3-4 mice per group. **p<0.01, *** p<0.001, **** p<0.0001

11. Akt/GSK3 β signaling defects in the cortex of chronically infected mice

Proteomic analysis of the synaptosome fraction revealed that chronic infection of the nervous system is associated with alterations of the Akt dependent signaling pathway (Figure 17). The Akt signaling pathway is a major upstream signaling regulator of GSK3 β . It is activated upon phosphorylation at threonine (Thr308) and serine (Ser473) residues, and once active phosphorylates downstream targets such as GSK3 β (273–275). Akt/GSK3 β pathway regulates multiple substrates, including metabolic, signaling, and structural proteins and transcription factors (274,275). It has been hypothesized that impaired Akt/GSK3 β signaling may provide an important molecular mechanism contributing to the pathology of neuropsychiatric illnesses (273–275), therefore we sought evidence for the presence of molecular and functional changes in the AKT/GSK3 β pathway.

First, we explored the effects of *T. gondii* induced neuroinflammation on cortical Akt protein expression and phosphorylation using western blot analyses. We found that chronic infection with *T. gondii* results in increased levels of Akt phosphorylation on threonine 308 and serine 473 sites, in whole cortex homogenates (Figure 21C, D, relative intensities normalized to GAPDH: pAkt (Ser473), control mice 0.587 ± 0.13 ; infected mice 1.753 ± 0.06 ; $p=0.0002$; pAkt (Thr308), control mice 1.356 ± 0.16 ; infected mice 2.212 ± 0.14 ; $p=0.01$; unpaired Student's t test). In contrast to these effects, the infection and neuroimmune activation did not significantly alter the expression of total Akt in the cortex (Figure 21A, B, relative intensities normalized to GAPDH: control mice 1.085 ± 0.03 ; infected mice 1.007 ± 0.07 ; $p=0.4$; unpaired Student's t test).

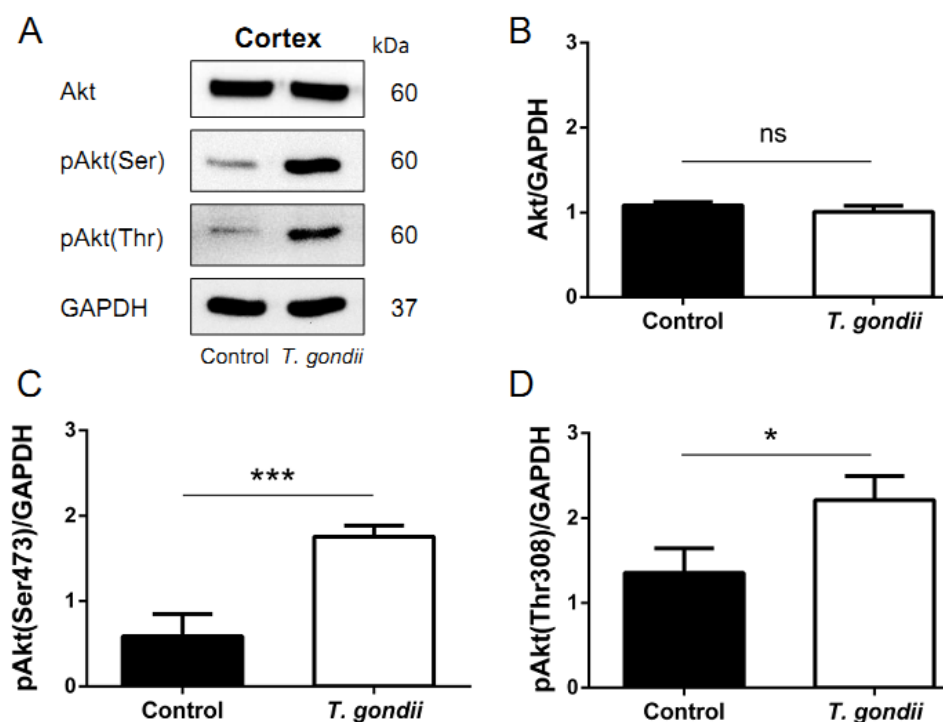


Figure 21. Effects of *T. gondii* induced neuroinflammation on Akt expression and phosphorylation

(A) Western blot analysis of total Akt (pan), phosphorylated Akt (Ser473) or Akt (Thr308) levels in extracts prepared from cortex homogenates of control and chronically infected mice. GAPDH was used as a loading control. (B-D) Densitometric analysis of Akt (B), pAkt (Ser473) (C), and pAkt (Thr308) (D) revealed that chronic toxoplasmosis is associated with a strong activation of Akt protein kinase as indicated by the significant increase of both phosphorylated Akt protein levels. Analysis was performed in two independent experiments. Data are expressed as mean \pm SEM, n=4-5 mice per group. *p<0.05, ***p<0.001, n.s, not significant

In the next step, we evaluated the effects of chronic neuroinflammation on the expression of total and phosphorylated GSK3 β , in the cortex, by measuring the mRNA and protein levels. As shown in Figure 22A, the samples from infected mice did not show a statistical difference in the GSK3 β mRNA levels as compared to controls (control mice 0.126 \pm 0.002; infected mice 0.119 \pm 0.002; p=0.3; unpaired Student's t test). In line with this result, no significant group differences were found with respect to the total GSK3 β protein levels (Figure 22B, C, relative intensities normalized to GAPDH: control mice 0.982 \pm 0.1; infected mice 0.848 \pm 0.04; p=0.2; unpaired Student's t test). However, an additional analysis of the phosphorylated GSK3 β protein demonstrated a statistically significant increase in the relative GSK3 β phosphorylation levels in the cortex of mice infected with *T. gondii* (Figure 22B, D: relative

intensities normalized to GAPDH: pGSK3 β (Ser9), control mice 1.187 ± 0.1 ; infected mice 1.502 ± 0.04 ; $p=0.03$).

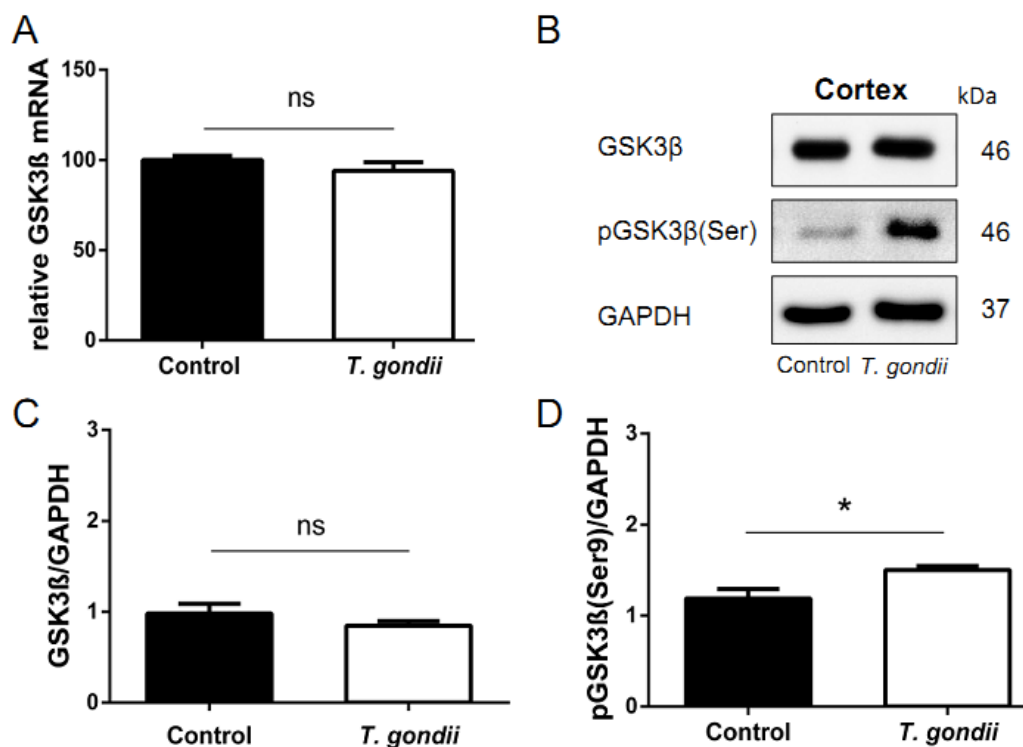


Figure 22. Effects of *T. gondii* induced neuroinflammation on GSK3 β expression and phosphorylation

(A) To assess the effect of *T. gondii* infection on GSK3 β protein kinase, mRNA expression for GSK3 β was assessed by real-time quantitative PCR (corrected for the housekeeping gene HPRT) after extracting total RNA from cortex. Data are normalized to control mice. (B) Photomicrographs show western blot samples for total GSK3 β and Ser9-phosphorylated GSK3 β in extracts prepared from cortex homogenates of noninfected (control) and chronically infected mice. GAPDH is shown as loading control for comparison. Densitometric analysis of total GSK3 β (C) and pGSK3 β (Ser9) (D) protein levels indicates that chronic toxoplasmosis elevates GSK3 β phosphorylation at Ser 9 site, suggesting an inhibitory activity over GSK3 β . Analysis was performed in two independent experiments. Data are expressed as mean \pm SEM, $n=4-5$ mice per group. * $p<0.05$, n.s, not significant

Discussion

Behavioral changes triggered by *T. gondii* in rodents have been extensively discussed in recent years (157,159,160,166,171,276,277). Several clinical studies claimed a possible association between *T. gondii* seropositivity and neurological diseases in humans, but no sufficient explanation or underlying mechanisms have been described to date (12,13,121,131–133,137,146,278,279). These specific behavioral and neurological changes occur, not exclusively, due to focal brain abnormalities associated with parasite cyst localization, but might be a result of pathological interactions between different brain areas. Furthermore, the dysregulation of the inflammatory milieu, neurotransmitter imbalance, as well as synaptic plasticity could contribute to this effect.

Converging evidence provided by advances in imaging techniques in recent years confirms a close relationship between disturbances in brain networks and debilitating neuropsychiatric disorders in humans with cognitive and psychomotor impairments (224,225,228,280–283). The core pathology of dysconnectivity syndromes resides mostly in aberrant synaptic plasticity due to disturbed interaction between neurotransmitters, neurotransmitter receptors and different immunological factors (216,217,223). Therefore, we have explored the impact of *T. gondii*-induced microlesions on the whole mouse brain neuronal circuitry as well as on the morphology of individual noninfected neurons, and we correlated the neuroanatomical alterations in those areas with changes in the synapse efficacy as possible contributing factors for the behavioral and neurological deficits.

In contrast to other studies, which have investigated the location of *T. gondii* cysts in specific brain areas, we focused our analysis on the position of *T. gondii*-induced lesions. These lesions are detectable in a variety of neuroanatomical areas where complex neuro-immunological dynamics occur. Initially, we combined the conventional MRI (based on T2- and T2*-contrasts) and DT-MRI with a global fiber tracking algorithm in order to identify the

brain areas with the highest density of *T. gondii*-induced lesions and to further assess their impact on the neuronal circuitry pattern. The SSC, motor cortices, hippocampus and striatal brain structures were depicted as primary sites with altered T2*-MR based contrast, suggesting substantial neuroanatomical changes within these brain regions of the infected mice. A previous study by Hermes *et al.* (284) evaluated the chronic *T. gondii* infection by T2-weighted MRI; however, they observed only moderate ventricular dilatation in infected mice. The reason for the disparate findings could be that T2-based MR contrast is less sensitive compared to T2*-weighted MRI for visualizing the brain microlesions. Alternatively, in their study, the authors have used a different mouse strain, thus the genetic resistance to infection of Swiss Webster mice could also play an important role.

Histological examination revealed that *T. gondii*-induced lesions were constituted by activated resident glia cells, as well as recruited mononuclear cells and a few neutrophil granulocytes and lymphocytes, similar to the description by Gulinello *et al.* (104,168). Cell-mediated immunity confers protection against *T. gondii* through the production of inflammatory molecules such as IL-1, IL-4, IL-5, IL-6, IL-8, IL-12, IL-15, IL-18, IL-22, TNF, IFN- γ , NO and others which engage distinct pathways and specific effector mechanisms required for the appropriate control of the infection (29,74,104,285,286).

Most of the inflammatory mediators are potentially toxic for neurons (287–289). For example, neurons are highly susceptible to NO, and the toxic effects of this molecule have a central role in the pathophysiology of several neurodegenerative and demyelinating disorders (290,291). Therefore, one would expect a high rate of degenerating neurons associated with the presence of *T. gondii* in the brain. Interestingly, by using specific markers for neuronal death (FluoroJadeB), we observed only limited neurodegeneration in the CNS of mice chronically infected. Moreover, another study performed in a murine model of Alzheimer's disease suggests that infection with *T. gondii* inhibits neuronal degeneration (292). A possible explanation is provided by a study of Rozenfeld *et al.* where they demonstrate that IFN- γ activated microglia have an active role in neuronal protection by stimulating the production of transforming growth factor beta-1 which inhibits iNOS (293). These results suggest that neurodegeneration is, at most, a marginal factor in the etiology of behavioral and neurological changes associated with chronic toxoplasmosis.

We observed random distribution of *T. gondii* cysts, with no preference to specific brain areas, corresponding with the previous results by Gulinello *et al.* (168) and Berenreiterová *et al.* (170), whereas other groups reported elevated cyst numbers in certain brain regions of infected animals (164,166). Furthermore, the location of the cysts was also random in one recent study investigating a rat model in which the infection is associated with limited inflammation (172). In our experiments, the low number of *T. gondii* cysts and the corresponding moderate number of infected neurons suggest that, in addition to the infected cells, other components might alter neuronal morphology and function.

The inflammatory milieu produced by resident glial cells as well as recruited immune cells, can specifically influence neuronal function and communication. It was previously described that increases of pro-inflammatory cytokines lead to abnormal synaptic plasticity (213,216,217). In the case of chronic *T. gondii* infection, it is possible that continuous production of inflammatory molecules will lead to changes in synaptic plasticity and abnormal wiring of brain connections. Further detailed studies should identify the specific pathophysiological mechanisms as well as the exact character and source of inflammatory mediators.

Detailed qualitative and quantitative analysis of neuronal fibers using DT-MRI and hrFM revealed the impact of *T. gondii* infection on regional and global mouse brain connective microstructure. This novel approach is currently the only methodology providing a non-invasive window into the whole brain structural connectivity (201). We took advantage of this new technique and demonstrated not only a loss of fiber continuity and density at lesion sites, but also substantial alterations in the general wiring scheme. This involved GM cortical and subcortical changes as assessed by the reduced FD and FA values, but also significant abnormalities along major WM tracts. DT-MRI findings in SSC were paralleled by modifications of neuronal cytoskeletal protein levels, verifying the validity of our *in vivo* approach. Notably, infected mice displayed reduced expression of neurofilament (clone SMI311) and microtubule (MAP2) in the SSC and hippocampus. Qualitative evaluation of immunofluorescence images revealed a clear reduction of SMI311 and MAP2 immunoreactivity, confirming abnormalities along the cortical and hippocampal dendritic trees. Importantly, quantification of MAP2 content in the cortex by western blot confirmed the reduced expression levels of this protein. Given the roles of neurofilaments and microtubules in the radial growth of axons and dendrites, leading to the stabilization and

maturation of neuronal connections (294–296), we suggest that the altered expression of these two proteins supports the existence of abnormalities in axonal and dendritic morphology in the SSC with possible functional consequences on behavior.

Moreover, our analysis unveiled a pattern of *T. gondii*-induced white matter pathology. We showed such modifications, first by *in vivo* DT-MRI and then by electron microscopy. Reduced FA values in white matter areas along with significantly increased radial diffusivity were associated with myelin abnormalities. The electron micrographs revealed clear decompaction as well as degeneration of the myelin lamellae in *T. gondii*-infected brains. To our knowledge, evidence of *T. gondii*-induced white matter microstructural changes has not been shown previously. Interestingly, white matter changes revealed by DT-MRI were located along important tracts, such as the corpus callosum, cingulum and internal capsule. Impaired inter-hemispherical callosal connectivity would certainly functionally affect the somatosensory system, given the direct connections of the left and right SSC through this pathway. Cingulum is another fiber pathway known for allowing communication between components of the limbic system and projecting in areas such as the entorhinal cortex or hippocampus. Such pathological processes characterized by white matter structural alterations in the mentioned brain areas are likely to contribute to functional impairments associated with behavioral modifications.

To further explore the structural alterations underlying the changes in the brain connectivity, we focused our study to closely investigate the morphological modifications suffered by noninfected pyramidal neurons in the somatosensory cortical layers II/III, upon chronic infection with *T. gondii*. Pyramidal cells in layer III are excitatory neurons involved in projections between various brain areas contributing to fundamental sensory and cognitive processes. Precise morphological analysis of individual pyramidal neurons from the indicated areas revealed impaired dendritic branching both for the apical and the basal dendrites in infected mice compared with noninfected controls. Extending these findings to the hippocampus, we report a reduction of total dendritic complexity of the neurons located in the CA1 and DG regions, suggesting that these changes might be intimately related to dysfunctions in the memory and learning processes of mice chronically infected with *T. gondii*. Changes in dendritic morphology predict changes in the number of dendritic spines that are responsible for information exchange. Dendritic spines are specialized membrane protrusions located on neuronal dendrites; they have a very complex structure and

fundamental functions in the synaptic physiology and plasticity (197). Spine abnormalities have been observed in several neurological and psychiatric disorders (197,297). We found a significant reduction in the number of spines within the pyramidal neurons of layers II/III for apical, as well as for basal dendrites. Morphological changes such as significant reduction in spine length were additionally detected. Because layer II/III pyramidal cells are intercortical neurons, the loss of dendritic spine number and morphological abnormalities can be associated with disrupted communications between higher cortical areas, thus providing a possible explanation for the behavioral alterations. Our results suggest that neuronal changes in chronic *T. gondii* infection is a consequence of the interplay between the host immune system and the CNS, rather than a direct effect of the parasites on individual neurons within a specific brain region.

Similar results were reported in other brain structures as well as in the neuronal components of the enteric nervous system. In an attempt to identify the possible mechanisms employed by *T. gondii* to reduce fear response as part of the manipulation of the host, Mitra *et al.* show in a rat model of chronic infection that *T. gondii* causes a retraction of dendritic arborization in basolateral amygdala neurons (298). The enteric nervous system is a collection of neurons that integrates all aspects of motility, secretion, immune and inflammatory processes of the gastrointestinal tract (299–301). Several studies provided experimental evidence that chronic infection with *T. gondii* elicits morphological changes of neuronal subpopulations found in the wall of different segments of the gastrointestinal tract (302–306). Nevertheless, all these results suggest that morphological alterations of the neurons during latent infection might not be an epiphenomenon and may be biologically relevant. Additional methods will need to be employed to test the functional implications of these findings and to clarify the precise nature of those alterations in *T. gondii* infected mice.

Synapses provide the physical basis for communication within the brain, and the ability of synapses to maintain their integrity and functionality is critical to maintain proper CNS function. Dysfunction in proteins that regulate synaptic plasticity likely contributes to the development of neuropsychiatric disorders (307–309). In my project I went beyond previous studies by analyzing the long-term effects of cerebral infection with *T. gondii* in adult cortical and hippocampal synapse. The study revealed reduced concentrations of multiple individual synaptic proteins, many of which are key to optimal synaptic efficacy. These findings are the first to provide molecular and cellular clues regarding the changes at the level of the synapse

to elucidate the known behavioral and neurological abnormalities in mice upon chronic infection with *T. gondii*. Importantly, we measured significantly lower synaptophysin and PSD95 protein levels in infected mice compared with noninfected mice by western blot, indicating clear alteration in integrity and functionality within mature synapses of mice infected with *T. gondii*. Synaptophysin is involved in modulation of the efficiency of the synaptic vesicle cycle (266,310), whereas the function of PSD95 is the correct assembly of the postsynaptic density complex (311,312). A recent study using synaptophysin-deficient mice reported impaired memory and spatial-learning capacities and reduced novelty recognition (313), similar to mice infected with *T. gondii*. Decreased expression of synaptophysin associated with cognitive decline has been described in the adult rat brain in a model of chronic induced neuroinflammation (314). PSD95 activity is tightly linked to normal regulation of synaptic plasticity (259,315). Abnormalities in PSD95 and related postsynaptic-density-complex molecules can contribute to abnormal synaptic plasticity, which structurally correlates to changes in the morphology or distribution of dendrites and dendritic spines (316,317).

Pathway analysis allowed us to uncover previously unknown negative effects of the infection on signaling pathways that play critical roles in adult cognitive function. A major finding is the lasting negative impact on glutamatergic neurotransmission, specifically on the NMDA receptors. Although the synaptoproteome analysis implicated both AMPA and NMDA receptors, western blot experiments demonstrate a significant reduced expression of NMDA receptor subunits NR1, NR2A and NR2B. The apparently contradictory results might be explained by the difference in the sample number. The structure and the role of NMDA receptors in a variety of normal and pathological brain processes have been extensively reviewed elsewhere (271,272,318). Particularly the roles of NR1, NR2A and NR2B subunits of NMDA receptor have been reported, in animal models as well as in humans, to have clinical implications.

NR1 is indispensable for all the constructions of NMDA receptors and distributes ubiquitously in the brain (319,320). The deficit with the expression of NR1 in the brain have been associated with depression and psychoses in animal models as well as in human patients (321–323). The NR2A subunits distributes widely, but the levels of its expression are higher in the cerebral cortex, the hippocampus and cerebellar granule cells (322). The diheteromeric NR1/NR2A subunits have been suggested to be involved in depression and

anxiety-like behaviour, and hippocampal-dependent behaviour (324–326). Studies performed in mice suggested NR2B to play essential roles in learning, memory and neuronal pattern formation, as mice overexpressing the NR2B subunits exhibit superior ability of learning and memory while mice lacking the subunit exhibit impaired formation of whisker-related neuronal barrelette structure in the somatosensory cortex (327). Recent reports indicate that alterations in the NR2B expression are involved in certain aspects of seizure disorder, schizophrenia, Alzheimer's disease and Huntington's disease (327). Interestingly, several studies investigating the neurological basis of anxiety have shown that blockade of NMDA receptors, using pharmacological antagonists, causes noninfected rats to approach cat odors fearlessly (328,329). Cytokines and inflammatory mediators such as IFN- γ , TNF, NO, IL-1 and IL-6, commonly present during toxoplasmic encephalitis may affect NMDA receptors via activation of indoleamine-2,3-dioxygenase enzyme (IDO). Increased expression of IDO elicits the degradation of tryptophan, the essential amino-acid, which is the precursor of serotonin (330,331). Tryptophan degradation by IDO leads to increased concentrations of two neuroactive metabolites, quinolinic acid (QA) and kynurenic acid (KA) (332). A recent study confirmed that one month after infection with a type II *T. gondii* strain, there was a dramatically increased concentration of both KA and QA in the brains of infected mice (333). In human patients, excessive QA and KA levels have been correlated with a number of neurodegenerative disorders, depression and schizophrenia (332,334–336). Produced primarily by microglia, QA binds to NMDARs inducing excitotoxicity and oxidative stress in the brain (332,337). Kynurenic acid, which is produced primarily in astrocytes, is a potent antagonist of NMDARs, leading thus to disturbances in glutamatergic and dopaminergic neurotransmission (332,337).

Another interesting finding resulted from pathway analysis is the involvement of phosphatidylinositol 3-OH kinase (PI3K) enzymes family via serine-threonine kinase Akt complex. PI3K signaling is involved in cellular functions such as cell growth, proliferation, differentiation, motility, survival and intracellular trafficking (338,339). Activation of PI3K occurs through binding to cellular receptors located on plasma membrane, including toll like receptors (TLRs) (339), and mediates the recruitment of Akt. After recruitment, Akt, which is a key regulator of PI3K pathway, is activated by phosphorylation at Thr308 and Ser473 (273,275). Activated Akt phosphorylates the constitutively active serine-threonine kinase GSK3 β (Ser9). Phosphorylation of GSK3 β (Ser9) results in its inhibition (275,340).

Akt/GSK3 β signaling pathway plays pivotal roles in the brain by regulating several metabolic, signaling, and structural proteins and transcription factors, and thus influences neuronal plasticity and neurodegeneration (275). Additionally, dysregulation of Akt/GSK3 β activity contribute to the pathogenesis of neuropsychiatric disorders, such as mood disorders and schizophrenia (341,342). In our study, following chronic infection with *T. gondii*, we could detect a vigorous expression of pAkt (Thr308) and pAkt (Ser473) protein levels in the cortex, indicating an increased activation of Akt. In line with this result we could show inhibition of GSK3 β activity, as reflected by increased pGSK3 β (Ser9) protein levels. We speculate that the increased activation of Akt might be, at least partially, due to presence of parasites which are recognized and activate TLRs (236). Moreover, the inhibition of GSK3 β could represent a protective mechanisms meant to reduce the impact of proinflammatory molecules on brain parenchyma. GSK3 β has been recognized as the control switch for the regulation of pro- and anti-inflammatory response (343). Several lines of evidence from studies with other pathogens, like *Burkholderia pseudomallei* and *Francisella tularensis*, indicated that pharmacological inhibition of GSK3 β is beneficial as indicated by the improved survivability of acutely infected mice and reduction of pro-inflammatory cytokine levels (344,345). Akt/GSK3 β pathway is also a therapeutic target for neurological disorders (346). For example, drugs like lithium chloride (LiCl), valproic acid, haloperidol, clozapine and olanzapine are known to inhibit GSK3, directly, or indirectly by activating Akt, and are now widely used in the treatment of several mental disorders (346). Interestingly, Webster *et al.* have demonstrated that *T. gondii*-infected rats treated with anti-psychotic (haloperidol) and mood stabilizing (valproic acid) medications did not developed altered behavioral profiles displayed by their untreated but infected littermates (347). Although the authors conclude that the effect on behavior is due to inhibited replication of *T. gondii* (138,347), thus reducing the parasite burden in the brain, no evidence to support this hypothesis is provided. Instead we suggest that the effect of the antipsychotic drugs could be due to modulation of Akt/GSK3 β pathway. Further experiments should address this hypothesis and clarify the involvement of Akt/GSK3 β upstream and downstream signaling molecules in the *T. gondii*-induced neuropathology.

In conclusion, the results presented herein indicate that upon latent infection with *T. gondii*, marked neuroanatomical and synaptic functional changes occur in CNS regions that are relevant to normal biological functions of the brain. We suggest that the described alterations

might contribute to the reported behavior and neuropsychiatric changes observed in chronic *T. gondii* infection, and establish a murine model for translational studies of chronic toxoplasmosis. Identification of the synaptic signaling pathways may allow more specific manipulations to alter their activity in order to demonstrate the causal effects of chronic infection with *T. gondii* as well as to establish targets for therapeutic development.

References

1. Tenter A, Heckeroth A, Weiss L. *Toxoplasma gondii*: from animals to humans. *Int J Parasitol* 2000. **30** : 1217–58.
2. Montoya JG, Liesenfeld O. Toxoplasmosis. *Lancet* 2004. **363** : 1965–76.
3. Dubey JP. The history of *Toxoplasma gondii*--the first 100 years. *J Eukaryot Microbiol* 2008. **55** : 467–75.
4. Ferguson DJP. *Toxoplasma gondii*: 1908-2008, homage to Nicolle, Manceaux and Splendore. *Mem Inst Oswaldo Cruz* 2009. **104** : 133–48.
5. Sabin A, Olitsky PK. *Toxoplasma* and obligate intracellular parasitism. *Science (80-)* 1906. **85** : 336–8.
6. Wolf A, Cowen D, Paige B. Human toxoplasmosis: occurrence in infants as an encephalomyelitis verified by transmission to animals. *Science (80-)* 1938. **89** : 1938–9.
7. Dubey JP. A review of toxoplasmosis in wild birds. *Vet Parasitol* 2002. **106** : 121–53.
8. Quencer RM, Post MJ. Spinal cord lesions in patients with AIDS. *Neuroimaging Clin N Am* 1997. **7** : 359–73.
9. Maciel E, Siqueira I, Queiroz AC, Melo A. *Toxoplasma gondii* myelitis in a patient with adult T-cell leukemia-lymphoma. *Arq Neuropsiquiatr* 2000. **58** : 1107–9.
10. Flegr J. Effects of *Toxoplasma* on human behavior. *Schizophr Bull* 2007. **33** : 757–60.
11. Flegr J. Influence of latent *Toxoplasma* infection on human personality, physiology and morphology: pros and cons of the *Toxoplasma*-human model in studying the manipulation hypothesis. *J Exp Biol* 2013. **216** : 127–33.
12. Yereli K, Balcioglu IC, Özbilgin A. Is *Toxoplasma gondii* a potential risk for traffic accidents in Turkey? *Forensic Sci Int* 2006. **163** : 34–7.
13. Fabiani S, Pinto B, Bruschi F. Toxoplasmosis and neuropsychiatric diseases: can serological studies establish a clear relationship? *Neurol Sci* 2013. **34** : 417–25.
14. Luft BJ, Brooks RG, Conley FK, McCabe RE, Remington JS. Toxoplasmic encephalitis in patients with acquired immune deficiency syndrome. *JAMA* 1984. **252** : 913–7.
15. Dubey JP, Lindsay DS, Speer CA. Structures of *Toxoplasma gondii* tachyzoites, bradyzoites, and sporozoites and biology and development of tissue cysts. *Clin Microbiol Rev* 1998. **11** : 267–99.
16. Barragan A, Sibley LD. Transepithelial migration of *Toxoplasma gondii* is linked to parasite motility and virulence. *J Exp Med* 2002. **195** : 1625–33.
17. Barragan A, Brossier F, Sibley LD. Transepithelial migration of *Toxoplasma gondii* involves an interaction of intercellular adhesion molecule 1 (ICAM-1) with the parasite adhesion MIC2. *Cell Microbiol* 2005. **7** : 561–8.
18. Saeij JPJ, Boyle JP, Coller S, et al. Polymorphic secreted kinases are key virulence factors in toxoplasmosis. *Science* 2006. **314** : 1780–3.
19. Dobrowolski JM, Sibley LD. *Toxoplasma* invasion of mammalian cells is powered by the actin cytoskeleton of the parasite. *Cell* 1996. **84** : 933–9.
20. Tomavo S. The differential expression of multiple isoenzyme forms during stage conversion of *Toxoplasma gondii*: An adaptive developmental strategy. *Int J Parasitol* 2001. **31** : 1023–31.

-
21. Lyons RE, McLeod R, Roberts CW. Toxoplasma gondii tachyzoite-bradyzoite interconversion. *Trends Parasitol* 2002. **18** : 198–201.
22. Sullivan WJ, Jeffers V. Mechanisms of Toxoplasma gondii persistence and latency. *FEMS Microbiol Rev* 2012. **36** : 717–33.
23. Dubey JP. Advances in the life cycle of Toxoplasma gondii. *Int J Parasitol* 1998. **28** : 1019–24.
24. Tilley M, Fichera ME, Jerome ME, Roos DS, White MW. Toxoplasma gondii sporozoites form a transient parasitophorous vacuole that is impermeable and contains only a subset of dense-granule proteins. *Infect Immun* 1997. **65** : 4598–605.
25. Poukchanski A, Fritz HM, Tonkin ML, et al. Toxoplasma gondii Sporozoites Invade Host Cells Using Two Novel Paralogues of RON2 and AMA1. *PLoS One* 2013. **8**.
26. Dubey JP. Toxoplasma gondii oocyst survival under defined temperatures. *J Parasitol* 1998. **84** : 862–5.
27. Torrey EF, Yolken RH. Toxoplasma oocysts as a public health problem. *Trends Parasitol* 2013. **29** : 380–4.
28. Tenter AM, Heckeroth AR, Weiss LM. Toxoplasma gondii: from animals to humans. *Int J Parasitol* 2000. **30** : 1217–58.
29. Hunter CA, Sibley LD. Modulation of innate immunity by Toxoplasma gondii virulence effectors. *Nat Rev Microbiol* 2012. **10** : 766–78.
30. Jones JL, Dubey JP. Foodborne toxoplasmosis. *Clin Infect Dis* 2012. **55** : 845–51.
31. Denkers EY, Gazzinelli RT. Regulation and function of T-cell-mediated immunity during Toxoplasma gondii infection. *Clin Microbiol Rev* 1998. **11** : 569–88.
32. Kang H, Remington JS, Suzuki Y. Decreased resistance of B cell-deficient mice to infection with Toxoplasma gondii despite unimpaired expression of IFN-gamma, TNF-alpha, and inducible nitric oxide synthase. *J Immunol* 2000. **164** : 2629–34.
33. Buzoni-Gatel D, Schulthess J, Menard LC, Kasper LH. Mucosal defences against orally acquired protozoan parasites, emphasis on Toxoplasma gondii infections. *Cell Microbiol* 2006. **8** : 535–44.
34. Kasper L, Courret N, Darche S, et al. Toxoplasma gondii and mucosal immunity. *Int J Parasitol* 2004. **34** : 401–9.
35. Ju C-H, Chockalingam A, Leifer CA. Early response of mucosal epithelial cells during Toxoplasma gondii infection. *J Immunol* 2009. **183** : 7420–7.
36. Munoz M, Liesenfeld O, Heimesaat MM. Immunology of Toxoplasma gondii. *Immunol Rev* 2011. **240** : 269–85.
37. Liesenfeld O, Kosek J, Remington JS, Suzuki Y. Association of CD4+ T cell-dependent, interferon-gamma-mediated necrosis of the small intestine with genetic susceptibility of mice to peroral infection with Toxoplasma gondii. *J Exp Med* 1996. **184** : 597–607.
38. Schreiner M, Liesenfeld O. Small intestinal inflammation following oral infection with Toxoplasma gondii does not occur exclusively in C57BL/6 mice: review of 70 reports from the literature. *Mem Inst Oswaldo Cruz* 2009. **104** : 221–33.
39. Courret N, Darche S, Sonigo P, et al. CD11c- and CD11b-expressing mouse leukocytes transport single Toxoplasma gondii tachyzoites to the brain. *Blood* 2006. **107** : 309–16.
40. Dunay IR, Sibley LD. Monocytes mediate mucosal immunity to Toxoplasma gondii. *Curr Opin Immunol* 2010. **22** : 461–6.
41. Dunay IR, DaMatta RA, Fux B, et al. Gr1+ Inflammatory Monocytes Are Required for Mucosal Resistance to the Pathogen Toxoplasma gondii. *Immunity* 2008. **29** : 306–17.
42. Unno A, Suzuki K, Xuan X, et al. Dissemination of extracellular and intracellular Toxoplasma gondii tachyzoites in the blood flow. *Parasitol Int* 2008. **57** : 515–8.
43. Channon JY, Seguin RM, Kasper LH. Differential infectivity and division of Toxoplasma gondii in human peripheral blood leukocytes. *Infect Immun* 2000. **68** : 4822–6.
44. Coombes JL, Charsar B a, Han S-J, et al. Motile invaded neutrophils in the small intestine of Toxoplasma gondii-infected mice reveal a potential mechanism for parasite spread. *Proc Natl Acad Sci U S A* 2013. **110** : E1913–22.
45. Fadul CE, Channon JY, Kasper LH. Survival of immunoglobulin G-opsonized Toxoplasma gondii in nonadherent human monocytes. *Infect Immun* 1995. **63** : 4290–4.
-

-
46. Blader IJ, Saeij JP. Communication between *Toxoplasma gondii* and its host: Impact on parasite growth, development, immune evasion, and virulence. *APMIS* 2009. **117** : 458–76.
47. Sinai AP, Payne TM, Carmen JC, et al. Mechanisms underlying the manipulation of host apoptotic pathways by *Toxoplasma gondii*. *Int J Parasitol* 2004. **34** : 381–91.
48. Lüder CGK, Stanway RR, Chaussepied M, Langsley G, Heussler VT. Intracellular survival of apicomplexan parasites and host cell modification. *Int J Parasitol* Australian Society for Parasitology Inc.; 2009. **39** : 163–73.
49. Lambert H, Hitziger N, Dellacasa I, Svensson M, Barragan A. Induction of dendritic cell migration upon *Toxoplasma gondii* infection potentiates parasite dissemination. *Cell Microbiol* 2006. **8** : 1611–23.
50. Hitziger N, Dellacasa I, Albiger B, Barragan A. Dissemination of *Toxoplasma gondii* to immunoprivileged organs and role of Toll/interleukin-1 receptor signalling for host resistance assessed by in vivo bioluminescence imaging. *Cell Microbiol* 2005. **7** : 837–48.
51. Lachenmaier SM, Deli MA, Meissner M, Liesenfeld O. Intracellular transport of *Toxoplasma gondii* through the blood-brain barrier. *J Neuroimmunol* 2011. **232** : 119–30.
52. Hunter CA, Roberts CW, Alexander J. Kinetics of cytokine mRNA production in the brains of mice with progressive toxoplasmic encephalitis. *Eur J Immunol* 1992. **22** : 2317–22.
53. Wilson EH, Hunter CA. The role of astrocytes in the immunopathogenesis of toxoplasmic encephalitis. *Int J Parasitol* 2004. **34** : 543–8.
54. Sarciron ME, Gherardi A. Cytokines involved in Toxoplasmic encephalitis. *Scand J Immunol* 2000. **52** : 534–43.
55. Suzuki Y. Immunopathogenesis of cerebral toxoplasmosis. *J Infect Dis* 2002. **186** : 234–40.
56. Suzuki Y. Host resistance in the brain against *Toxoplasma gondii*. *J Infect Dis* 2002. **185** : 58–65.
57. Chao CC, Hu S, Gekker G, et al. Effects of cytokines on multiplication of *Toxoplasma gondii* in microglial cells. *J Immunol* 1993. **150** : 3404–10.
58. Ferguson DJ, Hutchison WM, Pettersen E. Tissue cyst rupture in mice chronically infected with *Toxoplasma gondii*. An immunocytochemical and ultrastructural study. *Parasitol Res* 1989. **75** : 599–603.
59. Sims TA, Hay J, Talbot IC. An electron microscope and immunohistochemical study of the intracellular location of *Toxoplasma* tissue cysts within the brains of mice with congenital toxoplasmosis. *Br J Exp Pathol* 1989. **70** : 317–25.
60. Lüder CG, Giraldo-Velásquez M, Sendtner M, Gross U. *Toxoplasma gondii* in primary rat CNS cells: differential contribution of neurons, astrocytes, and microglial cells for the intracerebral development and stage differentiation. *Exp Parasitol* 1999. **93** : 23–32.
61. Fagard R, Van Tan H, Creuzet C, Pelloux H. Differential development of *Toxoplasma gondii* in neural cells. *Parasitol Today* 1999. **15** : 504–7.
62. Creuzet C, Robert F, Roisin MP, et al. Neurons in primary culture are less efficiently infected by *Toxoplasma gondii* than glial cells. *Parasitol Res* 1998. **84** : 25–30.
63. Melzer TC, Cranston HJ, Weiss LM, Halonen SK. Host Cell Preference of *Toxoplasma gondii* Cysts in Murine Brain: A Confocal Study. *J Neuroparasitology* 2010. **1** : 1–6.
64. Strack A, Asensio VC, Campbell IL, Schlüter D, Deckert M. Chemokines are differentially expressed by astrocytes, microglia and inflammatory leukocytes in *Toxoplasma* encephalitis and critically regulated by interferon-gamma. *Acta Neuropathol* 2002. **103** : 458–68.
65. Schlüter D, Deckert M, Hof H, Frei K. *Toxoplasma gondii* Infection of Neurons Induces Neuronal Cytokine and Chemokine Production, but Gamma Interferon- and Tumor Necrosis Factor-Stimulated Neurons Fail To Inhibit the Invasion. *Infect Immun* 2001. **69** : 7889–93.
66. Jebbari H, Roberts CW, Ferguson DJP, Bluethmann H, Alexander J. A protective role for IL-6 during early infection with *Toxoplasma gondii*. *Parasite Immunol* 1998. **20** : 231–9.
67. Suzuki Y, Conley FK, Remington JS. Importance of endogenous IFN-gamma for prevention of toxoplasmic encephalitis in mice. *J Immunol* 1989. **143** : 2045–50.
68. Suzuki Y, Sa Q, Gehman M, Ochiai E. Interferon-gamma- and perforin-mediated immune responses for resistance against
-

- Toxoplasma gondii in the brain. *Expert Rev Mol Med* 2011. **13**.
69. Gazzinelli RT, Xu Y, Hieny S, Cheever A, Sher A. Simultaneous depletion of CD4+ and CD8+ T lymphocytes is required to reactivate chronic infection with Toxoplasma gondii. *J Immunol* 1992. **149** : 175–80.
70. Reichmann G, Walker W, Villegas EN, et al. The CD40/CD40 ligand interaction is required for resistance to toxoplasmic encephalitis. *Infect Immun* 2000. **68** : 1312–8.
71. Andrade RM, Portillo J-AC, Wessendarp M, Subauste CS. CD40 signaling in macrophages induces activity against an intracellular pathogen independently of gamma interferon and reactive nitrogen intermediates. *Infect Immun* 2005. **73** : 3115–23.
72. Aline F, Bout D, Dimier-Poisson I. Dendritic cells as effector cells: gamma interferon activation of murine dendritic cells triggers oxygen-dependent inhibition of Toxoplasma gondii replication. *Infect Immun* 2002. **70** : 2368–74.
73. Adams LB, Hibbs JB, Taintor RR, Krahenbuhl JL. Microbiostatic effect of murine-activated macrophages for Toxoplasma gondii. Role for synthesis of inorganic nitrogen oxides from L-arginine. *J Immunol* 1990. **144** : 2725–9.
74. Dupont CD, Christian DA, Hunter CA. Immune response and immunopathology during toxoplasmosis. *Semin Immunopathol* 2012. **34** : 793–813.
75. Combe CL, Curiel TJ, Moretto MM, Khan IA. NK cells help to induce CD8(+)-T-cell immunity against Toxoplasma gondii in the absence of CD4(+) T cells. *Infect Immun* 2005. **73** : 4913–21.
76. Lütjen S, Soltek S, Virna S, Deckert M, Schlüter D. Organ- and disease-stage-specific regulation of Toxoplasma gondii-specific CD8-T-cell responses by CD4 T cells. *Infect Immun* 2006. **74** : 5790–801.
77. Denkers EY, Yap G, Schar-ton-Kersten T, et al. Perforin-mediated cytotoxicity plays a limited role in host resistance to Toxoplasma gondii. *J Immunol* 1997. **159** : 1903–8.
78. Yap GS, Shaw MH, Ling Y, Sher A. Genetic analysis of host resistance to intracellular pathogens: lessons from studies of Toxoplasma gondii infection. *Microbes Infect* 2006. **8** : 1174–8.
79. Tait ED, Hunter CA. Advances in understanding immunity to Toxoplasma gondii. *Mem Inst Oswaldo Cruz* 2009. **104** : 201–10.
80. Boehm U, Klamp T, Groot M, Howard JC. Cellular responses to interferon-gamma. *Annu Rev Immunol* 1997. **15** : 749–95.
81. Fentress SJ, Behnke MS, Dunay IR, et al. Phosphorylation of immunity-related GTPases by a toxoplasma gondii-secreted kinase promotes macrophage survival and virulence. *Cell Host Microbe* 2010. **8** : 484–95.
82. Howard JC, Hunn JP, Steinfeldt T. The IRG protein-based resistance mechanism in mice and its relation to virulence in Toxoplasma gondii. *Curr Opin Microbiol* 2011. **14** : 414–21.
83. Zhao YO, Khaminets A, Hunn JP, Howard JC. Disruption of the Toxoplasma gondii parasitophorous vacuole by IFN γ -inducible immunity-related GTPases (IRG proteins) triggers necrotic cell death. *PLoS Pathog* 2009. **5**.
84. Butcher BA, Greene RI, Henry SC, et al. p47 GTPases regulate Toxoplasma gondii survival in activated macrophages. *Infect Immun* 2005. **73** : 3278–86.
85. Brunet LR. Nitric oxide in parasitic infections. *Int Immunopharmacol* 2001. **1** : 1457–67.
86. Bogdan C. Nitric oxide and the immune response. *Nat Immunol* 2001. **2** : 907–16.
87. Forstermann U, Gath I, Schwarz P, Closs EI, Kleinert H. Isoforms of nitric oxide synthase. Properties, cellular distribution and expressional control. *Biochem Pharmacol* 1995. **50** : 1321–32.
88. Liesenfeld O, Kang H, Park D, et al. TNF- α , nitric oxide and IFN- γ are all critical for development of necrosis in the small intestine and early mortality in genetically susceptible mice infected perorally with Toxoplasma gondii. *Parasite Immunol* 1999. **21** : 365–76.
89. Schar-ton-Kersten TM, Yap G, Magram J, Sher A. Inducible nitric oxide is essential for host control of persistent but not acute infection with the intracellular pathogen Toxoplasma gondii. *J Exp Med* 1997. **185** : 1261–73.
90. Chakravorty D, Hensel M. Inducible nitric oxide synthase and control of intracellular bacterial pathogens. *Microbes Infect* 2003. **5** : 621–7.

-
91. Murray PJ. Macrophages as a battleground for toxoplasma pathogenesis. *Cell Host Microbe* 2011. **9** : 445–7.
92. Murray HW, Rubin BY, Carriero SM, Harris AM, Jaffee EA. Human mononuclear phagocyte antiprotozoal mechanisms: oxygen-dependent vs oxygen-independent activity against intracellular *Toxoplasma gondii*. *J Immunol* 1985. **134** : 1982–8.
93. Dimier IH, Bout DT. Interferon-gamma-activated primary enterocytes inhibit *Toxoplasma gondii* replication: A role for intracellular iron. *Immunology* 1998. **94** : 488–95.
94. Miller CM, Boulter NR, Ikin RJ, Smith NC. The immunobiology of the innate response to *Toxoplasma gondii*. *Int J Parasitol* 2009. **39** : 23–39.
95. Sibley LD, Messina M, Niesman IR. Stable DNA transformation in the obligate intracellular parasite *Toxoplasma gondii* by complementation of tryptophan auxotrophy. *Proc Natl Acad Sci U S A* 1994. **91** : 5508–12.
96. Gazzinelli RT, Eltoun I, Wynn TA, Sher A. Acute cerebral toxoplasmosis is induced by in vivo neutralization of TNF-alpha and correlates with the down-regulated expression of inducible nitric oxide synthase and other markers of macrophage activation. *J Immunol* 1993. **151** : 3672–81.
97. Schlüter D, Kwok L-Y, Lütjen S, et al. Both lymphotoxin-alpha and TNF are crucial for control of *Toxoplasma gondii* in the central nervous system. *J Immunol* 2003. **170** : 6172–82.
98. Yap GS, Schariton-Kersten T, Charest H, Sher A. Decreased resistance of TNF receptor p55- and p75-deficient mice to chronic toxoplasmosis despite normal activation of inducible nitric oxide synthase in vivo. *J Immunol* 1998. **160** : 1340–5.
99. Nathan CF, Murray HW, Wiebe ME, Rubin BY. Identification of interferon-gamma as the lymphokine that activates human macrophage oxidative metabolism and antimicrobial activity. *J Exp Med* 1983. **158** : 670–89.
100. Mordue DG, Sibley LD. A novel population of Gr-1+ activated macrophages induced during acute toxoplasmosis. *J Leukoc Biol* 2003. **74** : 1015–25.
101. Carruthers VB, Suzuki Y. Effects of *Toxoplasma gondii* infection on the brain. *Schizophr Bull* 2007. **33** : 745–51.
102. Pittella JEH. Pathology of CNS parasitic infections. *Handb Clin Neurol* 2013. **114** : 65–88.
103. Hunter CA, Remington JS. Immunopathogenesis of toxoplasmic encephalitis. *J Infect Dis* 1994. **170** : 1057–67.
104. Möhle L, Parlog A, Pahnke J, Dunay IR. Spinal cord pathology in chronic experimental *Toxoplasma gondii* infection. *Eur J Microbiol Immunol (Bp)* 2014. **4** : 65–75.
105. Silva MG da, Lino Jr R de S, da Costa TL, et al. Anatomopathological study in BALB/c mice brains experimentally infected with *Toxoplasma gondii*. *Braz J Infect Dis* 2008. **12** : 52–6.
106. Ferguson DJ, Graham DI, Hutchison WM. Pathological changes in the brains of mice infected with *Toxoplasma gondii*: a histological, immunocytochemical and ultrastructural study. *Int J Exp Pathol* 1991. **72** : 463–74.
107. Conley FK, Jenkins KA. Immunohistological study of the anatomic relationship of toxoplasma antigens to the inflammatory response in the brains of mice chronically infected with *Toxoplasma gondii*. *Infect Immun* 1981. **31** : 1184–92.
108. Boothroyd JC, Grigg ME. Population biology of *Toxoplasma gondii* and its relevance to human infection: do different strains cause different disease? *Curr Opin Microbiol* 2002. **5** : 438–42.
109. Caiaffa WT, Chiari CA, Figueiredo ARP, Orefice F, Antunes CMF. Toxoplasmosis and mental retardation: report of a case-control study. *Mem Inst Oswaldo Cruz* 1993. **88** : 253–61.
110. Torgerson PR, Mastroiacovo P. The global burden of congenital toxoplasmosis: a systematic review. *Bull World Health Organ* 2013. **91** : 501–8.
111. Moncada PA, Montoya JG. Toxoplasmosis in the fetus and newborn: an update on prevalence, diagnosis and treatment. *Expert Rev Anti Infect Ther* 2012. **10** : 815–28.
112. Berrébi A, Assouline C, Bessières M-H, et al. Long-term outcome of children with congenital toxoplasmosis. *Am J Obstet Gynecol* 2010. **203** : 552.e1–6.
-

-
113. Brown AS, Schaefer CA, Quesenberry CP, et al. Maternal exposure to toxoplasmosis and risk of schizophrenia in adult offspring. *Am J Psychiatry* 2005. **162** : 767–73.
114. Mortensen PB, Nørgaard-Pedersen B, Waltoft BL, et al. Toxoplasma gondii as a Risk Factor for Early-Onset Schizophrenia: Analysis of Filter Paper Blood Samples Obtained at Birth. *Biol Psychiatry* 2007. **61** : 688–93.
115. Selten JP, Kahn RS. Schizophrenia after prenatal exposure to Toxoplasma gondii? *Clin Infect Dis* 2002. **35** : 633–4.
116. Kasper LD, Braunwald E, Hauser S, et al. Protozoal infections-Toxoplasma infection. Principles of Internal Medicine 16th ed. McGraw-Hill Medical Publishing Division; 2005.
117. Holliman RE. Toxoplasmosis, behaviour and personality. *J Infect* 1997. **35** : 105–10.
118. Webster JP. Rats, cats, people and parasites: The impact of latent toxoplasmosis on behaviour. *Microbes Infect* 2001. **3** : 1037–45.
119. Havlíček J, Gasová ZG, Smith AP, Zvára K, Flegr J. Decrease of psychomotor performance in subjects with latent “asymptomatic” toxoplasmosis. *Parasitology* 2001. **122** : 515–20.
120. Beste C, Getzmann S, Gajewski PD, Golka K, Falkenstein M. Latent Toxoplasma gondii infection leads to deficits in goal-directed behavior in healthy elderly. *Neurobiol Aging* 2014. **35** : 1037–44.
121. Flegr J, Havlíček J, Kodym P, Malý M, Smahel Z. Increased risk of traffic accidents in subjects with latent toxoplasmosis: a retrospective case-control study. *BMC Infect Dis* 2002. **2** : 11.
122. Flegr J, Klose J, Novotná M, Berenreitterová M, Havlíček J. Increased incidence of traffic accidents in Toxoplasma-infected military drivers and protective effect RhD molecule revealed by a large-scale prospective cohort study. *BMC Infect Dis* 2009. **9** : 72.
123. Kocazeybek B, Oner YA, Turksoy R, et al. Higher prevalence of toxoplasmosis in victims of traffic accidents suggest increased risk of traffic accident in Toxoplasma-infected inhabitants of Istanbul and its suburbs. *Forensic Sci Int* 2009. **187** : 103–8.
124. Stock AK, Heintschel von Heinegg E, Köhling HL, Beste C. Latent Toxoplasma gondii infection leads to improved action control. *Brain Behav Immun* 2014. **37** : 103–8.
125. Yolken RH, Dickerson FB, Fuller Torrey E. Toxoplasma and schizophrenia. *Parasite Immunol* 2009. **31** : 706–15.
126. Flegr J, Zitková S, Kodym P, Frynta D. Induction of changes in human behaviour by the parasitic protozoan Toxoplasma gondii. *Parasitology* 1996. **113** : 49–54.
127. Flegr J, Hrdý I. Influence of chronic toxoplasmosis on some human personality factors. *Folia Parasitol (Praha)* 1994. **41** : 122–6.
128. Lindova J, Novotna M, Havlicek J, et al. Gender differences in behavioural changes induced by latent toxoplasmosis. *Int J Parasitol* 2006. **36** : 8.
129. Freedman R. Schizophrenia. *N Engl J Med* 2003. **349** : 1738–49.
130. Brown AS. Prenatal infection as a risk factor for schizophrenia. *Schizophr Bull* 2006. **32** : 200–2.
131. Wang HL, Wang GH, Li QY, et al. Prevalence of Toxoplasma infection in first-episode schizophrenia and comparison between Toxoplasma-seropositive and Toxoplasma-seronegative schizophrenia. *Acta Psychiatr Scand* 2006. **114** : 40–8.
132. Torrey EF, Yolken RH. Toxoplasma gondii and schizophrenia. *Emerg Infect Dis* 2003. **9** : 1375–80.
133. Hinze-Selch D, Däubener W, Eggert L, et al. A controlled prospective study of Toxoplasma gondii infection in individuals with schizophrenia: Beyond seroprevalence. *Schizophr Bull* 2007. **33** : 782–8.
134. Arias I, Sorlozano A, Villegas E, et al. Infectious agents associated with schizophrenia: A meta-analysis. *Schizophr Res* 2012. **136** : 128–36.
135. Torrey EF, Bartko JJ, Lun ZR, Yolken RH. Antibodies to Toxoplasma gondii in patients with schizophrenia: A meta-analysis. *Schizophr Bull* 2007. **33** : 729–36.
136. Amminger GP, McGorry PD, Berger GE, et al. Antibodies to Infectious Agents in Individuals at Ultra-High Risk for Psychosis. *Biol Psychiatry* 2007. **61** : 1215–7.
137. Zhu S. Psychosis may be associated with toxoplasmosis. *Med Hypotheses* 2009. **73** : 799–801.
-

138. Goodwin DG, Strobl JS, Lindsay DS. Evaluation of five antischizophrenic agents against *Toxoplasma gondii* in human cell cultures. *J Parasitol* 2011. **97** : 148–51.
139. Jones-Brando L. Drugs used in the treatment of schizophrenia and bipolar disorder inhibit the replication of *Toxoplasma gondii*. *Schizophrenia Research*. 2003. p. 237–44.
140. Pearce BD, Kruszon-Moran D, Jones JL. The relationship between *Toxoplasma Gondii* infection and mood disorders in the third national health and nutrition survey. *Biol Psychiatry* 2012. **72** : 290–5.
141. Kar N, Misra B. *Toxoplasma* seropositivity and depression: a case report. *BMC Psychiatry* 2004. **4** : 1.
142. Gror MW, Yolken RH, Xiao JC, et al. Prenatal depression and anxiety in *Toxoplasma gondii* positive women. *Am J Obstet Gynecol* 2011. **204**.
143. Miman O, Mutlu EA, Ozcan O, et al. Is there any role of *Toxoplasma gondii* in the etiology of obsessive-compulsive disorder? *Psychiatry Res* 2010. **177** : 263–5.
144. Brynska A, Tomaszewicz-Libudziec E, Wolanczyk T. Obsessive-compulsive disorder and acquired toxoplasmosis in two children. *Eur Child Adolesc Psychiatry* 2001. **10** : 200–4.
145. Okusaga O, Langenberg P, Sleemi A, et al. *Toxoplasma gondii* antibody titers and history of suicide attempts in patients with schizophrenia. *Schizophr Res* 2011. **133** : 150–5.
146. Arling TA, Yolken RH, Lapidus M, et al. *Toxoplasma gondii* antibody titers and history of suicide attempts in patients with recurrent mood disorders. *J Nerv Ment Dis* 2009. **197** : 905–8.
147. Yagmur F, Yazar S, Temel HO, Cavusoglu M. May *Toxoplasma gondii* increase suicide attempt-preliminary results in Turkish subjects? *Forensic Sci Int* 2010. **199** : 15–7.
148. Kusbeci OY, Miman O, Yaman M. Could *Toxoplasma gondii* Have any Role in Alzheimer Disease? 2011. **25** : 1–3.
149. Celik T, Kamisli O, Babur C, et al. Is there a relationship between *Toxoplasma gondii* infection and idiopathic Parkinson's disease? *Scand J Infect Dis* 2010. **42** : 604–8.
150. Miman O, Kusbeci OY, Aktepe OC, Cetinkaya Z. The probable relation between *Toxoplasma gondii* and Parkinson's disease. *Neurosci Lett* 2010. **475** : 129–31.
151. Brown AS. Epidemiologic studies of exposure to prenatal infection and risk of schizophrenia and autism. *Dev Neurobiol* 2012. **72** : 1272–6.
152. Krause D, Matz J, Weidinger E, et al. Association between intracellular infectious agents and Tourette's syndrome. *Eur Arch Psychiatry Clin Neurosci* 2010. **260** : 359–63.
153. Akyol A, Bicerol B, Ertug S, Ertabaklar H, Kiylioglu N. Epilepsy and seropositivity rates of *Toxocara canis* and *Toxoplasma gondii*. *Seizure* 2007. **16** : 233–7.
154. Prandota J. The importance of *toxoplasma gondii* infection in diseases presenting with headaches. Headaches and aseptic meningitis may be manifestations of the Jarisch-Herxheimer reaction. *Int J Neurosci* 2009. **119** : 2144–82.
155. Prandota J. Migraine associated with patent foramen ovale may be caused by reactivation of cerebral toxoplasmosis triggered by arterial blood oxygen desaturation. *Int J Neurosci* 2010. **120** : 81–7.
156. Webster JP. Prevalence and transmission of *Toxoplasma gondii* in wild brown rats, *Rattus norvegicus*. *Parasitology* 1994. **108** (Pt 4) : 407–11.
157. Hutchinson WM, Bradley M, Cheyne WM, Wells BW, Hay J. Behavioural abnormalities in *Toxoplasma*-infected mice. *Ann Trop Med Parasitol* 1980. **74** : 337–45.
158. Webster JP, Brunton CFA, Macdonald DW. Effect of *Toxoplasma-Gondii* Upon Neophobic Behavior in Wild Brown-Rats, *Rattus-Norvegicus*. *Parasitology* 1994. **109** : 37–43.
159. Berdoy M, Webster JP, Macdonald DW. The manipulation of rat behaviour by *Toxoplasma gondii*. *Mammalia* 1995. **59**.
160. Berdoy M, Webster JP, Macdonald DW. Fatal attraction in rats infected with *Toxoplasma gondii*. *Proc Biol Sci* 2000. **267** : 1591–4.
161. Biben M. Predation and predatory play behaviour of domestic cats. *Animal Behaviour*. 1979. p. 81–94.
162. Blackshaw JK. *The Domestic Cat: The Biology of its Behaviour*. Applied Animal Behaviour Science. 2001. p. 259–61.

-
163. Vyas A, Kim SK, Sapolsky RM. The effects of toxoplasma infection on rodent behavior are dependent on dose of the stimulus. *Neuroscience* 2007. **148** : 342–8.
164. Haroon F, Handel U, Angenstein F, et al. Toxoplasma gondii actively inhibits neuronal function in chronically infected mice. *PLoS One* 2012. **7**.
165. Ingram WM, Goodrich LM, Robey EA, Eisen MB. Mice Infected with Low-Virulence Strains of Toxoplasma gondii Lose Their Innate Aversion to Cat Urine, Even after Extensive Parasite Clearance. *PLoS One* 2013. **8**.
166. Vyas A, Kim S-K, Giacomini N, Boothroyd JC, Sapolsky RM. Behavioral changes induced by Toxoplasma infection of rodents are highly specific to aversion of cat odors. *Proc Natl Acad Sci U S A* 2007. **104** : 6442–7.
167. Lamberton PHL, Donnelly CA, Webster JP. Specificity of the Toxoplasma gondii-altered behaviour to definitive versus non-definitive host predation risk. *Parasitology* 2008. **135** : 1143–50.
168. Gulinello M, Acquarone M, Kim JH, et al. Acquired infection with Toxoplasma gondii in adult mice results in sensorimotor deficits but normal cognitive behavior despite widespread brain pathology. *Microbes Infect* 2010. **12** : 528–37.
169. Gatkowska J, Wiczorek M, Dziadek B, Dzitko K, Długonska H. Behavioral changes in mice caused by Toxoplasma gondii invasion of brain. *Parasitol Res* 2012. **111** : 53–8.
170. Berenreiterová M, Flegr J, Kuběna AA, Nĕmec P. The distribution of Toxoplasma gondii cysts in the brain of a mouse with latent toxoplasmosis: implications for the behavioral manipulation hypothesis. *PLoS One* 2011. **6** : e28925.
171. McConkey GA, Martin HL, Bristow GC, Webster JP. Toxoplasma gondii infection and behaviour - location, location, location? *J Exp Biol* 2013. **216** : 113–9.
172. Evans AK, Strassmann PS, Lee IP, Sapolsky RM. Patterns of Toxoplasma gondii cyst distribution in the forebrain associate with individual variation in predator odor avoidance and anxiety-related behavior in male Long-Evans rats. *Brain Behav Immun* 2014. **37** : 122–33.
173. LeDoux J. The emotional brain, fear, and the amygdala. *Cellular and Molecular Neurobiology*. 2003. p. 727–38.
174. Fanselow MS, Poulos AM. The neuroscience of mammalian associative learning. *Annu Rev Psychol* 2005. **56** : 207–34.
175. Berenreiterova M, Flegr J, Kubena AA, Nemecek P. The distribution of Toxoplasma gondii cysts in the brain of a mouse with latent toxoplasmosis: Implications for the behavioral manipulation hypothesis. *PLoS One* 2011. **6**.
176. Maeda T, Fujii T, Matsumura T, et al. AIDS-related cerebral toxoplasmosis with hyperintense foci on T1-weighted MR images: A case report. *J Infect* 2006. **53**.
177. Suzuki K, Masuya M, Matsumoto T, et al. High-intensity signals in the basal ganglia from gadolinium-enhanced T1-weighted MRI as an early change in toxoplasma encephalitis in an AIDS patient. *J Infect Chemother* 2010. **16** : 135–8.
178. Strittmatter C, Lang W, Wiestler OD, Kleihues P. The changing pattern of human immunodeficiency virus-associated cerebral toxoplasmosis: a study of 46 postmortem cases. *Acta Neuropathol* 1992. **83** : 475–81.
179. Conejero-Goldberg C, Torrey EF, Yolken RH. Herpesviruses and Toxoplasma gondii in orbital frontal cortex of psychiatric patients. *Schizophr Res* 2003. **60** : 65–9.
180. Gaskell EA, Smith JE, Pinney JW, Westhead DR, McConkey GA. A unique dual activity amino acid hydroxylase in Toxoplasma gondii. *PLoS One* 2009. **4**.
181. Prandovszky E, Gaskell E, Martin H, et al. The neurotropic parasite toxoplasma gondii increases dopamine metabolism. *PLoS One* 2011. **6**.
182. Money KM, Stanwood GD. Developmental origins of brain disorders: roles for dopamine. *Front Cell Neurosci* 2013. **7** : 260.
183. Brisch R, Saniotis A, Wolf R, et al. The role of dopamine in schizophrenia from a neurobiological and evolutionary perspective: old fashioned, but still in vogue. *Front psychiatry* 2014. **5** : 47.
184. Hamon M, Blier P. Monoamine neurocircuitry in depression and strategies for new treatments. *Prog Neuro-Psychopharmacology Biol Psychiatry* 2013. **45** : 54–63.
-

-
185. Mittal SK, Eddy C. The role of dopamine and glutamate modulation in Huntington disease. *Behav Neurol* 2013. **26** : 255–63.
186. Segura-Aguilar J, Paris I, Muñoz P, et al. Protective and toxic roles of dopamine in Parkinson's disease. *J Neurochem* 2014. **129** : 898–915.
187. Gatkowska J, Wiczorek M, Dziadek B, Dzitko K, Dlugonska H. Sex-dependent neurotransmitter level changes in brains of *Toxoplasma gondii* infected mice. *Exp Parasitol* 2013. **133** : 1–7.
188. Stibbs HH. Changes in brain concentrations of catecholamines and indoleamines in *Toxoplasma gondii* infected mice. *Ann Trop Med Parasitol* 1985. **79** : 153–7.
189. Saeij JPJ, Collier S, Boyle JP, et al. *Toxoplasma* co-opts host gene expression by injection of a polymorphic kinase homologue. *Nature* 2007. **445** : 324–7.
190. Boothroyd JC. Have It Your Way: How Polymorphic, Injected Kinases and Pseudokinases Enable *Toxoplasma* to Subvert Host Defenses. *PLoS Pathog* 2013. **9**.
191. Koshy AA, Dietrich HK, Christian DA, et al. *Toxoplasma* co-opts host cells it does not invade. *PLoS Pathog* 2012. **8** : 18.
192. Klein SL. Parasite manipulation of the proximate mechanisms that mediate social behavior in vertebrates. *Physiol Behav* 2003. **79** : 441–9.
193. Kaushik M, Lamberton PHL, Webster JP. The role of parasites and pathogens in influencing generalised anxiety and predation-related fear in the mammalian central nervous system. *Horm Behav* 2012. **62** : 191–201.
194. Kavaliers M, Colwell DD. Decreased predator avoidance in parasitized mice: neuromodulatory correlates. *Parasitology* 1995. **111** : 257–63.
195. Nokes C, Bundy DA. Does helminth infection affect mental processing and educational achievement? *Parasitol Today* 1994. **10** : 14–8.
196. Kandel E, Schwartz J, Jessell T. Principles of Neural Science. 4th ed. New York: McGraw-Hill; 2000.
197. Nimchinsky EA, Sabatini BL, Svoboda K. Structure and function of dendritic spines. *Annu Rev Physiol* 2002. **64** : 313–53.
198. Citri A, Malenka RC. Synaptic plasticity: multiple forms, functions, and mechanisms. *Neuropsychopharmacology* 2008. **33** : 18–41.
199. Brown A, Weaver LC. The dark side of neuroplasticity. *Experimental Neurology*. 2012. p. 133–41.
200. Pascual-Leone A, Freitas C, Oberman L, et al. Characterizing brain cortical plasticity and network dynamics across the age-span in health and disease with TMS-EEG and TMS-fMRI. *Brain Topogr* 2011. **24** : 302–15.
201. Harsan L-A, Dávid C, Reisert M, et al. Mapping remodeling of thalamocortical projections in the living reeler mouse brain by diffusion tractography. *Proc Natl Acad Sci U S A* 2013. **110** : E1797–806.
202. Le Bihan D. Looking into the functional architecture of the brain with diffusion MRI. *Int Congr Ser* 2006. **1290** : 1–24.
203. Reisert M, Mader I, Anastasopoulos C, et al. Global fiber reconstruction becomes practical. *Neuroimage* 2011. **54** : 955–62.
204. Mori S, Zhang J. Principles of diffusion tensor imaging and its applications to basic neuroscience research. *Neuron* 2006. **51** : 527–39.
205. Mori S, Van Zijl PCM. Fiber tracking: Principles and strategies - A technical review. *NMR in Biomedicine*. 2002. p. 468–80.
206. Rauskolb S, Zagrebelsky M, Dreznjak A, et al. Global deprivation of brain-derived neurotrophic factor in the CNS reveals an area-specific requirement for dendritic growth. *J Neurosci* 2010. **30** : 1739–49.
207. Heneka MT, Kummer MP, Stutz A, et al. NLRP3 is activated in Alzheimer's disease and contributes to pathology in APP/PS1 mice. *Nature* 2013. **493** : 674–8.
208. Streit WJ, Mrak RE, Griffin WST. Microglia and neuroinflammation: a pathological perspective. *J Neuroinflammation* 2004. **1** : 14.
209. Lyman M, Lloyd DG, Ji X, Vizcaychipi MP, Ma D. Neuroinflammation: The role and consequences. *Neurosci Res* 2014. **79** : 1–12.
210. Hemmer B, Archelos JJ, Hartung H-P. New concepts in the immunopathogenesis of multiple sclerosis. *Nat Rev Neurosci* 2002. **3** : 291–301.
-

-
211. Yirmiya R, Goshen I. Immune modulation of learning, memory, neural plasticity and neurogenesis. *Brain Behav Immun* Elsevier Inc.; 2011. **25** : 181–213.
212. Pribiag H, Stellwagen D. Neuroimmune regulation of homeostatic synaptic plasticity. *Neuropharmacology* Elsevier Ltd; 2014. **78** : 13–22.
213. Di Filippo M, Sarchielli P, Picconi B, Calabresi P. Neuroinflammation and synaptic plasticity: theoretical basis for a novel, immune-centred, therapeutic approach to neurological disorders. *Trends Pharmacol Sci* 2008. **29** : 402–12.
214. Haroon E, Raison CL, Miller AH. Psychoneuroimmunology Meets Neuropsychopharmacology: Translational Implications of the Impact of Inflammation on Behavior. *Neuropsychopharmacology* 2012. **37** : 137–62.
215. Wang X, Suzuki Y. Microglia produce IFN-gamma independently from T cells during acute toxoplasmosis in the brain. *J Interferon Cytokine Res* 2007. **27** : 599–605.
216. Coogan A, O'Connor JJ. Inhibition of NMDA receptor-mediated synaptic transmission in the rat dentate gyrus in vitro by IL-1 beta. *Neuroreport* 1997. **8** : 2107–10.
217. Curran B, O'Connor JJ. The pro-inflammatory cytokine interleukin-18 impairs long-term potentiation and NMDA receptor-mediated transmission in the rat hippocampus in vitro. *Neuroscience* 2001. **108** : 83–90.
218. Najjar S, Pearlman DM, Alper K, Najjar A, Devinsky O. Neuroinflammation and psychiatric illness. *J Neuroinflammation* 2013. **10** : 1–24.
219. Brietzke E, Stabellini R, Grassi-Oliveira R, Lafer B. Cytokines in Bipolar Disorder: Recent Findings, Deleterious Effects But Promise for Future Therapeutics. *CNS Spectr* 2011. **16** : 157–68.
220. Mansur RB, Zugman A, Asevedo EDM, et al. Cytokines in schizophrenia: Possible role of anti-inflammatory medications in clinical and preclinical stages. *Psychiatry Clin Neurosci* 2012. **66** : 247–60.
221. Miller BJ, Buckley P, Seabolt W, Mellor A, Kirkpatrick B. Meta-Analysis of Cytokine Alterations in Schizophrenia: Clinical Status and Antipsychotic Effects. *Biol Psychiatry* 2011. **70** : 663–71.
222. Stephan KE, Friston KJ, Frith CD. Dysconnection in Schizophrenia: From abnormal synaptic plasticity to failures of self-monitoring. *Schizophr Bull* 2009. **35** : 509–27.
223. Stephan KE, Baldeweg T, Friston KJ. Synaptic Plasticity and Dysconnection in Schizophrenia. *Biol Psychiatry* 2006. **59** : 929–39.
224. Vasic N, Walter H, Sambataro F, Wolf RC. Aberrant functional connectivity of dorsolateral prefrontal and cingulate networks in patients with major depression during working memory processing. *Psychol Med* 2009. **39** : 977–87.
225. Zalesky A, Fornito A, Seal ML, et al. Disrupted axonal fiber connectivity in schizophrenia. *Biol Psychiatry* 2011. **69** : 80–9.
226. Friston KJ. The disconnection hypothesis. *Schizophr Res* 1998. **30** : 115–25.
227. Hahn C, Lim HK, Lee CU. Neuroimaging findings in late-onset schizophrenia and bipolar disorder. *J Geriatr Psychiatry Neurol* 2014. **27** : 56–62.
228. Menzies L, Williams GB, Chamberlain SR, et al. White matter abnormalities in patients with obsessive-compulsive disorder and their first-degree relatives. *Am J Psychiatry* 2008. **165** : 1308–15.
229. Najjar S, Pearlman DM. Neuroinflammation and white matter pathology in schizophrenia: systematic review. *Schizophr Res* 2014.
230. Horacek J, Flegr J, Tintera J, et al. Latent toxoplasmosis reduces gray matter density in schizophrenia but not in controls: Voxel-based-morphometry (VBM) study. *World J Biol Psychiatry* 2012. **13** : 501–9.
231. Saper CB, Romanovsky AA, Scammell TE. Neural circuitry engaged by prostaglandins during the sickness syndrome. *Nat Neurosci* 2012. **15** : 1088–95.
232. Zheng X, Zhang X, Kang A, et al. Thinking outside the brain for cognitive improvement: Is peripheral immunomodulation on the way? *Neuropharmacology* Elsevier Ltd; 2014.
233. Carter CJ. Schizophrenia: a pathogenetic autoimmune disease caused by viruses and pathogens and dependent on genes. *J Pathog* 2011. **2011** : 128318.
234. Buzoni-Gatel D, Werts C. Toxoplasma gondii and subversion of the immune system. *Trends Parasitol* 2006. **22** : 448–52.
-

235. Denkers EY. Toll-like receptor initiated host defense against toxoplasma gondii. *J Biomed Biotechnol* 2010. **2010**.
236. Yarovinsky F. Innate immunity to Toxoplasma gondii infection. *Nat Rev Immunol* 2014. **14** : 109–21.
237. Müller N, Schwarz M. Schizophrenia as an inflammation-mediated dysbalance of glutamatergic neurotransmission. *Neurotoxicity Research*. 2006. p. 131–48.
238. Spedding M, Gressens P. Neurotrophins and cytokines in neuronal plasticity. *Novartis Found Symp* 2008. **289** : 222–33; discussion 233–40.
239. Harsan L-A, Steibel J, Zaremba A, et al. Recovery from chronic demyelination by thyroid hormone therapy: myelinogenesis induction and assessment by diffusion tensor magnetic resonance imaging. *J Neurosci* 2008. **28** : 14189–201.
240. Calamante F, Tournier JD, Kurniawan ND, et al. Super-resolution track-density imaging studies of mouse brain: Comparison to histology. *Neuroimage* 2012. **59** : 286–96.
241. Paxinos G, Franklin KBJ. *Mouse Brain in Stereotaxic Coordinates*. Second Ed. Academic Press; 2001.
242. Mawrin C, Kirches E, Dietzmann K. Single-cell analysis of mtDNA in amyotrophic lateral sclerosis: towards the characterization of individual neurons in neurodegenerative disorders. *Pathol Res Pract* 2003. **199** : 415–8.
243. Steiner J, Bielau H, Brisch R, et al. Immunological aspects in the neurobiology of suicide: Elevated microglial density in schizophrenia and depression is associated with suicide. *J Psychiatr Res* 2008. **42** : 151–7.
244. Smalla K-H, Patricia K, Wyneken U. *Isolation of the Postsynaptic density: A Specialization of the Subsynaptic Cytoskeleton. The cytoskeleton: Imaging, Isolation, and Interaction* Springer Science, Humana press; 2013. p. 265–80.
245. Stoppini L, Buchs P a, Muller D. A simple method for organotypic cultures of nervous tissue. *J Neurosci Methods* 1991. **37** : 173–82.
246. Gogolla N, Galimberti I, DePaola V, Caroni P. Preparation of organotypic hippocampal slice cultures for long-term live imaging. *Nat Protoc* 2006. **1** : 1165–71.
247. Scheiter M, Lau U, van Ham M, et al. Proteome analysis of distinct developmental stages of human natural killer (NK) cells. *Mol Cell Proteomics* 2013. **12** : 1099–114.
248. Van Ham M, Kemperman L, Wijers M, Fransen J, Hendriks W. Subcellular localization and differentiation-induced redistribution of the protein tyrosine phosphatase PTP-BL in neuroblastoma cells. *Cell Mol Neurobiol* 2005. **25** : 1225–44.
249. Reinl T, Nimtz M, Hundertmark C, et al. Quantitative phosphokinome analysis of the Met pathway activated by the invasive internalin B from *Listeria monocytogenes*. *Mol Cell Proteomics* 2009. **8** : 2778–95.
250. Sun SW, Liang HF, Trinkaus K, et al. Noninvasive detection of cuprizone induced axonal damage and demyelination in the mouse corpus callosum. *Magn Reson Med* 2006. **55** : 302–8.
251. Song SK, Yoshino J, Le TQ, et al. Demyelination increases radial diffusivity in corpus callosum of mouse brain. *Neuroimage* 2005. **26** : 132–40.
252. Li KW, Miller S, Klychnikov O, et al. Quantitative proteomics and protein network analysis of hippocampal synapses of CaMKIIalpha mutant mice. *J Proteome Res* 2007. **6** : 3127–33.
253. Mallei A, Giambelli R, Gass P, et al. Synaptoproteomics of learned helpless rats involve energy metabolism and cellular remodeling pathways in depressive-like behavior and antidepressant response. *Neuropharmacology* 2011. **60** : 1243–53.
254. Li KW, Jimenez CR. Synapse proteomics: current status and quantitative applications. *Expert Rev Proteomics* 2008. **5** : 353–60.
255. Filiou MD, Turck CW, Martins-De-Souza D. Quantitative proteomics for investigating psychiatric disorders. *Proteomics - Clinical Applications*. 2011. p. 38–49.
256. Bomar JM, Benke PJ, Slattery EL, et al. Mutations in a novel gene encoding a CRAL-TRIO domain cause human Cayman ataxia and ataxia/dystonia in the jittery mouse. *Nat Genet* 2003. **35** : 264–9.
257. Dick O, Tom Dieck S, Altmann WD, et al. The presynaptic active zone protein bassoon is essential for photoreceptor ribbon synapse formation in the retina. *Neuron* 2003. **37** : 775–86.

258. Tao Y-X, Rumbaugh G, Wang G-D, et al. Impaired NMDA receptor-mediated postsynaptic function and blunted NMDA receptor-dependent persistent pain in mice lacking postsynaptic density-93 protein. *J Neurosci* 2003. **23** : 6703–12.
259. Migaud M, Charlesworth P, Dempster M, et al. Enhanced long-term potentiation and impaired learning in mice with mutant postsynaptic density-95 protein. *Nature* 1998. **396** : 433–9.
260. Masson J, Darmon M, Conjard A, et al. Mice lacking brain/kidney phosphate-activated glutaminase have impaired glutamatergic synaptic transmission, altered breathing, disorganized goal-directed behavior and die shortly after birth. *J Neurosci* 2006. **26** : 4660–71.
261. Schwenk J, Metz M, Zolles G, et al. Native GABA(B) receptors are heteromultimers with a family of auxiliary subunits. *Nature* 2010. **465** : 231–5.
262. Tu W, Xu X, Peng L, et al. DAPK1 Interaction with NMDA Receptor NR2B Subunits Mediates Brain Damage in Stroke. *Cell* 2010. **140** : 222–34.
263. Wang X, Kibschull M, Laue MM, et al. Aczonin, a 550-kD putative scaffolding protein of presynaptic active zones, shares homology regions with Rim and Bassoon and binds profilin. *J Cell Biol* 1999. **147** : 151–62.
264. Crowder KM, Gunther JM, Jones TA, et al. Abnormal neurotransmission in mice lacking synaptic vesicle protein 2A (SV2A). *Proc Natl Acad Sci U S A* 1999. **96** : 15268–73.
265. Janz R, Goda Y, Geppert M, Missler M, Südhof TC. SV2A and SV2B function as redundant Ca²⁺ regulators in neurotransmitter release. *Neuron* 1999. **24** : 1003–16.
266. Janz R, Südhof TC, Hammer RE, et al. Essential roles in synaptic plasticity for synaptogyrin I and synaptophysin I. *Neuron* 1999. **24** : 687–700.
267. Moechars D, Weston MC, Leo S, et al. Vesicular glutamate transporter VGLUT2 expression levels control quantal size and neuropathic pain. *J Neurosci* 2006. **26** : 12055–66.
268. Beal MF. Mechanisms of excitotoxicity in neurologic diseases. *FASEB J* 1992. **6** : 3338–44.
269. Petroff OAC. GABA and glutamate in the human brain. *Neuroscientist* 2002. **8** : 562–73.
270. Chang PK-Y, Verbich D, McKinney RA. AMPA receptors as drug targets in neurological disease—advantages, caveats, and future outlook. *Eur J Neurosci* 2012. **35** : 1908–16.
271. Paoletti P, Bellone C, Zhou Q. NMDA receptor subunit diversity: impact on receptor properties, synaptic plasticity and disease. *Nat Rev Neurosci* 2013. **14** : 383–400.
272. Zhou Q, Sheng M. NMDA receptors in nervous system diseases. *Neuropharmacology* 2013. **74** : 69–75.
273. Emamian ES. AKT/GSK3 signaling pathway and schizophrenia. *Frontiers in Molecular Neuroscience*. 2012.
274. Salcedo-Tello P, Ortiz-Matamoros A, Arias C. GSK3 Function in the Brain during Development, Neuronal Plasticity, and Neurodegeneration. *Int J Alzheimers Dis* 2011. **2011** : 189728.
275. Grimes CA, Jope RS. The multifaceted roles of glycogen synthase kinase 3beta in cellular signaling. *Prog Neurobiol* 2001. **65** : 391–426.
276. Webster JP, Brunton CF, MacDonald DW. Effect of *Toxoplasma gondii* upon neophobic behaviour in wild brown rats, *Rattus norvegicus*. *Parasitology* 1994. **109** (Pt 1 : 37–43.
277. Worth AR, Lymbery AJ, Thompson RCA. Adaptive host manipulation by *Toxoplasma gondii*: Fact or fiction? *Trends Parasitol* 2013. **29** : 150–5.
278. Hinze-Selch D, Däubener W, Erdag S, Wilms S. The diagnosis of a personality disorder increases the likelihood for seropositivity to *Toxoplasma gondii* in psychiatric patients. *Folia Parasitol (Praha)* 2010. **57** : 129–35.
279. Pedersen MG, Mortensen PB, Norgaard-Pedersen B, Postolache TT. *Toxoplasma gondii* infection and self-directed violence in mothers. *Arch Gen Psychiatry* 2012. **69** : 1123–30.
280. Lawrie SM, Whalley HC, Job DE, Johnstone EC. Structural and functional abnormalities of the amygdala in schizophrenia. *Ann N Y Acad Sci* 2003. **985** : 445–60.
281. Goghari VM, Lang DJ, Flynn SW, MacKay AL, Honer WG. Smaller corpus callosum subregions containing motor fibers in schizophrenia. *Schizophr Res* 2005. **73** : 59–68.

282. Woodward ND. Thalamocortical Dysconnectivity in Schizophrenia. *Am J Psychiatry* 2012. **169** : 1092.
283. Anticevic A, Brumbaugh MS, Winkler AM, et al. Global prefrontal and fronto-amygdala dysconnectivity in bipolar i disorder with psychosis history. *Biol Psychiatry* 2013. **73** : 565–73.
284. Hermes G, Ajioka JW, Kelly KA, et al. Neurological and behavioral abnormalities, ventricular dilatation, altered cellular functions, inflammation, and neuronal injury in brains of mice due to common, persistent, parasitic infection. *J Neuroinflammation* 2008. **5** : 48.
285. Gaddi PJ, Yap GS. Cytokine regulation of immunopathology in toxoplasmosis. *Immunol Cell Biol* 2007. **85** : 155–9.
286. Randall LM, Hunter CA. Parasite dissemination and the pathogenesis of toxoplasmosis. *Eur J Microbiol Immunol (Bp)* 2011. **1** : 3–9.
287. Fritz-French C, Tyor W. Interferon- α (IFN α) neurotoxicity. *Cytokine Growth Factor Rev* 2012. **23** : 7–14.
288. Zanelli S, Naylor M, Kapur J. Nitric oxide alters GABAergic synaptic transmission in cultured hippocampal neurons. *Brain Res* 2009. **1297** : 23–31.
289. Zindler E, Zipp F. Neuronal injury in chronic CNS inflammation. *Best Pract Res Clin Anaesthesiol* 2010. **24** : 551–62.
290. Giovannoni G, Heales SJR, Land JM, Thompson EJ. The potential role of nitric oxide in multiple sclerosis. *Multi Scler* 1998. **4** : 212–6.
291. Law A, Gauthier S, Quirion R. Say NO to Alzheimer ' s disease: the putative links between nitric oxide and dementia of the Alzheimer ' s type. *Brain Res Rev* 2001. **35** : 73–96.
292. Jung B-K, Pyo K-H, Shin KY, et al. Toxoplasma gondii Infection in the Brain Inhibits Neuronal Degeneration and Learning and Memory Impairments in a Murine Model of Alzheimer's Disease. *PLoS One* 2012. **7** : e33312.
293. Rozenfeld C, Martinez R, Seabra S, et al. Toxoplasma gondii prevents neuron degeneration by interferon-gamma-activated microglia in a mechanism involving inhibition of inducible nitric oxide synthase and transforming growth factor-beta1 production by infected microglia. *Am J Pathol* 2005. **167** : 1021–31.
294. Al-Chalabi A, Miller CCJ. Neurofilaments and neurological disease. *BioEssays* 2003. **25** : 346–55.
295. Penzes P, Srivastava DP, Woolfrey KM. Not Just Actin? A Role for Dynamic Microtubules in Dendritic Spines. *Neuron* 2009. **61** : 3–5.
296. Sanchez C, Diaz-Nido J, Avila J. Phosphorylation of microtubule-associated protein 2 (MAP2) and its relevance for the regulation of the neuronal cytoskeleton function. *Prog Neurobiol* 2000. **61** : 133–68.
297. Glantz LA, Lewis DA. Decreased dendritic spine density on prefrontal cortical pyramidal neurons in schizophrenia. *Arch Gen Psychiatry* 2000. **57** : 65–73.
298. Mitra R, Sapolsky RM, Vyas A. Toxoplasma gondii infection induces dendritic retraction in basolateral amygdala accompanied by reduced corticosterone secretion. *Dis Model Mech* 2012.
299. Hansen MB. The enteric nervous system I: organisation and classification. *Pharmacol Toxicol* 2003. **92** : 105–13.
300. Hansen MB. The enteric nervous system II: gastrointestinal functions. *Pharmacol Toxicol* 2003. **92** : 249–57.
301. Hansen MB. The enteric nervous system III: a target for pharmacological treatment. *Pharmacol Toxicol* 2003. **93** : 1–13.
302. Hermes-Uliana C, Pereira-Severi LS, Luerdes RB, et al. Chronic infection with Toxoplasma gondii causes myenteric neuroplasticity of the jejunum in rats. *Auton Neurosci Basic Clin* 2011. **160** : 3–8.
303. Odorizzi L, Moreira NM, Gonçalves GF, et al. Quantitative and morphometric changes of subpopulations of myenteric neurons in swines with toxoplasmosis. *Auton Neurosci Basic Clin* 2010. **155** : 68–72.
304. Papazian-Cabanas RM, Araújo EJA, Silva AV da, Sant'Ana DMG. Myenteric neuronal plasticity induced by Toxoplasma gondii (genotype III) on the duodenum of rats. *An Acad Bras Cienc* 2012. **84** : 737–46.
305. Silva LS, Sartori AL, Zaniolo LM, et al. Toxoplasma gondii: Myenteric neurons of intraperitoneally inoculated rats show quantitative and morphometric alterations. *Exp Parasitol* 2011. **129** : 5–10.

-
306. Zaniolo LM, Da Silva AV, Sant'Ana D de MG, Araújo EJ de A. Toxoplasma gondii infection causes morphological changes in caecal myenteric neurons. *Exp Parasitol* 2012. **130** : 103–9.
307. Clinton SM, Meador-Woodruff JH. Abnormalities of the NMDA Receptor and Associated Intracellular Molecules in the Thalamus in Schizophrenia and Bipolar Disorder. *Neuropsychopharmacology* 2004. **29** : 1353–62.
308. Eastwood SL. The synaptic pathology of schizophrenia: Is aberrant neurodevelopment and plasticity to blame? *Int Rev Neurobiol* 2003. **59** : 47–72.
309. Meador-Woodruff JH, Clinton SM, Beneyto M, McCullumsmith RE. Molecular Abnormalities of the Glutamate Synapse in the Thalamus in Schizophrenia. *Ann N Y Acad Sci* 2003. **1003** : 75–93.
310. Valtorta F, Pennuto M, Bonanomi D, Benfenati F. Synaptophysin: Leading actor or walk-on role in synaptic vesicle exocytosis? *BioEssays* 2004. **26** : 445–53.
311. Chetkovich DM, Bunn RC, Kuo S-H, et al. Postsynaptic targeting of alternative postsynaptic density-95 isoforms by distinct mechanisms. *J Neurosci* 2002. **22** : 6415–25.
312. Cao J, Viholainen JI, Dart C, et al. The PSD95-nNOS interface: a target for inhibition of excitotoxic p38 stress-activated protein kinase activation and cell death. *J Cell Biol* 2005. **168** : 117–26.
313. Schmitt U, Tanimoto N, Seeliger M, Schaeffel F, Leube RE. Detection of behavioral alterations and learning deficits in mice lacking synaptophysin. *Neuroscience* 2009. **162** : 234–43.
314. Deng XH, Ai WM, Lei DL, et al. Lipopolysaccharide induces paired immunoglobulin-like receptor B (PirB) expression, synaptic alteration, and learning-memory deficit in rats. *Neuroscience* 2012. **209** : 161–70.
315. Montgomery JM, Madison D V. Discrete synaptic states define a major mechanism of synapse plasticity. *Trends Neurosci* 2004. **27** : 744–50.
316. Rajan I, Cline HT. Glutamate receptor activity is required for normal development of tectal cell dendrites in vivo. *J Neurosci* 1998. **18** : 7836–46.
317. Monfils MH, Teskey GC. Induction of long-term depression is associated with decreased dendritic length and spine density in layers III and V of sensorimotor neocortex. *Synapse* 2004. **53** : 114–21.
318. Bartlett TE, Wang YT. The intersections of NMDAR-dependent synaptic plasticity and cell survival. *Neuropharmacology* 2013. **74** : 59–68.
319. Zukin RS, Bennett M V. Alternatively spliced isoforms of the NMDAR1 receptor subunit. *Trends Neurosci* 1995. **18** : 306–13.
320. Cull-Candy S, Brickley S, Farrant M. NMDA receptor subunits: Diversity, development and disease. *Current Opinion in Neurobiology*. 2001. p. 327–35.
321. Kelly JP, Wrynn AS, Leonard BE. The olfactory bulbectomized rat as a model of depression: An update. *Pharmacology and Therapeutics*. 1997. p. 299–316.
322. Wang D, Noda Y, Tsunekawa H, et al. Behavioural and neurochemical features of olfactory bulbectomized rats resembling depression with comorbid anxiety. *Behav Brain Res* 2007. **178** : 262–73.
323. Law AJ, Deakin JF. Asymmetrical reductions of hippocampal NMDAR1 glutamate receptor mRNA in the psychoses. *Neuroreport* 2001. **12** : 2971–4.
324. Sun H, Jia N, Guan L, et al. Involvement of NR1, NR2A different expression in brain regions in anxiety-like behavior of prenatally stressed offspring. *Behav Brain Res* 2013. **257** : 1–7.
325. Sun H, Guan L, Zhu Z, Li H. Reduced levels of NR1 and NR2A with depression-like behavior in different brain regions in prenatally stressed juvenile offspring. *PLoS One* 2013. **8**.
326. Kannagara TS, Eadie BD, Bostrom C a, et al. GluN2A-/- Mice Lack Bidirectional Synaptic Plasticity in the Dentate Gyrus and Perform Poorly on Spatial Pattern Separation Tasks. *Cereb Cortex* 2014. **1500** : 1–12.
327. Loftis JM, Janowsky A. The N-methyl-D-aspartate receptor subunit NR2B: localization, functional properties, regulation, and clinical implications. *Pharmacol Ther* 2003. **97** : 55–85.
328. Adamec RE, Burton P, Shallow T, Budgell J. Unilateral block of NMDA receptors in the amygdala prevents predator stress - Induced lasting increases in anxiety-like behavior and unconditioned startle - Effective hemisphere
-

- depends on the behavior. *Physiol Behav* 1998. **65** : 739–51.
329. Adamec RE, Burton P, Shallow T, Budgell J. NMDA receptors mediate lasting increases in anxiety-like behavior produced by the stress of predator exposure - Implications for anxiety associated with posttraumatic stress disorder. *Physiol Behav* 1998. **65** : 723–37.
330. Catena-Dell'Osso M, Rotella F, Dell'Osso A, Fagiolini A, Marazziti D. Inflammation, serotonin and major depression. *Curr Drug Targets* 2013. **14** : 571–7.
331. Saito K, Markey SP, Heyes MP. Chronic effects of gamma-interferon on quinolinic acid and indoleamine-2,3-dioxygenase in brain of C57BL6 mice. *Brain Res* 1991. **546** : 151–4.
332. Schwarcz R, Pellicciari R. Manipulation of brain kynurenes: glial targets, neuronal effects, and clinical opportunities. *J Pharmacol Exp Ther* 2002. **303** : 1–10.
333. Notarangelo FM, Wilson EH, Horning KJ, et al. Evaluation of kynurenine pathway metabolism in *Toxoplasma gondii*-infected mice: Implications for schizophrenia. *Schizophr Res* 2014. **152** : 261–7.
334. Guidetti P, Schwarcz R. 3-Hydroxykynurenine and quinolinate: pathogenic synergism in early grade Huntington's disease? *Adv Exp Med Biol* 2003. **527** : 137–45.
335. Guillemin GJ, Meininger V, Brew BJ. Implications for the kynurenine pathway and quinolinic acid in amyotrophic lateral sclerosis. *Neurodegener Dis* 2006. **2** : 166–76.
336. Schwarcz R, Rassoulpour A, Wu HQ, et al. Increased cortical kynurenate content in schizophrenia. *Biol Psychiatry* 2001. **50** : 521–30.
337. Guillemin GJ, Smythe G, Takikawa O, Brew BJ. Expression of indoleamine 2,3-dioxygenase and production of quinolinic acid by human microglia, astrocytes, and neurons. *Glia* 2005. **49** : 15–23.
338. Gross C, Bassell GJ. Neuron-specific regulation of class I PI3K catalytic subunits and their dysfunction in brain disorders. *Front Mol Neurosci* 2014. **7** : 12.
339. Cantley LC. The phosphoinositide 3-kinase pathway. *Science* 2002. **296** : 1655–7.
340. Cross DA, Alessi DR, Cohen P, Andjelkovich M, Hemmings BA. Inhibition of glycogen synthase kinase-3 by insulin mediated by protein kinase B. *Nature* 1995. **378** : 785–9.
341. Cole AR. Glycogen synthase kinase 3 substrates in mood disorders and schizophrenia. *FEBS J* 2013. **280** : 5213–27.
342. Salcedo-Tello P, Ortiz-Matamoros A, Arias C. GSK3 Function in the Brain during Development, Neuronal Plasticity, and Neurodegeneration. *Int J Alzheimers Dis* 2011. **2011** : 189728.
343. Cortes-Vieyra R, Bravo-Patino A, Valdez-Alarcon JJ, et al. Role of glycogen synthase kinase-3 beta in the inflammatory response caused by bacterial pathogens. *J Inflamm* 2012. **9** : 23.
344. Tay TF, Maheran M, Too SL, et al. Glycogen synthase kinase-3 β inhibition improved survivability of mice infected with *Burkholderia pseudomallei*. *Trop Biomed* 2012. **29** : 551–67.
345. Zhang P, Katz J, Michalek SM. Glycogen synthase kinase-3 β (GSK3 β) inhibition suppresses the inflammatory response to *Francisella* infection and protects against tularemia in mice. *Mol Immunol* 2009. **46** : 677–87.
346. Beaulieu J-M, Gainetdinov RR, Caron MG. Akt/GSK3 signaling in the action of psychotropic drugs. *Annu Rev Pharmacol Toxicol* 2009. **49** : 327–47.
347. Webster JP, Lambertson PHL, Donnelly CA, Torrey EF. Parasites as causative agents of human affective disorders? The impact of anti-psychotic, mood-stabilizer and anti-parasite medication on *Toxoplasma gondii*'s ability to alter host behaviour. *Proc Biol Sci* 2006. **273** : 1023–30.

Annex

Differentially expressed synaptosomal proteins identified by iTRAQ.

No.	Symbol	Entrez Gene Name	Accession	Location	Fold change
1	ABCA13	ATP-binding cassette, sub-family A (ABC1), member 13	Q5SSE9	Extracellular	-1.460
2	ACADVL	acyl-CoA dehydrogenase, very long chain	P50544	Cytoplasm	1.723
3	ACLY	ATP citrate lyase	Q91V92	Cytoplasm	-1.513
4	ALB	albumin	P07724	Extracellular	5.839
5	ANKS1B	ankyrin repeat and sterile alpha motif domain containing 1B	Q8BIZ1	Nucleus	-1.792
6	APOD	apolipoprotein D	P51910	Extracellular	3.948
7	APOE	apolipoprotein E	P08226	Extracellular	2.287
8	ARHGDIB	Rho GDP dissociation inhibitor (GDI) beta	Q61599	Cytoplasm	1.799
9	ATCAY	ataxia, cerebellar, Cayman type	Q8BHE3	Plasma Membrane	-2.012
10	B2M	beta-2-microglobulin	P01887	Plasma Membrane	7.610
11	BCAS1	breast carcinoma amplified sequence 1	Q80YN3	Plasma Membrane	1.852
12	C19orf10	chromosome 19 open reading frame 10	Q9CPT4	Extracellular	1.720
13	C4A/C4B	complement component 4B (Chido blood group)	P01029	Extracellular	1.991
14	CALU	calumenin	O35887	Cytoplasm	2.099
15	CHGA	chromogranin A (parathyroid secretory protein 1)	P26339	Cytoplasm	1.843

No.	Symbol	Entrez Gene Name	Accession	Location	Fold change
16	CHGB	chromogranin B (secretogranin 1)	P16014	Extracellular	2.304
17	CLU	clusterin	Q06890	Cytoplasm	1.939
18	CST3	cystatin C	P21460	Extracellular	2.070
19	CTSD	cathepsin D	P18242	Cytoplasm	1.827
20	CTSZ	cathepsin Z	Q9WUU7	Cytoplasm	3.062
21	DLG2	discs, large homolog 2 (Drosophila)	Q91XM9	Plasma Membrane	-1.488
22	DLG4	discs, large homolog 4 (Drosophila)	Q62108	Plasma Membrane	-1.942
23	DNAJC5	DnaJ (Hsp40) homolog, subfamily C, member 5	P60904	Plasma Membrane	-1.626
24	DSP	desmoplakin	E9Q557	Plasma Membrane	1.736
25	ESYT2	extended synaptotagmin-like protein 2	Q3TZZ7	Plasma Membrane	-1.517
26	GABBR2	gamma-aminobutyric acid (GABA) B receptor, 2	Q80T41	Plasma Membrane	-1.645
27	GABRA1	gamma-aminobutyric acid (GABA) A receptor, alpha 1	P62812	Plasma Membrane	-1.473
28	GBP2	guanylate binding protein 2, interferon-inducible	Q9Z0E6	Cytoplasm	3.800
29	GFAP	glial fibrillary acidic protein	P03995	Cytoplasm	2.302
30	GIMAP4	GTPase, IMAP family member 4	Q99JY3	Nucleus	-1.471
31	GLS	glutaminase	D3Z7P3	Cytoplasm	-1.558
32	GLUL	glutamate-ammonia ligase	P15105	Cytoplasm	-2.519
33	GRIA2	glutamate receptor, ionotropic, AMPA 2	P23819	Plasma Membrane	-1.582
34	GRIA3	glutamate receptor, ionotropic, AMPA 3	Q9Z2W9	Plasma Membrane	-2.004
35	GRIN1	glutamate receptor, ionotropic, N-methyl D-aspartate 1	P35438	Plasma Membrane	-1.490
36	GSTM5	glutathione S-transferase mu 5	P10649	Cytoplasm	-1.495
37	H2AFZ	H2A histone family, member Z	POC0S6	Nucleus	4.505

No.	Symbol	Entrez Gene Name	Accession	Location	Fold change
38	HCLS1	hematopoietic cell-specific Lyn substrate 1	P49710	Nucleus	1.867
39	HIST1H1C	histone cluster 1, H1c	P15864	Nucleus	2.254
40	HLA-A	major histocompatibility complex, class I, A	P01899	Plasma Membrane	3.919
41	HOMER1	homer homolog 1 (Drosophila)	Q9Z2Y3	Plasma Membrane	-1.718
42	HSP90B1	heat shock protein 90kDa beta (Grp94), member 1	P08113	Cytoplasm	1.810
43	IFIT3	interferon-induced protein with tetratricopeptide repeats 3	Q64345	Cytoplasm	5.093
44	Ighg2a	immunoglob heavy constant γ -2A	P01864	Extracellular	3.606
45	Iigp1	interferon inducible GTPase 1	Q9QZ85	Other	3.248
46	Irgm1	immunity-related GTPase family M member 1	Q60766	Cytoplasm	4.670
47	JUP	junction plakoglobin	Q02257	Plasma Membrane	1.781
48	KCTD16	potassium channel tetramerization domain containing 16	Q5DTY9	Plasma Membrane	-1.433
49	KIAA0513	KIAA0513	Q8R0A7	Other	-1.642
50	KRT16	keratin 16	Q9Z2K1	Cytoplasm	2.513
51	KRT17	keratin 17	Q9QWL7	Cytoplasm	2.030
52	Krt2	keratin 2	Q3TTY5	Cytoplasm	1.959
53	KRT35	keratin 35	Q497I4	Cytoplasm	-2.309
54	Krt42	keratin 42	Q6IFX2	Other	2.700
55	KRT5	keratin 5	Q922U2	Cytoplasm	2.031
56	KRT6B	keratin 6B	P50446	Cytoplasm	1.773
57	KRT75	keratin 75	Q8BGZ7	Cytoplasm	1.813
58	KRT76	keratin 76	Q3UV17	Cytoplasm	2.275
59	LAMP2	lysosomal-associated membrane protein 2	P17047	Plasma Membrane	4.186
60	LAP3	leucine aminopeptidase 3	Q9CPY7	Cytoplasm	1.825

No.	Symbol	Entrez Gene Name	Accession	Location	Fold change
61	LCP1	lymphocyte cytosolic protein 1 (L-plastin)	Q61233	Cytoplasm	2.524
62	LGALS1	lectin, galactoside-binding, soluble, 1	P16045	Extracellular	1.816
63	LGI1	leucine-rich, glioma inactivated 1	Q9JIA1	Plasma Membrane	-1.471
64	LRRC7	leucine rich repeat containing 7	Q80TE7	Plasma Membrane	-1.701
65	MAL2	mal, T-cell differentiation protein 2 (gene/pseudogene)	Q8BI08	Plasma Membrane	-1.473
66	NAMPT	nicotinamide phosphoribosyltransferase	Q99KQ4	Extracellular	2.606
67	NDUFA4	NDUFA4, mitochondrial complex associated	Q62425	Cytoplasm	-1.527
68	NDUFB5	NADH dehydrogenase (ubiquinone) 1 beta subcomplex, 5	Q9CQH3	Cytoplasm	-1.715
69	Nptn	neuroplastin	P97300	Plasma Membrane	-1.443
70	OGT	O-linked N-acetylglucosamine (GlcNAc) transferase	Q8CGY8	Cytoplasm	-1.587
71	PCSK1N	proprotein convertase subtilisin/kexin type 1 inhibitor	Q9QXV0	Extracellular	1.872
72	PDIA3	protein disulfide isomerase family A, member 3	P27773	Cytoplasm	1.723
73	PFN1	profilin 1	P62962	Cytoplasm	1.995
74	PLBD2	phospholipase B domain containing 2	Q3TCN2	Extracellular	1.708
75	PLCB1	phospholipase C, beta 1 (phosphoinositide-specific)	Q9Z1B3	Cytoplasm	-1.626
76	PPIB	peptidylprolyl isomerase B (cyclophilin B)	P24369	Cytoplasm	2.290
77	PPP1R1B	protein phosphatase 1, regulatory (inhibitor) subunit 1B	Q60829	Cytoplasm	2.094
78	PPT1	palmitoyl-protein thioesterase 1	O88531	Cytoplasm	1.728
79	PRDX1	peroxiredoxin 1	P35700	Cytoplasm	1.772
80	PRDX3	peroxiredoxin 3	P20108	Cytoplasm	1.767
81	PRDX6	peroxiredoxin 6	O08709	Cytoplasm	2.318

No.	Symbol	Entrez Gene Name	Accession	Location	Fold change
82	PRKACA	protein kinase, cAMP-dependent, catalytic, alpha	P05132	Cytoplasm	-1.821
83	Ptma	prothymosin alpha	P26350	Nucleus	1.759
84	Ptprd	protein tyrosine phosphatase, receptor type, D	Q64487	Plasma Membrane	-1.431
85	PURB	purine-rich element binding protein B	O35295	Nucleus	-2.336
86	PVALB	parvalbumin	P32848	Cytoplasm	1.835
87	RAB3A	RAB3A, member RAS oncogene family	P63011	Cytoplasm	-1.499
88	RAB3B	RAB3B, member RAS oncogene	Q9CZT8	Cytoplasm	-1.938
89	RHOG	ras homolog family member G	P84096	Cytoplasm	2.142
90	RIMS1	regulating synaptic membrane exocytosis 1	Q99NE5	Plasma Membrane	-1.522
91	RPL18	ribosomal protein L18	P35980	Cytoplasm	2.064
92	Rpl23a	ribosomal protein L23A	P62751	Nucleus	1.746
93	RPL30	ribosomal protein L30	P62889	Cytoplasm	1.914
94	RPL5	ribosomal protein L5	P47962	Cytoplasm	2.301
95	RPL7	ribosomal protein L7	P14148	Nucleus	1.891
96	RPLP2	ribosomal protein, large, P2	P99027	Cytoplasm	2.067
97	RTN4	reticulon 4	Q99P72	Cytoplasm	1.714
98	S100A4	S100 calcium binding protein A4	P07091	Cytoplasm	4.802
99	S100A6	S100 calcium binding protein A6	P14069	Cytoplasm	2.612
100	SCAI	suppressor of cancer cell invasion	Q8C8N2	Other	-1.451
101	SCG2	secretogranin II	Q03517	Extracellular	2.068
102	SFXN1	sideroflexin 1	Q99JR1	Cytoplasm	-1.531
103	SH3BGRL3	SH3 domain binding glutamate-rich protein like 3	Q91VW3	Nucleus	1.797

No.	Symbol	Entrez Gene Name	Accession	Location	Fold change
104	SLC12A5	solute carrier family 12 (potassium/chloride transporter), member 5	Q91V14	Plasma Membrane	-1.529
105	SLC17A6	solute carrier family 17 (vesicular glutamate transporter), member 6	Q8BLE7	Plasma Membrane	-1.572
106	SLC1A2	solute carrier family 1 (glial high affinity glutamate transporter), member 2	P43006	Plasma Membrane	-2.347
107	SLC4A4	solute carrier family 4 (sodium bicarbonate cotransporter), member 4	O88343	Plasma Membrane	-1.490
108	SLC4A8	solute carrier family 4, sodium bicarbonate cotransporter, member 8	Q8JZR6	Plasma Membrane	-1.546
109	SLC6A11	solute carrier family 6 (neurotransmitter transporter), member 11	P31650	Plasma Membrane	-1.681
110	STAT1	signal transducer and activator of transcription 1, 91kDa	P42225	Nucleus	2.205
111	SV2A	synaptic vesicle glycoprotein 2A	Q9JIS5	Cytoplasm	-1.462
112	SV2B	synaptic vesicle glycoprotein 2B	Q8BG39	Plasma Membrane	-1.460
113	SYNGAP1	synaptic Ras GTPase activating protein 1	F6SEU4	Plasma Membrane	-1.439
114	SYNGR3	synaptogyrin 3	Q8R191	Plasma Membrane	-1.587
115	SYP	synaptophysin	Q62277	Cytoplasm	-1.695
116	TAPBP	TAP binding protein (tapasin)	Q9R233	Cytoplasm	3.530
117	TF	transferrin	Q921I1	Extracellular	1.702
118	TPM3	tropomyosin 3	P21107	Cytoplasm	1.704
119	WDR7	WD repeat domain 7	Q920I9	Other	-1.460
120	WFS1	Wolfram syndrome 1 (wolframin)	P56695	Cytoplasm	1.924

Selbständigkeitserklärung

Hiermit erkläre ich, dass ich die von mir eingereichte Dissertation zum Thema:

Neuronal alterations in chronic cerebral *Toxoplasma gondii* infection

selbstständig verfasst, nicht schon als Dissertation verwendet habe und die benutzten Hilfsmittel und Quellen vollständig angegeben wurden.

Weiterhin erkläre ich, dass ich weder diese noch eine andere Arbeit zur Erlangung des akademischen Grades doctor rerum naturalium (Dr. rer. nat.) an anderen Einrichtungen eingereicht habe.

Magdeburg, den 20.11.2014

Alexandru Parlog

Curriculum vitae

Name	Alexandru Parlog
Birth date	26.03.1982
Birth place	Tulcea, Romania
Nationality	Romanian
Address	Fermersleber Weg 45D 39112 Magdeburg
Phone	0049 (0) 1785326038
E-mail	alexandru_parlog@yahoo.com

Education

- 2011-2015 Otto-von-Guericke University, Magdeburg, Faculty of Natural Sciences, PhD in Neuroscience.
- 2008-2010 Strasbourg University, Strasbourg, Faculty of Life Science, Master in Neuroscience, Degree: *Master of Science in Neuroscience (MSc)*.
- 2001-2007 University of Agronomy and Veterinary Medicine, Bucharest, Faculty of Veterinary Medicine, Degree: *Doctor of veterinary medicine (DVM)*.

Work experience

- 2011-2015: PhD student, Institute of Medical Microbiology and Hospital Hygiene, Immunoparasitology Group, Magdeburg, Germany.
- 2010-2011: Research assistant, Institute of Genetics and Molecular and Cellular Biology, Translational Medicine and Neurogenetics Department, Strasbourg, France.
- 2009-2010: Master internship, University Medical Center, Medical Physics, Animal Molecular Imaging Research Center, Freiburg, Germany.
- 2007-2008: Veterinary doctor, Tulcea County, Romania.
-